SDN-BASED ADAPTIVE DATA ENABLED CHANNEL ESTIMATION IN THE INTERNET OF MARITIME THINGS FOR QoS ENHANCEMENT IN NAUTICAL RADIO NETWORKS

by

Owoicho Emmanuel Ijiga

Submitted in partial fulfillment of the requirements for the degree

Philosophiae Doctor (Computer Engineering)

in the

Department of Electrical, Electronic and Computer Engineering

Faculty of Engineering, Built Environment and Information Technology

UNIVERSITY OF PRETORIA

17th February 2021

SUMMARY

SDN-BASED ADAPTIVE DATA ENABLED CHANNEL ESTIMATION IN THE INTERNET OF MARITIME THINGS FOR QoS ENHANCEMENT IN NAUTICAL RADIO NETWORKS

by

Owoicho Emmanuel Ijiga

Promoter:	Prof. R. Malekian
Co-promoter:	Dr. U. C. Okonkwo
Department:	Electrical, Electronic and Computer Engineering
University:	University of Pretoria
Degree:	Philosophiae Doctor (Computer Engineering)
Keywords:	Channel Estimation, Data Rate, Emergent Configurations, Fading, Industrial Internet of Things, Maritime Industry, Multi Path Propagation, Nautical Radio Networks, Oil & Gas Production, Outage Probability, QoS Provision, Software Defined Networking, Ubiquitous Computing.

Several heterogeneous, intelligent and distributed devices can be connected to interact with one another over the internet in what is known as the internet of things (IoT). Also, the concept of IoT can be exploited in the industrial environment for increasing the production output of goods and services and for mitigating the risk of disaster occurrences. This application of IoT for enhancing industrial production is known as industrial IoT (IIoT). More so, the benefits of IoT technology can be particularly exploited across the maritime industry in what is termed the internet of maritime things (IoMT) where sensors and actuator devices are implanted on marine equipment in order to foster the communication efficacy of nautical radio networks. Marine explorations may suffer from unwanted situations such as transactional delays, environmental degradation, insecurity, seaport congestions, accidents and collisions etc, which could arise from severe environmental conditions. As a result, there is a need to develop proper communication techniques that will improve the overall quality of service (QoS) and quality of experience (QoE) of marine users. To address these, the merits of

contemporaneous technologies such as ubiquitous computing, software-defined networking (SDN) and network functions virtualization (NFV) in addition to salubrious communication techniques including emergent configurations (EC), channel estimation (CE) and communication routing protocols etc, can be utilized for sustaining optimal operation of pelagic networks.

Emergent configuration (EC) is a technology that can be adapted into maritime radio networks to support the operation and collaboration of IoT connected devices in order to improve the efficiency of the connected IoT systems for maximum user satisfaction. To meet user goals, the connected devices are required to cooperate with one another in an adaptive, interoperable, and homogeneous manner. In this thesis, a survey on the concept of IoT is presented in addition to a review of IIoT systems. The applications of ubiquitous computing and SDN technology are employed to design a newfangled network architecture which is specifically propounded for enhancing the throughput of oil and gas production in the maritime ecosystem. The components of this architecture work in collaboration with one another by attempting to manage and control the exploration process of deep ocean activities especially during emergencies involving anthropogenic oil and gas spillages.

On the other hand, CE is a utilitarian communication technique that can be exploited during maritime exploration processes which offer additional reinforcement to the capacities of the nautical radio network. This technique enables the receivers of deep-sea networks to efficiently approximate the channel impulse response (CIR) of the wireless communication channel so that the effects of the communication channel on the transmitting aggregated cluster head information can be proficiently understood and predicted for useful decision-making procedures. Two CE schemes named inter-symbol interference/ average noise reduction (ISI/ANR) and reweighted error-reducing (RER) are designed in this study for estimating maritime channels for supporting the communication performances of nautical radio networks in both severe and light-fading environmental conditions. In the proposed RER method, the Manhattan distance of the CIR of an orthodox adaptive estimator is taken, which is subsequently normalised by a stability constant $(\ddot{\varepsilon})$ whose responsibility is for correcting any potential numerical system instability that may arise during the updating stages of the estimation process. To decrease the received signal error, a log-sum penalty function is eventually multiplied by an adjustable leakage factor $(\hat{\varepsilon})$ that provides additional stability to the oscillating channel behaviour. The performance of the proposed RER method is further strengthened and made resilient against channel effects by the introduction of a reweighting attractor that further contracts the mean square error of this proposed estimator. In the ISI/ANR technique, the effects of possible ISI that may arise

from maritime transmissions is considered and transformed using a low-pass filter that is incorporated for eliminating the effects of channel noise possible effects of multipath propagation. The RER scheme offered superior CE performances in comparison to other customary techniques such as the adaptive recursive least squares and normalised least mean square method in addition to conventional linear approaches such as least squares, linear minimum mean square error and maximum-likelihood estimation method. The proposed ISI/ANR technique offered an improved MSE performance in comparison to all considered linear methods. Finally, from this study, we were able to establish that accurate CE methods can improve the QoS and QoE of nautical radio networks in terms of network data rate and system outage probability.

DEDICATION

The entire research work and thesis write-up is dedicated to God, the Father of all mankind and His Son, Jesus Christ together with His Holy Spirit, the Paraclete.

ACKNOWLEDGEMENTS

I wish to firstly express distinctive gratitude to God, the Father almighty for his incessant inspirations, blessings, guidance and provisions during the entire period of this research work.

My profound gratitude goes to my supervisor, Professor Reza Malekian who consistently provided effective and beneficial advice and also worked to ensure that my basic needs were met in a bid to effectively implement and actualize the goals of this study. I sincerely appreciate all efforts made as he always created time to ensure the progress of this research work. My appreciation goes to my co-supervisor Dr Uche A. K. Okonkwo, who took out time to go through the work to meet very high standards. I sincerely appreciate the head of the ASN research group, Prof. Herman Myburgh for his effective leadership, maturity and assistance during the periods of this research work. Also, I would like to give appreciation to the head of department, Prof. Johan Jourbet for his effective leadership and guidance not forgetting the dean of the faculty, Prof. Sunil Maharaj, for being a part of my academic success over recent years. Furthermore, I would like to acknowledge my superiors during my services to the department as an assistant lecturer including Dr Suzanne Smith, Dr Derik le Roux and Prof. Pieter de Villiers for their unending supports and encouragements during the period of this research work. Not forgetting the administrative staff of the department, I give special thanks to Ms Mari Ferreira, Ms Cornel Freislich and Ms Helena Gous for providing the needed administrative support in the realization of this project.

I convey overwhelming thanks to my parents Mr and Mrs Eche F. Ijiga, who kept on encouraging me by providing motivation, financial support and prayers to ensure this research comes to a completion. I also give distinctive appreciation to my siblings Onuh M. Ijiga, Oyiwoja M. Onmonya, Onma J. Enyejo and Amina C. Ijiga, who kept on praying for me and providing words of encouragements, not forgetting Mr and Mrs Boniface Ankeli, Mrs Esther Odekina, Dr Mrs Angelina Ogwuche, Prof. and Mrs Abraham Idoko, Mr Adigwu Joseph Ichapi, Mr and Mrs Joseph Ijiga, Mr and Mrs Yakubu Ogwuche, Dr and Mrs Godfrey Akpakwu and all my extended family members whose names are too numerous to mention and who kept motivating and praying for me throughout the duration of this research work.

I am grateful to all friends and family who motivated me during difficult times especially; Dr and Mrs Daniel E. Ewim, Dr and Mrs Muyiwa B. Balogun, Dr and Mrs Olayinka O. Ogundile, Dr and Mrs

Azubike Onuora-Oguno, Dr George Dosunmu, Engr Taiwo Folayan, Mr and Mrs Louis Nsisong, Mr and Mrs Malcolm M. Sande, Mr and Mrs Augustine K. Nkulu, Mr and Mrs Ebetsamang Thupae, Mr Timothy Fay, Ms Priscilla Colon, Ms Yuping Huang, Mr Fortunatus Lamola, Mr Samuel Atache, Engr and Mrs Atoo A. Abraham and all members of the advanced sensor networks research group, University of Pretoria.

I appreciate the Association of Catholic Students, University of Pretoria and give special thanks to the chaplain, Rev. Fr Manuel Graça, for providing me with spiritual guidance during the period of this research. I appreciate all members of the Saint Cecelia choir, Saint Martins de Porres Catholic Church, Sunnyside, Pretoria and would also like to acknowledge Patrick Lenk and Dan Gibson music, whose exhilarating Gregorian chants (available on YouTube) provided me with the much needed spiritual inspirations in addition to physical motivations during critical thinking moments of this study.

Lastly, the financial support of the University of Pretoria Doctoral research grant, the South African National Research Foundation/Research and Innovation Support and Advancement (NRF/RISA) research grant and the centre for connected intelligence, advanced sensor networks research group, University of Pretoria is highly acknowledged.

LIST OF ABBREVIATIONS

4G	Fourth Generation
5G	Fifth Generation
AWGN	Additive White Gaussian Noise
AoDV	Ad-hoc on-demand Distance Vector
AoMDV	Ad-hoc on-demand Multipath Distance Vector
AMI	Advance Metering Infrastructure
AMQP	Advanced Message Queuing Protocol
ACF	Autocorrelation Function
AUV	Autonomous Underwater Vehicles
BS	Base Station
BYOD	Bring Your Own Device
BYOK	Bring Your Own Key
CDF	Cumulative Density Function
CE	Channel Estimation
CH	Cluster Head
CIR	Channel Impulse Response
CM	Cluster Members
CoAP	Constrained Application Protocol
CP-OFDM	Cyclic Prefix Orthogonal Frequency Division Multiplexing
CPSS	Cyber-Physical-Social Systems
CSI	ChannelState Information
D2D	Device-to-Device
DA	Directional Antennas
DAML	DARPA Agent Markup Language
DM	Device Manager
DRS	Demand Response Systems
DSC	Digital Selective Calling
EC	Emergent Configuration
ECM	Emergent Configuration Manager
ETC	Expected Transmission Count

GEO	GEostationary Orbit
GPA	Group Pair-selection Algorithm
HTTP	HyperText Transfer Protocol
IIoT	Industrial Internet of Things
IoMT	Internet of Maritime Things
IoT	Internet of Things
ISI	Inter-Symbol Interference
ISI/ANR	Inter-Symbol Interference/ Average Noise Reduction
LAN	Local-Area Network
LEO	Low Earth Orbit
LMMSE	Linear Minimum Mean Square Error
LoS	Line of Sight
LR-WPAN	Low-Rate Wireless Personal Area Network
LS	Least Square
LTE	Long Term Evolution
M2M	Machine-to-Machine
MAPE-K	Monitor, Analyse, Plan, Execute, system-KB
MariComm	MARItime broadband COMMunication
MIMO	Multiple Input Multiple Output
ML	Maximum Likelihood
MUE	Marine User Equipment
MQTT	Message Queue Telemetry Transport
NAVDAT	NAVigation DATa
NFC	Near Field Communication
NFV	Network Functions Virtualization
NLMS	Normalised Least Mean Squares
NLoS	Non Line of Sight
OLSR	Optimized Link-state Routing Protocol
OSV	Offshore Supply Vessel
OWL	Oil on Water Locator
PBS	Pair Broadcast Synchronization
PDF	Probability Density Function

PSD	Power Spectral Density
PSV	Platform Supply Vessel
QoE	Quality of Experience
QoS	Quality of Service
RER	Reweighted Error-Reducing
RFID	Radio Frequency IDentification
RLS	Recursive Least Squares
ROV	Remotely Operated Underwater Vehicle
RPAS	Remotely Piloted Aircraft System
R-sync	Robust SYNChronization
SDN	Software-Defined Networking
SINR	Signal Interference to Noise Ratio
SNR	Signal to Noise Ratio
SoA	Service-oriented Architecture
STETS	Spanning Tree-based Energy-efficient Time Synchronization
TBR	Ticket-Based Routing
TCP/IP	Transmission Control Protocol/Internet Protocol
UA	User Agent
UAV	Unmanned Aerial Vehicle
UCSS	Ubiquitous Computing Service System
UDDI	Universal Description Discovery and Integration
VB-RA	Voyage-Based cooperative Resource Allocation
VDES	Very high-frequency Data Exchange System
VSAT	Very Small Aperture Terminal
Wi-Fi	Wireless Fidelity
WLAN	Wireless Local Area Network
WMAN	Wireless Metropolitan Area Network
WPAN	Wireless Personal Area Network
WSN	Wireless Sensor Network
xG	Next Generation
XML	eXtensible Markup Language
XMPP	eXtensible Messaging and Presence Protocol

LIST OF SYMBOLS

$\mathbf{A}_{yy}[\ddot{D}_i, i]$	Auto-covariance matrix of received information
$(.)^*$	Conjugation operator
$\mathbf{J}_{cf}[\ddot{D}_i, i]$	Cost function for minimizing MSE
$\mathbf{A}_{cy}[\ddot{D}_i, i]$	Cross-covariance matrix between the CIR and receiver signal
$\vec{\mathring{R}}_i$	Data rate of vessel i
f_d	Doppler frequency
$\|.\|$	Euclidean norm
$\mathbb{E}$	Expectation operator
$\mathbb{F}[\ddot{D}_i, i]$	forgetting factor
$\|.\|_F$	Frobenius norm operator
$\vec{\eth}[\ddot{D}_i, i]$	Gain vector of the adaptive estimator
$\varpi_k(0)$	Generalized Erlang random variable PDF
$(.)^H$	Hermitian transpose operator
$e_r^*[\ddot{D}_i, i]$	Instantaneous CE error
$\bar{\Upsilon}_{RLS}[\ddot{D}_i, i]$	Inverse autocorrelation matrix of the transmitting signal
$\varpi_k(0)$	Lagrange basis polynomial
$\hat{\mathbf{C}}_{LMMSE}[\ddot{D}_i, i]$	LMMSE channel estimate
$\hat{\mathbf{C}}_{LS}[\ddot{D}_i, i]$	LS channel estimate
$\hat{\mathbf{C}}_{NLMS}[\ddot{D}_i, i]$	NLMS channel estimate
$P_{out}(.)$	Outage probability
α	Path loss exponent
$\overline{E}_p$	Power of the CH-aggregated signal
P_E	Power of the multipath component
$P_{QoS}(.)$	QoS-grarantee probability
$\mathbf{y}[\ddot{D}_i, i]$	Received signal at service cloud
λ	Regularization factor
$\hat{\mathbf{C}}_{RER}[\ddot{D}_i, i]$	RER channel estimate
$\hat{\varepsilon}$	RER Leakage factor
$\ddot{\varepsilon}$	RER stability constant
$\hat{\mathbf{C}}_{RLS}[\ddot{D}_i, i]$	RLS channel estimate

sgn(.)	Signum function
γ_i	SNR at reception
μ	Step size parameter
$\mathbf{g}[\ddot{D}_i, i]$	Transmitting information signal
σ_w^2	Variance of zero-mean complex white Gaussian noise
v	Velocity of the mobile CH
λ_w	Wavelength of propagating signal
$M_{a,b}(.)$	Whittaker function
$\mathbf{w}[\ddot{D}_i, i]$	Zero-mean complex white Gaussian noise

TABLE OF CONTENTS

List of Figures

List of Tables

CHAPTER 1 Introduction

1.1 BACKGROUND

The concept of "internet of things (IoT)" find utilitarian applications across a wide variety of fields ranging from smart homes, smart cities, smart grids, healthcare, intelligent transportation system, smart agriculture and industries etc. This entrancing concept attempts to amalgamate the virtual domain with the physical world through active internet connections using objects such as sensor nodes, actuators, software applications and electronics for the efficient and reliable collection and exchange of information over the connected network of things. The IoT technology is distinct from traditional internet connections because, in the former, human roles are not required for operation whereas, in the latter, there are numerous needs for human involvements [1]. Due to this capability, IoT systems can be deployed for environmental monitoring, traceability, machine control and process automation in what is termed self-organisation and configuration [2].

The IoT technology find major applications in the industrial sector not excluding manufacturing, agriculture and transportation etc. This technology is currently met with interesting implementations across the automobile and aviation industries for the development of safe transportation networks over reliable internet communication systems. Similarly, the IoT concept can find beneficial applications in the maritime sector of the transportation industry. However, the convenience of IoT technology in the development of marine communication networks is poorly studied in the literature. Consequently, this research aims at exploiting the boundless rewards of IoT technology for the development of nautical communication networks.

The maritime industry is limited to wide network coverage areas and cost-effectiveness [3]. Satellite communication systems can provide substantial wide network coverage for marine communication

networks but on the contrary, it is not cost-effective. Hence, there is an urgent need to develop communication technologies that will offer an appreciable tradeoff between the network coverage strength and cost effectiveness. As a result, the IoT technology can be deployed to enhance the communication performances of nautical radio networks in what is termed internet of maritime things (IoMT). In the IoMT technology, sensors are embedded on marine objects and are subsequently configured to collaborate with one another so as to assist valuable marine services such as oceanographic data collection and analysis, environmental monitoring, disaster prevention and management, oceanic sampling, and assisted navigation applications etc. If IoT technology is required for enhancing the signal coverage and quality of service (QoS) of marine radio networks, then techniques such as routing, channel estimation (CE), cryptography, resource allocation and machine learning etc should be well considered and designed for enhancing the network quality, data rate and throughput etc. The QoS of a marine communication network can be described as a measurement of the entire network performance of the marine communication system which could be related to nautical communication services such as outage probability, signal to noise ratio (SNR), packet loss, transmission delay, mean square error (MSE), and bit rate, etc. The quality of experience (QoE) of marine communication networks on the other hand is a measure of the gratification or exasperation of the marine users' experiences with the communication services offered by the thalassic radio network. From the aforementioned techniques, we consider CE for the realisation of IoMT which is evaluated in terms of MSE, SNR and outage probability.

The sensors deployed in the formation of IoMT are strategically positioned across the marine environment to collect useful environmental data that can be used for maritime decision-making processes. The IoMT-installed sensor networks are usually affordable (low cost) communication systems, which can be enacted in the development of perceptible cost-effective communication meshes in the nautical radio networks. However, the aggregated information to be propagated across the maritime channel will have traits such as low speed and low power, since the travelling sensor information will have low and weak transmission capabilities. As a result of the absence of carrier frequency signal transmission (or modulation) technique and due to the limitations of the sensor-based networks such as low-speed transmissions, the transmitting cluster head (CH) information in an IoMT system will most likely experience severe effects of multipath propagation and fading. Consequently, to mitigate these effects and to improve the communication quality, efficient CE methods are required in the pelagic network. Channel estimation techniques are required for aiding the seashore mounted receivers to approximate the channel impulse response (CIR) of the marine channel so that it could understand and

predict the nature and underlying consequences of the channel impact on propagating aggregated CH information since the propagating CH information may experience channel fading. Fading is described as a phenomenon that may be experienced when signals propagate across a wireless communication channel resulting in a variation of signal attenuation with time, frequency or geographical position. Thus, CE is required to improve the network performance of nautical communication systems since the signal received at the seashore base station (BS) can experience the aforementioned attenuation due to signal interactions with environmental obstacles and marine atmospheric conditions. Consequently, the network configuration of the nautical system may likely experience small fading.

Fading can generally be classified into either large scale fading or small scale fading. In large scale fading, the attenuation of the average signal power occurs as a result of signal transmissions over large areas leading to the effects of shadowing on the received signals. Statistical distributions such as the lognormal distribution are generally accepted channel models for modelling large scale fading environments. On the other hand, in small scale fading scenarios (which is applicable to maritime communication networks), the changes in the amplitude and phase of the transmitting signals occur from little changes in the spatial distances between the network transmitters and receivers. Consequently, the received signal may either experience the effects of multipath propagation or Doppler spread such as frequency selective and flat fading. When the channel experiences Doppler spread as a result of the time variations of the channel, the propagating signal will either experience slow or fast signal fading which are either characterised by slow or rapid variations of the CIR within packet durations. Statistical channel models such as Rayleigh, Rice, Nakagami-*m* and Hoyt etc, are well-known distributions for modelling small-scale fading networks which are relevant for modelling the fading channel of both terrestrial and nautical radio networks. Orthodox CE techniques such as least square (LS), linear minimum mean square error (LMMSE), maximum likelihood (ML), Normalised least mean square (NLMS) and recursive least squares (RLS) methods are well suitable for terrestrial broadband communication systems involving long-distance transmission using signal modulation techniques. They may also find application in maritime communication networks in the estimating of the channel conditions. However, their performances will be limited and unstable in these communication networks since the power of the transmitting sensor aggregated CH-information is low. Thus, there is a need for the development of suitable CE methods in the estimation of the behaviour of maritime radio environments that will offer more system stability to the marine sensor-based systems for the performance improvement of the QoS and QoE in nautical radio networks. In this thesis, the CE performances of a linear-based technique named inter-symbol interference/ average

noise reduction (ISI/ANR) CE and an adaptive method named reweighted error-reducing (RER) CE for estimating the CIR of nautical radio networks is proposed and evaluated in comparison to some existing classical methods (that are either classified as linear or adaptive as elaborated in Chapter 4) for reinforcing the QoS and QoE requirements of ocean-faring users. For the proposed ISI/ANR technique, possible effects of ISI that can occur during channel transmissions are considered, where the use of lowpass filters is adopted for mitigating the channel noise effects and multipath propagation. In the proposed RER method, the Manhattan distance of the CIR obtained from conventional RLS method is normalised after which a variable leakage factor is introduced to control a log-sum penalty function whose undertaking is to offer system stability to the proposed adaptive estimator over other considered traditional techniques. Moreover, we introduce a reweighting attractor to further shrink the CE error in order to offer substantial mean square error (MSE) advantage to the RER estimator over all other analysed estimators. To end, the QoS requirements of pelagic communication networks are eventually analysed and documented in terms of network data rate, outage probability and QoS-guaranteed probability at different ranges of SNR values when different numbers of directional antennas (DA) are deployed.

The reminder of this Chapter is structured as follows. The problem statement attributed to this research is mentioned and concisely presented in Section 1.2 where the context of the research problem and research gaps are identified and synoptically discussed. In Section 1.3, a summary of research objectives and research questions are given thereafter, the research hypothesis and approach is reported in Section 1.4. Furthermore, the research goals and contributions are respectively recorded in Section 1.5, 1.6 and 1.7 while the delineation and limitations of this research is documented in Section 1.8. Finally, the thesis overview is presented in Section 1.9.

1.2 PROBLEM STATEMENT

In the exploration of marine environments, oceanic investigation and extraction processes such as fishing, oil & gas drilling, snorkelling, scuba diving, sailing, rafting, and wakeboarding etc, are confronted with countless challenges ranging from environmental degradation, traffic clearance delays, congestion and insecurity issues etc. The objectives of the aforestated nautical exploration activities can be enriched by incorporating the IoT technology and CE methods where sensors are embedded on marine user equipment (MUE) with the intention of providing oceanographic information for useful

decision-making procedures. The CE techniques could be deployed to enhance the limitations of wireless sensor networks (WSN) since the sensor nodes that constitute the IoMT technology have ample transmission capabilities and battery life. These methods can considerably mitigate the above-listed challenges of marine explorations. In this study, the context of research problem and gaps are respectively presented in Section 1.2.1 and 1.2.2.

1.2.1 Context of the problem

As mentioned, marine explorations can take the brunt of surrounding limitations such as ocean degradation, complication of traffic management and security/safety issues. Other significant objections currently experienced during marine exploration activities include wide area network coverage and cost-effectiveness [3]. If the above activities should deploy marine user security, then there is a need to develop efficient and cost-effective communication systems for maritime operations. Although satellite communication systems are designed to offer marine users wider network coverage during explorations, they are not known to be cost-effective and deploying them for maritime networks can be exceptionally expensive. As such, developing simple and cost-effective WSN for ocean-going explorations is necessary with the intention to improve the QoE of thalassic users.

The use of sensor networks in marine communication networks results in the formation of an acceptable low-cost communication system. Nevertheless, the transmission of information across the IoMT network can experience adverse effects of multipath propagation and Doppler spread since the transmitting sensor information is characterised by low transmission power. In other words, in small scale fading environments such as that of marine explorations, broadcasting signals can be affected by the undesired effects of saltwater signal phenomena such as multipath propagation and possible shadowing. These may arise due to profound environmental conditions like extreme temperatures, unstable weather conditions including snowfalls, torrential rainfalls and fogs etc, in addition to deep-ocean waves, unstable ship movements and shore side highlands such as mountains, plateaus, trees and sea valleys. Thus, the line of sight (LoS) transmission path could be obstructed and several channel models that have been designed in application to terrestrial communication networks which considers both LoS and non LoS (NLoS) path propagation can find application in the marine networks for the evaluation of the worst case scenario. However, in broadband terrestrial communication systems, the message to be sent across the wireless channel is prepared with more signal strength and robustness against the

adverse effects of channel conditions through modulation techniques where the information signal is enveloped onto a carrier frequency signal. This modulation method can improve the transmitting power and reception quality of the travelling information even though they could still experience limited effects of attenuation from environmental obstacles. Because the sensors deployed in maritime wireless communication networks transmit under low power condition, there is a need to develop methods that will efficiently enhance the quality of the IoMT communication systems since the transmitting information are highly vulnerable to the effects of attenuation. To alleviate these challenges, there is a further need to develop efficient telecommunication techniques that will take into consideration, the effects of all unwanted environmental scenarios mentioned above so as to realise quality transmissions in marine networks for adequate decision-making procedures. One such technique is CE, where the behaviour of the channel can be predicted for the sake of improving the QoS and QoE requirements of maritime users. Here, the receivers approximate the CIR of the CH propagating information through the use of short preambles in furtherance of guaranteeing accurate signal reception. In this thesis, novel CE methods that significantly improve the system stability and QoS performances of nautical radio networks (in terms of data rate and outage probability) is designed.

1.2.2 Research gap

At present, only a few research works in the literature have considered enriching the experiences of nautical communication systems in an effort to improving the QoS and QoE requirements of hydrographic explorers. As a result, a lot of works need to be carried out in the maritime industry in a manner that the consequences of global trade barriers, marine explorations and pernicious economic losses would be alleviated. The utilization of state-of-the-art network technologies such as software-defined networking (SDN), network function virtualization (NFV), narrowband IoT, edge and cloud computing, artificial intelligence, machine learning, serverless and quantum computing etc are not well considered for enhancing the operation of marine networks. Developing novel techniques, for instance, energy-efficient and energy-balanced routing protocols for nautical radio networks in addition to developing acceptable CE methods for saltwater communications is still an open research gap for the operation of IoMT-configured operations. In this thesis, two novel CE methods named ISI/ANR and RER techniques are developed for improving the QoS and QoE of midwater explorers.

1.3 RESEARCH OBJECTIVE AND QUESTIONS

This research aims to address the limitations of WSN transmissions over maritime communication systems using CE techniques for improving the QoS experience of maritime networks. As such, the research objectives and questions are highlighted as follows:

1.3.1 Research Objectives

Thus, the research objectives of this study are mentioned as follows:

- To design an IoT-based framework for improving the QoS requirements in application to maritime operations and management.
- To design and develop novel CE methods for improving the quality of nautical radio network transmissions.
- To verify the system design through computer-based simulations and numerical analysis where the proposed CE methods are validated in terms of MSE whereas, the QoS requirements for pelagic communication systems are evaluated in terms of system data rate, outage probability and QoS-guaranteed probability.

1.3.2 Research Questions

The research questions to be addressed are grouped into main research questions and sub-research questions presented as follows:

1.3.2.1 Main Research Questions

The main questions to be addressed in this research are listed as follows.

- Can CE techniques be developed to enhance the QoS and QoE of maritime radio Networks?
- How will mercurial ambient conditions affect the transmission quality of navigational communication networks?

1.3.2.2 Sub-Research Questions

Five sub-research questions that partly address the main research questions are itemised as follows:

- How do adaptive CE schemes perform in comparison to their linear counterparts for nautical radio networks?
- How well does the proposed RER technique perform in contrast with other considered adaptive and linear estimators for the IoMT?
- Can the proposed ISI/ANR estimator offer significant performance improvement over other linear methods such as LS, LMMSE and maximum likelihood ML-based CE for the IoMT?
- What is the data rate of a naval radio network when the aggregated CH information travels at various levels of SNR over line of sight (LoS) and non-line of sight (NLoS) channel conditions?
- How will the system outage probability be affected in a maritime radio system when CH signals are transmitted over Rayleigh and Rician fading channel environments?

1.4 HYPOTHESIS AND APPROACH

1.4.1 Research Hypothesis

Due to the requirements for a cost-effective nautical communication network that will provide wider and efficient network coverages to improve the QoS and QoE of deep-ocean explorers, there is need to develop state-of-the-art network technologies based on IoT that will improve the production output of marine explorations.

Accurate CE techniques are generally known to enable wireless communication networks by assisting the receiver side to substantially approximate the CIR of general communication systems. This research also attempts to deploy the use of CE for improving the QoS and QoE of maritime radio networks where an adaptive and linear method is proposed for improving nautical communication networks over the performances of other customary techniques in a maritime radio network. Hence, the hypothesis for investigation in this research is stated as:

- Adopting accurate and stable CE methods in nautical radio networks can result in a considerable increase in the QoS and QoE of marine users during explorations of the maritime environment.

1.4.2 Research Approaches

The following approaches were adopted to address the research questions and hypothesis of this study.

- Intensive literature study to identify contemporary technologies applicable in the IIoT particularly in the maritime sector in addition to finding research gaps in the field of study.
- Comprehensive literature survey of CE techniques and existing research opportunities for supporting the QoS and QoE of marine users in the IoMT.
- Design and development of a pragmatic IoT-enabled framework for maritime explorations.
- Design and development of two novel CE methods for improving the quality of nautical radio network transmissions and reception so as to improve the production output of maritime explorations.
- Formulation of carefully designed mathematical models and sequential procedures for realising the proposed CE schemes in comparison with classical methods for nautical radio networks.
- A comparative performance analysis of proposed estimators in comparison with orthodox linear and adaptive methods through computer-based simulations using MATLAB programming language.
- Evaluation and documentation of the QoS requirements of pelagic communication systems in terms of outage probability and network data rate assuming LoS and NLoS communications.

1.5 RESEARCH GOALS

The goals of this research are presented as follows:

- To develop novel CE methods that will improve the QoS and QoE of marine radio networks.
- To evaluate the QoS performances of nautical radio networks in terms of network data rate and outage probability under heavy frequent and light infrequent fading environments.

1.6 RESEARCH CONTRIBUTION

The contributions of this research work are listed as follows.

- Development of a comprehensive literature review of the applications of IoT technology across industrial activities particularly in the maritime sector is presented in Chapter 2.
- An IoT-based framework is designed in Chapter 4.2 for improving the QoS requirements in application to maritime operations and management where off-shore navigating vessels are equipped with environmental sensing equipment in communication with a cluster head user equipment that transmits aggregated seawater sensor information via the marine channel to a shoreward located central BS.
- Development of two novel CE techniques is presented in Chapter 4.3 for improving the performances of maritime communication systems named RER and ISI/ANR CE that both attempt to improve the performance of conventional schemes such as ML-based estimation and RLS techniques in order to reduce the CE error of the maritime communication network using combinational techniques that involve summing the instantaneous square error with a log-sum penalty which is subsequently realised by the normalisation of the Manhattan distance of the system CIR. Additionally, a simple step by step procedures for deriving our considered marine estimators is elaborately documented for the benefits of intending readers.
- Evaluation of the QoS performances in terms of system data-rate, outage probability and QoS-guaranteed probabilities is documented in Chapter 5.3 for improving nautical user QoE over signal transmissions in both heavy frequent and light infrequent shadowing conditions of oceanic signal propagation.

1.7 RESEARCH OUTPUT

The research output from this study primarily focuses on the application of IoT across the industrial sector. The main sectors considered are the maritime and the agriculture industries. Thus, the research outputs from this study are listed as follows:

- O. E. Ijiga, R. Malekian and U. C. Okonkwo, "Enabling Emergent Configurations in the Industrial Internet of Things for Oil and Gas Explorations: A Survey, *Electronics*, vol. 9, no. 8, pp. 1-34, 2020.
- O. E. Ijiga, R. Malekian and U. C. Okonkwo, "Performance Analysis of Nautical Radio Networks based on Channel Estimation and QoS Provisions for the Maritime IoT, in *IEEE Internet of Things journal*, pp. 1-30, 2020 (Submitted).
- E. Botha, R. Malekian and O. E. Ijiga, "IoT in Agriculture: Enhanced Throughput in South African Farming Applications," *2019 IEEE 2nd Wireless Africa Conference (WAC)*, Pretoria, South Africa, 2019, pp. 1-5.

1.8 DELINEATION AND LIMITATIONS

The application of IoT technology for improving the production outputs and also for safeguarding marine lives and properties is poorly considered as observed from the intensive literature studies of this research work. Initially, obtaining articles that could serve as a benchmark to validate our research questions and hypothesis was difficult since, only very few works have considered deploying IoT in the creation of smart oceans. Accordingly, the works in [3, 4] then provided the much-required foundation to build the research hypothesis of this study. Therefore, as a direction of future works, a pragmatic test-bed in a naturalistic marine environment can be carried out, where simulations can be evaluated in comparison to experimental data for the IoMT. In this testing, both software and hardware tools can be adopted. Thus, the benefits of open-source traffic monitoring applications such as Wireshark and Tcpdump can be exploited in the design of IoMT software testbed while signal integrity check and transceiver emulators like digital storage oscilloscope and software-defined radios (SDR) in addition to security testing, measurements and analysis, and network management modules like wi-Fi enabled micro-controllers and programmable logic controllers, etc, can be deployed in the development of the hardware testbed of IoMT networks.

1.9 OVERVIEW OF STUDY

The remaining Chapters of this Thesis are organised as follows:

Chapter 2 gives a fundamental review of IoT applications in industrial environments. It further narrows down this application to the maritime sector which is the primary focus of this study. Furthermore, an overview of SDN and ubiquitous computing technology is presented for enabling EC across the maritime industry particularly for oil & gas explorations. In Chapter 3, the mechanism of signal propagation across the wireless channels is expatiated where the elementary concepts of multipath propagation and fading in terrestrial and maritime environment are explicitly described. The underlying concepts of CE are expressly documented in this Chapter where the mainstream estimators (adopted to evaluate against the proposed estimators) are outlined. A framework of the considered IoT-enabled maritime environment is presented in Chapter 4 after which the formulation of the network model is described in details given elaborate mathematical descriptions. Then, the proposed CE techniques for improving pelagic communication networks are described in details. Likewise, a comprehensive analysis of the QoS requirements of pelagic communication networks is expounded in this Chapter. In the proceeding Chapter 5, results obtained from simulations are analysed and documented for the proposed CE schemes in addition to the evaluations of the QoS provisions of nautical radio networks. Finally, in Chapter 6, valid conclusions are drawn from this research work that authenticates our research hypothesis and answers the questions drawn from this study. Future research directions are also then highlighted to conclude the Chapters of this thesis.

CHAPTER 2 AN OVERVIEW OF IoT IN INDUSTRIAL APPLICATIONS

2.1 INTRODUCTION

Many researchers have suggested different definitions for IoT in literature. Two concise and important definitions of IoT are presented in [5]. IoT is defined in this article as an interaction between the physical and digital world where these interactions (physical and digital world interactions) are made possible using a plethora of actuators and sensors. It further defines IoT as a paradigm that embeds computing and networking in any kind of conceivable object where devices and appliances are connected to collaborate with one another in order to achieve some complex task that requires very high degree of intelligence.

In modern-day communication technologies, computing devices such as desktop computers, laptops, palmtops, servers, smartphones etc are interconnected to communicate with one another over the internet. The concept of IoT tries to incorporate non-electronic everyday objects such as household appliances, clothing, buildings, roads, vehicles, food etc in such a manner that they can communicate with one another and with the internet by the use of some embedded sensors, actuators and microprocessors [6–11] . It is documented in [12], that the number of connected things to the internet currently exceeds the number of people living on the planet. It is also mentioned that the number of things (or devices) connected to the internet in 2003 is 500 million whereas, the population of the world is estimated to be 6.3 billion people in same year. Furthermore, the Cisco internet business solutions group (IBSG) predicted (in 2011 as documented in [13]) that the number of internet connected devices will rise to about 50 billion by 2020. Presently, John Chambers, the former Cisco chief executive

predicts that this number will rise to 500 billion by 2025. This will consequently result in higher revenue opportunities for internet service providers and mobile network operators.

IoT can be adopted for a large number of applications such as smart homes, health care/fitness, smart cities, social life/entertainment, smart environment, agriculture and industries [14–16]. The benefits of IoT can be exploited in the industries so as to yield higher through-put and maximize gains [17, 18]. This application of IoT technologies for enhancing the safety of lives and properties as well as for increasing production output in the industrial sector gives birth to the concept of Industrial Internet of Things (IIoT). The oil and gas industry is faced with numerous challenges. One of the major challenges of this industrial sector is the speed and efficiency of drilling operation processes. For this challenge to be effectively addressed, the use of contemporary and autonomous technologies can be deployed to boost oil exploration procedures in addition to speeding up other internal operations. Consequently, the benefits of EC are propounded in this thesis for enhancing the processes of business interactions in the oil and gas industry. Furthermore, this chapter presents a state-to-the-art review and classification of IoT-based technologies for enhancing the throughput in the stages of industrial operations. More so, EC can be adopted for dynamically approaching and engineering IoT systems. It is described as “a set of things with their functionalities and services that connect and cooperate temporarily to achieve a goal" [19]. As aforementioned, EC is propounded for managing oil and gas spillages in maritime environments during offshore oil and gas explorations.

The rest of this chapter is structured as follows. Section 2.2 presents a brief review of the concept of IoT while an overview of IIoT is presented in Section 2.3. The application of EC in combating oil and gas emergencies for offshore maritime hydrocarbon exploration is propounded in Section 2.4 whereas the conclusions from this research presented in Section 2.5.

2.2 INTERNET OF THINGS: APPLICATIONS AND EMERGING NETWORKS

The paradigm of IoT involves equipping everyday objects with identifying, sensing, networking and processing capabilities that enable the objects to communicate with one another and with other devices and services over the internet in order to solve a particular task [12]. In this section, an overview of IoT applications in contemporary communication networks is briefly discussed.

2.2.1 Overview of Internet of Things Applications

The importance of the features of IoT technologies in human lives cannot be overemphasized. This technology (IoT) is essential for building smart societies, enhancing the throughput of industrial processes and for boosting security systems as summarized in Figure 2.1. In smart society applications, IoT is employed for building smart homes, smart offices and intelligent environments, where sensors embedded devices are deployed for efficient management of public assets and resources. Additionally, IoT technology is useful for urban management, where information and communication technology (ICT) models are brought into service for addressing the ever-growing urbanization challenges. In IoT urban management applications, electronic data collection sensors are employed for improving the quality of life. This is achieved by the transmission of information using wireless and cloud-based technologies in order to enhance business transactions and influence better daily decision making processes by the citizens living across municipalities.

It is briefly mentioned in Section 2.1 and 2.3 that the benefits of IoT can as well be exploited to boost the production of industrial output in addition to protection of industrial lives, properties and environment. The manufacturing, transportation, healthcare, energy and food production sector of an economy are prominent industries that exploit the benefits of IoT technologies as summarized in Figure 2.1, where smart sensors are deployed to monitor environmental conditions. The manufacturing industry comprises of automotive industries, consumer electronics and pharmaceuticals etc. Additionally, IoT applies to the transportation industry with specific reference to aviation, smart car production, smart parking, 3D assisted driving and traffic congestion management. Home healthcare, hospital management, electronic health (e-health) and mobile health (m-health) are all examples of IoT applications in smart healthcare industries while smart grid and lightning are applications of IoT in smart energy environments. Lastly, smart farming can be employed in both plant and animal food production industries such as agriculture and aquaculture [20, 21], where individual animals and plants are monitored using smart electronic sensors that provide information of their location, environmental and health condition. Smart sensors and actuators can also be used to control agricultural equipment and pumps while regulating environmental conditions such as temperature, pressure, chemical levels of the soil and humidity. This present-day technology (IoT) can also find application in the oil and gas sector. In this thesis, the application of IoT in offshore oil and gas exploration using the concept of EC is propounded for future development as documented in Section 2.4.

The concept of IoT generally finds pragmatic applications in security systems. End to end security scheme is an essential rumination for implementing IoT technologies. It is worthy to mention that IoT devices can be expertly coded to offer enhanced integrity and confidentiality of the transmitted messages. Methodical end to end encryption on devices, networks, and cloud infrastructures can prevent hackers (or attackers) from unauthorized access to user information (or properties). Furthermore, professionally programmed IoT-based software applications in sensor embedded computing devices can be exploited to enhance the operation of IoT-based systems. The implementation of these well-organized security sensor devices find use in home automation, industrial machine-to-machine (M2M) communication, electronic wearables and smart energy grids e.t.c., for device tracking and monitoring. On the other hand, cyber-physical-social (CPS) computing involves the processing of data/knowledge obtained from the CPS world for the integration, correlation, interpretation and provision of relevant abstractions to individuals for meaningful decision-making [22–24]. Also, CPS systems (CPSS) consists of the interaction between the cyberspace, physical space, human knowledge, and sociocultural elements for meaningful decision making. The importance of CPS security cannot be overemphasized in cyber-physical systems. CPS security is required to mitigate the security vulnerability of cyber-physical systems such as intelligent transportation systems, healthcare, smart grid and so on against unlicensed users. The IoT technology can be exploited in the defense sector to stimulate/enhance the economic growth and public safety of any nation, where sensor embedded surveillance devices and other electronic wearables are employed for motoring/tracking defense equipment, aircraft maintenance/ operation, crime detection and public protection as well as rapid response to other emergency services. Aerospace comprising of commercial and military aviation and use of unmanned aerial vehicles (UAV) are also prominent areas where the benefits of IoT is exploited to aid security and defense of citizens which proportionally foster economic growth of the nation.

To improve industrial productions, the benefits of IoT has been exploited in manufacturing industries such that smart factories are built using cyber-physical technologies. The authors in [25] propose an IoT-based hierarchical architecture for smart factories, where key technologies such as IoT, big data and cloud computing are used to enhance industrial productions. Contemporary research works have also reviewed the benefits of present-day IoT-enhanced technologies such as blockchain, software define networking (SDN) and network function virtualization (NFV) for IIoT applications as documented in [26–31]. Furthermore, numerous IoT-based technologies have been proposed for improving the output of industrial operations in the transportation, health care, smart energy and agricultural sector in particular. For more information on recent research works in the aforementioned IoT applications,

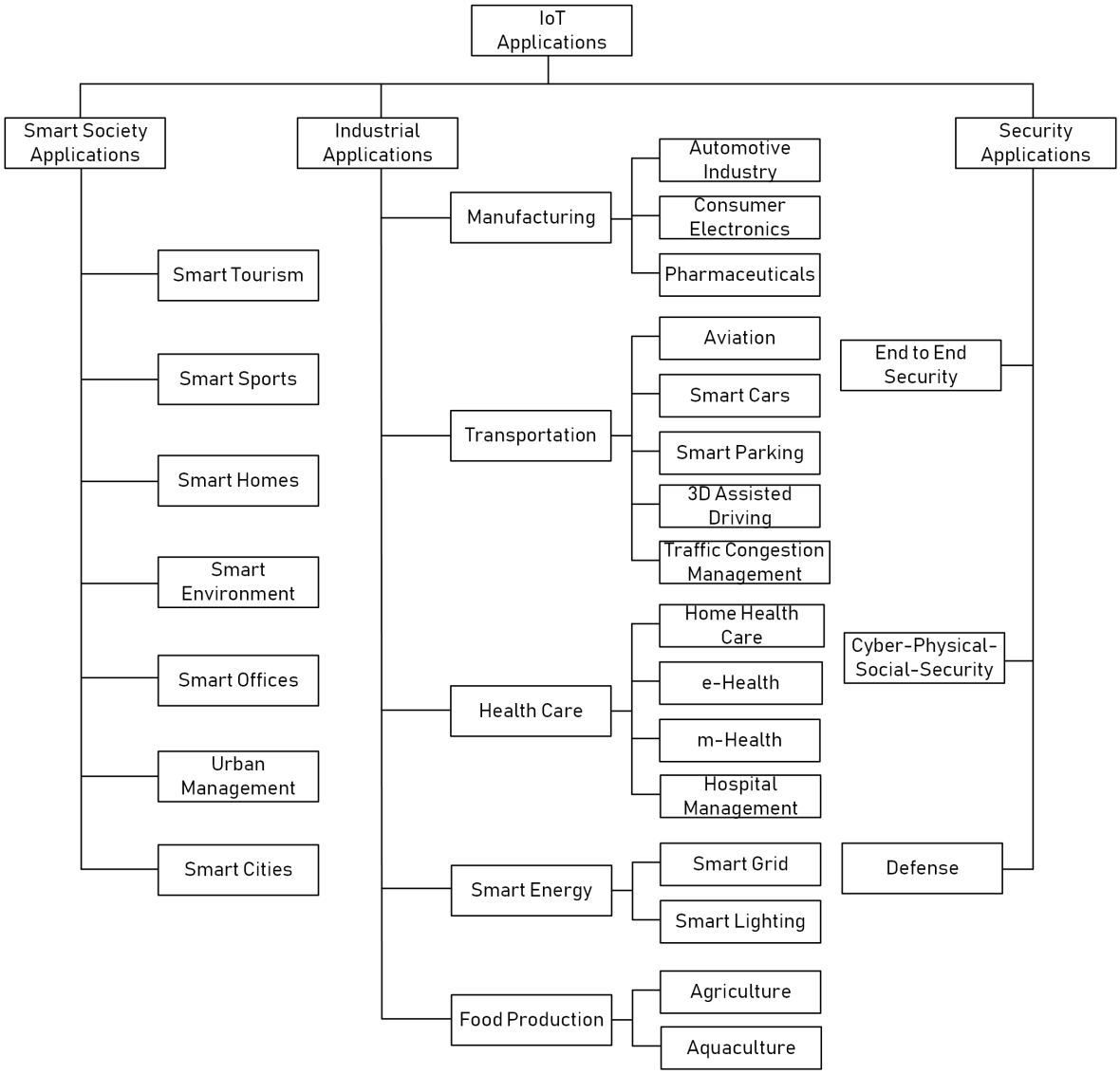

Figure 2.1. Summary of IoT Applications

interested readers are referred to [32–43].

2.2.2 Internet of Things and Next Generation Networks

The current 4G/LTE networks in comparison with the previous generation of networks is designed using CP-OFDM technology to specifically offer higher data transmission rates in addition to enhanced system capacity due to the high demands for the sparely available radio frequency spectrum. As earlier mentioned, it is estimated that the number of internet-connected devices will exceed 50 billion by 2020. Hence, it is required that contemporary network technologies having the capabilities of offering higher

data rate applications, ultra-low/reliable end-to-end latency, very high reliability/scalability, improved security features in addition to low power consumption capacity be developed so as to enhance the QoS delivery in addition to the QoE requirements of network users . As such, next-generation (xG) networks are carefully designed to meet the above-mentioned fundamental requirements. It is important to note that the emerging xG network is the fifth generation (5G) network of technologies which are designed to offer about $10-100$ times higher data rates in addition to lower energy consumptions as compared to the current LTE-based networks. Consequently, about 10 enabling technologies have been proposed as promising air interface for realizing xG networks [44]. These technologies include SDN, NFV, massive multiple-input multiple-output (MIMO), radio access techniques, mobile cloud computing, millimetre-wave communication, IoT, device to device (D2D) communications, green communications and ultra-densification. 5G networks generally possess the capabilities of managing and supporting the high demanding requirements of D2D-based IoT communication applications by integrating numerous heterogeneous access technologies for seamless connectivity of devices/objects with the internet. Interested readers are referred to [45–50] for more information on applications of IoT for xG networks.

2.3 INTERNET OF THINGS IN INDUSTRIAL APPLICATIONS

The concept of IoT can be deployed in the manufacturing sector to boost production efficiency and reduce manufacturing cost without compromising the quality of the industrial products. IIoT [51] involves the deployment of the concept of IoT and its technologies in industrial systems such as small-scale and automobile manufacturing sector, transportation, medicine, and logistics systems. Adopting the IoT concept in industries and smart factories offer several operational benefits such as test time reduction and calibration, production downtime minimization, warranty cost reduction, improved yield, quality and supply chain efficiency as well as the performance of predictive maintenance [52–54]. In this section, a review of IIoT is presented. In addition, findings from recent research works in the area of IIoT as documented in the literature are summarized and illustrated in Table 2.1. To sum up this section, recent research efforts made particularly in the maritime industrial IoT is documented in session 2.3.2 and summarised in Table 2.4.

2.3.1 Review of Contemporary Research Developments in the IIoT

The privileges of wireless sensor networks (WSN) technology as earlier-stated, find rewarding applications in the industries in what is termed IIoT. The numerous benefits of this technology can be exploited in a considerable number of industries such as the fire industry, manufacturing, power generation and transmission industry, security systems etc [55]. Some neoteric findings have been made for use of WSN in IIoT and are discussed as follows.

An update of research trends and challenges in the fire industry are summarized as reported in [56]. A service-oriented architecture (SoA) for fire IoT consisting of four layers namely sensing layer, network layer, service layer and interface layer is also presented in this chapter. The importance of IoT in the fire industry cannot be overemphasized as fire security technologies offer warning information to industry owners, security agencies such as police and fire brigade services as well as other emergency management services for the safeguarding of lives and industrial properties. The timely fire information provided by the IIoT technologies can be used to alert occupants/workers to minimize the occurrence of injury, destruction of properties and possible death that may arise from fire emergencies. The fire IoT is designed to integrate several devices which are equipped with identification, sensing, processing, communication and networking devices for the minimization of fire disaster in the industry. Furthermore, IoT technology can be employed in the industries for check-mating the disastrous effects of fire explosions through the fusion of correlated sensor measurements. This IoT-based fire detection technique is achieved by fusing sensor data connected between nodes. As such, a data fusion fire detection method consisting of the fusion of temperature and relative humidity smart nodes is proposed in [57], where the correlation of both temperature and relative humidity sensors are resolved using copular theory. The performances of the proposed sensor fusion-based scheme are compared with existing techniques such as conditional independence sensor scheme and bivariate Gaussian method as proposed in [58]. Results obtained demonstrated that the copula-based detection scheme enhances the performances of local detection across nodes in a significant manner in comparison with the compared schemes. Interested readers are referred to [57, 59, 60] for further reading on copula functions.

In [61], the concept of IoT is adopted for environmental monitoring under the aid of robotics where the robots are designed to move autonomously while interacting with the environment. A good example of an IoT-aided robotic system is a self-driving car [62]. In this article, an experimental test bed is

Table 2.1. Summary of research trends in the IIoT.

Reference	Aim of research	Technological Approach	Methodology	Contributions	Conclusions
[54]	To address the key distribution challenges of end-to-end private key cryptography using BYOK principle based on NFC technology in order to enhance the protection and confidentiality of transmitted data in IIoT environments.	Transfer of generated key materials using NFC technology between devices with use of authenticated encryption (AE) for cryptographic protection of transferred data.	A prototypical implementation of end-to-end encrypted data transfer using Nexus S smart phone installed with Android 4.1.2 Jelly Bean.	Development of key generation technology using BYOK principle based on the trustworthiness of devices and operators.	The developed BYOK prototype demonstrated robustness against external effects that may occur due to adding more interfaces into manufacturing devices.
[56]	A review of current research trends, industrial challenges, technologies and application of IoT in industries for fire disaster management.	Use of low power and low cost multiple sensor nodes for WSN-based fire detection and elimination applications in industries.	Extensive literature review.	• Development of a four-layered IoT-based SoA for industrial fire disaster management. • Description of issues/challenges in the fire industries.	IoT-based devices can be deployed for automated monitoring, management, control and maintenance of fire disaster occurrence/equipment in industrial applications.
[57]	Minimization of fire accidents using IoT-based technologies in the fire industry.	Use of fused sensors that are integrated based on copula theory.	Fusion of temperature and relative humidity sensors for fire detection and use of a fusion center for integrating all network node decisions in order to enhance final decision making.	Development of a novel fire detection method based on copula functions.	Copula-based detection scheme outperforms two other existing schemes when compared for local fire detection.
[61]	To investigate the characteristic performances of IoT-aided robotic aided systems for environmental monitoring.	Use of IoT devices connected to a drone (UAV) for environmental monitoring and creation of IoT network for environmental data sensing.	Extensive experimental analysis to determine the pros and cons of IoT-aided robotic systems.	• Documentation of the scientific background and interaction of robotic systems over 6TiSCH technology. • Development and documentation of experimental testbed that evaluates the operation of connected IoT devices on robotic systems.	• IoT-aided objects do not attract significant overhead as a result of onboard IoT-based equipment (e.g. mote). • Surveying and patrolling activities of IoT-aided robotic systems are achieved with good performances in terms of network joining time, packet loss ratio and data retrieval delay.
[63]	Development of an energy-efficient and robust time synchronization scheme (without isolated nodes) named R-Sync in addition to the design of a root selection algorithm for life time extension of sensor networks using energies between nodes for the IIoT.	Use of two timers where one is used for time synchronization while the other is used for connecting isolated nodes to synchronized networks.	Experimentation through computer-based simulation using NS-2 as well as experiment testbed using wireless hardware nodes where the proposed R-Sync is compared with existing synchronization schemes such as TPSN, GPA and STETS.	• Implementation and performance analysis of a novel robust time synchronization scheme (R-Sync) for IIoT. • Development and documentation of a root note selection algorithm for balancing sensor node energy consumption. .	• Results show that R-Sync consumes less energy compared to GPA and TPSN. Best performance of scheme shown in densely connected and large-scale networks. • Percentage of synchronized nodes is more in R-Sync in comparison to STETS. • Energy consumption of R-sync is more balanced than GPA and TPSN.

Table 2.1. Summary of research trends in the IIoT.

Reference	Aim of research	Technological Approach	Methodology	Contributions	Conclusions
[64]	To develop optimal ticket-based QoS routing protocol using generic algorithms for smart grid WSN applications.	Use of GA-TBR algorithm for optimal route selection among sensor nodes in smart grid WSN applications.	Use of genetic algorithms for 72 improving the initial population with high-quality outcomes which consequently improves the discovery of route selection using TBR	• Design and implementation of an efficient, reliable and low computational complexity GA-TBR algorithm for optimal route selection in accordance with a predefined set of QoS requirements using minimal probing tickets. • Evaluation of an in-depth performance analysis of GA features such as validity checking in addition to fitness function	Results obtained demonstrated that the proposed GA-TBR scheme offers 28% improvement in the routing selection path as compared to the IEEE 802.11s adopted AODV.
[65]	Design of novel SDN IIoT-based technology for resiliency support during failures or natural disturbances in smart grid networks.	Exchange of updating information with the associated SDN switches by use of OpenFlow protocol. Experimental validation of proposed SDN platform for enhanced resilience in smart grid applications using three topologies named fault detection, conventional network and network upgrading topology.	Use of SDN controller in smart grid networks for multi-functionality control and optimal performance using real-time data monitoring.	• Development of SDN platform for industrial real-time data energy profiles dynamic route establishment for grid control in smart grid IIoT networks. • Evaluation and documentation of different topologies for re-routing data among SDN switches in smart grid applications.	• The network upgrading topology demonstrated lower end-to-end latency at all interval of time in comparison to conventional network topology which offered lower latency as compared to fault detection scenarios. • Network upgrading scenarios offered highest data flow traffic at various time intervals in comparison to other scenarios. • The dynamic end to end route can be achieved within tens of milliseconds.
[66]	• To review fog computing infrastructures and protocols in application to IIoT. • To identify IIoT challenges and proffer working solutions to the mentioned.	Description of routing protocols, resource allocation methods and load balancing for fog computing in application to IIoT.	Description and classification of fog computing technology in particular application to sensor enhanced industrial operations.	• Review and documentation of state-of-the-art techniques in application to fog computing technology for enabling IIoT. • Comprehensive classification of the "industrial revolution" theory in relation to enabling IIoT. Furthermore, the discussion of elaborate open research domains with respect to fog computing as an enabler in application to IIoT is presented.	• The fog computing technology gives an alternative platform for controlling, computing, managing and storing IIoT devices in comparison to cloud computing techniques. • Fog computing will enhance sensor supported industrial operations when integrated with efficient communication technologies such as SDN, NFV, 5G, and CPS systems.

developed consisting of an IoT device that is connected to an UAV (commonly known as drone) which executes a monitoring mission around a specified area having an IoT network for the exploration

of environmental data. In general, robotic networks consist of many robots working together in a collaborative manner, where the robots are equipped with sensing, computing and communication devices in order to enhance the exchange of information over a communication network so that a particular task can be effectively accomplished. Results obtained from this work [61] (which can be developed further in larger-scale environment) shows that onboard of IoT equipment to the UAV does not incur significant overhead while the overall QoS expressed in terms of data retrieval delay, network joining time and packet loss ratio satisfies the requirements of this experiment.

In industrial wireless applications, a robust time synchronization scheme is required for efficient exchange of information and data processing. The synchronization schemes are necessary to enhance the collaborative coordination of the wireless sensor nodes in order to accomplish some useful task for the industrial environment. A good number of time synchronization schemes have been presented in literature for achieving high accuracy and productivity in IIoT systems. Pair broadcast synchronization protocol (PBS), group pair selection algorithm (GPA) and spanning tree-based energy-efficient time synchronization (STETS) [63], are few examples of time synchronization schemes for IIoT as documented in literature. In [63], a robust time synchronization scheme named R-sync is proposed for distributed systems in IIoT that adopts two timers for timing synchronization using two-way message exchange synchronization. A root node selection algorithm is also presented in this article [63] for balancing the energy consumption of connected sensor nodes and for extending the lifetime of IIoT networks. It is noteworthy to note that energy consumption and accuracy are crucial consideration points to bear in mind when designing time synchronization schemes because the energy of sensor nodes are usually limited. The performances of the proposed robust synchronization scheme (R-sync) is compared with three existing time synchronization schemes including GPA, STETS and timing-sync protocol for sensor networks (TPSN) using NS-2 simulation tool as well as experimental-based evaluation using wireless hardware nodes. Results obtained demonstrated the superior performance of the proposed R-sync time synchronization scheme in comparison to GPA, STETS and TPSN. From the results obtained, all nodes were synchronized with greater energy-efficiency hence, the proposed R-sync algorithm demonstrated better timing synchronization in comparison to other synchronization schemes. The number of broadcast messages using R-sync, GPA and TPSN algorithms are compared together in the experiment using different communication range for the entire network, where 240 different sensor nodes are deployed in a random manner over an area. The number of broadcast message is need for analysing the energy-efficiency of an algorithm as propagating messages require maximum consumption of energy during the life time of a node. Further results obtained from the

experiment showed that as the communication range increases, R-sync requires a much lower number of broadcast message in comparison to other analyzed synchronization algorithms. The number of broadcast messages are also compared with different number of sensor nodes assuming R-sync, GPA and TPSN with each node set to a communication range of 85 m. The results obtained demonstrated that R-sync offered the least broadcast messages while increasing much slower in comparison to GPA and TPSN. Based on these results, it can be concluded that the energy consumption of R-sync is much lower than other compared synchronization algorithms especially in large-scale and densely connected IIoT systems.

The IoT technology also finds beneficial applications in the power generation, power transmission and power distribution industries in application to wireless sensor network (WSN)-based smart grid. A smart grid can simply be described as a fast-emerging and next-generation electricity grid technology that aims at enhancing the efficiency and reliability of the present conventional electric power grid infrastructures through the use of contemporary WSN-enhanced communication technologies for the efficient controls and automation of power grid systems. Since the demand and supply of electric power are designed to be automatically controlled using a two-way communication system in smart grid WSN applications, there is an enormous necessity for developing energy-efficient and energy-balanced routing protocols that will coordinate the transmission and reception of electric power for enhanced reliability and efficiency in electric energy consumption. As a result, a ticket-based routing (TBR) optimization using a genetic algorithm is developed for smart grid applications in [64]. Furthermore, a genetic algorithm is used to minimize the overhead of discovery messages in addition to minimizing the number of tickets. This is aimed at developing a novel GA-TBR protocol for optimal selection of routes in WSN smart grid environments. Results obtained showed that the GA-TBR algorithm could select optimal routes with minimum possible delays. More so, a 20% performance improvement is observed when the GA-TBR protocol is compared with the existing IEEE 802.11s (wireless LAN standard for mesh networking) ad-hoc on demand distance vector routing (AoDV) protocol. Additionally, the concept of SDN is adopted in [65] for IIoT in the context of smart grid infrastructure, in order to meet the high demands of seamless data transmission during critical events such as natural disturbances or system failures. SDN is a useful technology adopted to enhance the application of IoT in the industry by providing dynamic reconfiguration for the improvement of data network robustness. A new SDN platform is proposed in this paper for IIoT systems in order to support resiliency by reacting immediately whenever a failure occurs. This is fore the recovery of smart grid networks using real-time monitoring techniques. In order to achieve multi-functionality control and

over come the challenges of optimization by operators, an SDN controller is adopted for providing real-time data monitoring in order to manage demand and increase system reliability and resources. The proposed IIoT SDN platform uses a three layer controller namely; infrastructure layer, control layer and application layer. The physical layer carries all physical equipment and hardware components for route switching performance between the network clusters and SDN switches. The devices contained in this infrastructure layer include smart sensors and actuators, demand response systems (DRS), advance metering infrastructure (AMI) and field bus control. The control layer receives routing information from SDN switches whenever new traffic flows are received by the switches. In other words, it serves as an interface between the application layer and the physical infrastructure. Data path allocation procedures are then allocated by the control layer after which requested paths are processed by the assignment of new routing rules and policies in agreement with the application layer. The application layer is the top most layer of the proposed SDN platform. Services for utility authentication are managed by this layer at the back-end system where information of each service request is exchanged and delivered. Data centers, storage, servers, processing, analysis and applications all constitute the application layer of the SDN platform. Experimental results obtained from this investigation revealed that SDN controllers showed great potentials for supporting resilience of smart grids even at faulty situations. The results demonstrated that the dynamic end-to-end reroute can be realized in few milliseconds, hence SDN based IIoT systems can significantly improve grid reliability for smart grid resilience enhancement.

The bring your own key (BYOK) principle based on near field communication (NFC) is proposed in [54] for mitigating the drawbacks of end-to-end private key cryptography and factory installed keys in the IIoT systems. For confidential and relevant production information to be transmitted over the internet in industrial systems, appropriate cryptography methods [67] such as end-to-end encryption using transport layer security (TLS) needs to be employed. Asymmetric cryptography provides an end-to-end encryption method that is not feasible in large data applications. Symmetric cryptography on the other hand, can be adopted for this purpose but requires both the sender and receiver to share the same key as a direct connection cannot be established using MQTT protocols and key exchange algorithms like the Diffie-Hellman cannot be adopted. The proposed BYOK scheme in this work is used to mitigate these drawbacks where device owners can change keys needed for end-to-end encryption and NFC technology is employed for transferring key materials between devices. In this proposed method, the transferred keys using NFC technology is protected using authenticated encryption (AE) so as to ensure confidentiality, authenticity and integrity of the transmitted keys. The concept of BYOK

principle originates from the bring your own device (BYOD) concept where employees can use their own tablets, laptops, phones and computers in company networks. Two key generating scenarios are also proposed in this research work which depends on the trustworthiness of the connected devices and its corresponding operators. In the first scenario, if an untrustworthy personnel and/or device deploys keys, then the keys will be generated at the back end. The key material is then encrypted and sent to the device and the keys will subsequently be protected from extraction and use by unwanted users with the aid of the applied encryption. In the second scenario, keys are generated directly at the connected device if the personnel and connected devices are considered trustworthy in the second scenario.

2.3.2 Recapitulation of Present-time Research Trends in the Maritime IIoT

A synopsis of research progress in the IIoT is briefly presented in previous Section 2.3.1. In this section, the evolution of WSN technology in specific application to the maritime sector is discussed.

A limited number of research works have attempted to design and analyse the performances of various communication techniques, which are capable of enhancing the operation of maritime activities. As mentioned, sensors can be strategically stationed to enhance the communication performance and throughput in a variety of industries ranging from consumer electronics, healthcare, agriculture, industrial automation, transportation, construction, and maritime operations etc, for higher profit applications, environmental monitoring, offshore explorations, disaster mitigation and management, and assisted navigations etc [3,4]. Thus, sensor networks can still be adapted in the maritime industry to monitor both onshore and offshore activities where vessels are implanted with sensors to communicate with one and other in addition to a remotely controlled base station as illustrated in Figure 4.5. To guarantee the QoS and QoE requirements of marine users, many factors including the consideration of wide network coverage area in addition to deployment of cost-effective systems must be considered for the modelling and the enabling of oceanographic propagations, since maritime networks require wider signal coverages in comparison to their terrestrial counterparts. As such, the QoS requirements of over-sea users are expected to be satisfied similarly to that of other terrestrial applications. To achieve these, the propagation of marine signals may be enhanced using massive directional antennas for better user QoS experience in the maritime sector. As such, a limited number of technologies have been developed in the literature to address maritime communication systems. These technologies are subsequently discussed and summarized as organised in Table 2.4.

An appreciable amount of research works is currently advancing in different parts of the globe (especially in the Republic of Korea) where attempts are been made to improve the performances of maritime operational activities. Consequently, a variety of maritime communication projects such as digital selective calling (DSC), automatic identification system (AIS), navigation data (NAVDAT), very high-frequency data exchange system (VDES) and India project etc., have attempted to improve the QoS requirements of nautical communication networks at tremendously low cost. Nonetheless, the maximum data rate offered by the aforementioned riverine communication projects is limited in comparison to other high implementation cost technologies such as satellite communication nexus. Satellite communication systems are generally designed to offer high data rates in addition to continental communication coverages. Nevertheless, these communication systems are not well capable to efficiently support underwater communication systems and are known to habitually communicate at a significant high cost due to the launching of satellites into the orbit, where onboard antennas require stabilization. As such, geostationary orbit (GEO) and low earth orbit (LEO) satellite projects such as international maritime satellite (INMARSAT), maritime very small aperture terminal (MVSAT) systems and iridium are subsequently developed to provide remarkable wide-area network coverages for maritime operations based on their very high frequency (VHF) communication capabilities. Nevertheless, these communication systems are not cost-effective for the ever-increasing needs of marine users since they require high implementation cost to launch satellites into orbits, that require stabilizers for on-board antennas. Besides, VHF-aided terrene networks do not have the capacity to effortlessly support high data rate services due to the limited bandwidth. To provide a remarkable trade-off between the high cost of satellite communication and a acceptable system data rate, the benefits of communication systems such as WISEPORT, TRION, BLUECOM+ and maritime broadband communication (MariComm) are exploited, where the characteristics of these nautical communication projects are recapitulated as illustrated in Table 2.3 [68]. More so, Table 2.2 [69] presents additional information on the various types and main features of satellite orbits.

Since, VHF-aided terrene networks do not have the capacity to effortlessly support high data rate services due to the limited bandwidth, there is consequently a need to consider adopting cost-efficient terrestrial communication technologies such as WiFi, WiMAX, LTE and 5G to support the QoS requirements of maritime operations. Additionally, green wireless networks can be utilized as alternative sources of energy in modern-day maritime communication systems. The use of the above-mentioned technologies can significantly reduce the cost of establishing and maintaining maritime wireless networks. Thus, exploiting the merits of this technology, the energy sustainability and network throughput

for green energy-powered wireless nautical networks are evaluated in [70], where a green energy buffer is modelled as a G/G/1 queueing system in which two heuristic algorithms are developed for the optimization of network energy sustainability and throughput. The proposed algorithms show that high network throughput and energy sustainability can be achieved for green-powered wireless communications. To improve on the QoE of pelagic user applications, a WiMAX-based routing protocol named MAC-based routing protocol for TRITON (MRPT) is developed to enhance the performances of maritime network connectivity in addition to reliable delivery of propagating marine packets. This over-sea routing protocol is designed to piggyback routing information (without significant control overhead) on the WiMAX-based mesh MAC messages. It is demonstrated in this work [71] that the proposed MRPT outperforms some terrestrial multi-hop wireless mesh protocols such as optimized link-state routing protocol (OLSR), AoDV and AOMDV in terms of average packet delay, initial system delay and throughput for traffic, from vessel to onshore-positioned BS. Furthermore, the authors in [72, 73] provide an overview of network technologies that can be deployed for the establishment of reliable and resilient wireless mesh maritime communication systems while a list of challenges and key management opportunities for nautical communication networks including automation and traffic engineering management opportunities are documented in [74]. In these works, the system architecture of maritime wireless mesh networks such as integrated wireless maritime communication networks (IWMCN), nautical ad-hoc networks (NANET) and MaritimeManets are expounded while the topologies of numerous maritime multi-hop routing protocols are discussed for applications in maritime wireless mesh networks. A communication architecture is also proposed in [75] to boost the efficiency of data transmissions in coastal networks, where the characteristics of key terrestrial next-generation technologies such as D2D communications and MIMO technology is capitalized upon. The architecture consists of two parts which include; underwater and over-water sections. The underwater part is designed to collect information about underwater conditions where the collected underwater data is subsequently transmitted to the over-water network configuration that consists of a hybrid network of elements such as communication buoys, vessels and transceiver-equipped unmanned aerial vehicles (UAVs). Similarly, a wireless-based heterogeneous OceanNet architecture is proposed for improving the QoE of marine users in [76], where wireless multi-hop backhaul networks are considered for providing improved connectivity across naval ad-hoc mesh networks in addition to the extension of oceanic signal coverage areas. The throughput enhancement in this investigation [76] is achieved by designing an elimination algorithm that aims at selecting the best path from the maritime user's end device, where the quality of communication links that constitute the network is analysed using signal to noise ratio (SNR) and extended transmission count. The developed path selection scheme

demonstrates an improvement in the packet delivery ratio. The works done in [68] further investigates the viability of high-speed maritime WSN technology based on LTE, where a testbed is developed for pelagic operations constituting the embedment of propagating oceanic vessels with marine routers so that they can easily communicate with coastal-mounted base stations and operation centres for useful decision-making procedures in the monitoring and control of surrounding marine activities. The projects embarked in this work [68] aims at designing WSN-based seawater networks that are capable of providing large volumes and varieties of data services to marine users at considerably high data rates. More so, the enhancement of the maritime communication capacity, data rate and spectral efficiency can be achieved using LTE technology such that the merits of advanced communication techniques such as MIMO and aggregation are exploited to achieve a communication coverage of about 100 km from the coastline.

Table 2.2. Overview of satellite orbits and characteristics. Taken from [77], ©2020 IEEE.

Satellite Orbit	Height Over Equator (km)
LEO: Low Earth Orbit	200 - 2000
MEO: Medium Earth Orbit	10,000 - 20,000
GEO: Geostationary Orbit	35, 786
HEO: High Elliptical Orbit	500 - 50, 000

In [78], appreciable efforts are made to support real-time and affordable internet broadband access for maritime communication systems by developing a communication architecture that offers a tradeoff between the consumption of network power and the users' communication quality. In this method, shipborne base stations are adopted for maritime operations such that a voyage-based cooperative resource allocation scheme (VB-RA) is designed for mitigating the effects of dynamic system inter-cell interference in addition to user handoff procedures for seamless QoS experiences during thalassic operations. The VB-RA scheme is designed to do shipborne BS switching for recovering blocked user vessels from link failures in addition to management of the inter-cell interference caused by overlap coverages of shipborne stations. Additionally, this allocation scheme reduces system power consumption by considering the sailing position of the farthest user vessel of individual shipborne base station as a constraint. The proposed scheme is compared with a conventional allocation scheme named dynamic traffic-and-interference aware in terms of signal interference to noise ratio (SINR), number of user ship handover and the number of hand over-related link failures. The proposed VB-RA scheme demonstrates superior performances in comparison to classical methods even when

the average power consumption of shipborne-base station is considered. Because of the demerits of satellite and cellular communication systems which include high cost and network coverage for maritime applications, marine users habitually find it difficult to connect with other vessels and people based onshore. To support better communication applications such as extended signal coverages and connectivity improvements, a wireless multi-hop backhaul network is developed in [77] by selecting the best path from marine user devices to onshore based terrestrial users. This is achieved by the elimination of quality degraded links using system signal to noise ratio (SNR) in long-range Wi-Fi networks. Furthermore, the expected transmission count (ETC) metric of OLSR protocol is adopted for determining the quality of the links between access routers in the developed ad-hoc mesh networks.

As wireless navigation between nautical vessels is required for safe operation and management of marine activities, there is every need to design and develop high-gain DAs in order to enable the extension of signal transmissions across maritime environments. As a result, maritime broadband wireless communication (MariComm) networks are deployed to extend terrestrial-based wireless network services to the ocean thereby providing high-speed internet services for marine users. To actualise these needs, a novel antenna tracking method is introduced for MariComm systems in [79] that consist of the use of multiple DA tracking modules to cover 360^0 in azimuth for the purpose of enhancing the quality of maritime communications. The designed antenna tracking module is solely brought to service for littoral systems in order to extend the oceanic communication range, improve data throughput and for reducing the DA switching times. Additionally, to achieve an improved maritime broadband coverage and efficient nautical transmission rate, a massive MIMO BS is designed in [80] by the hybridization of digital and analogue precoding in such a way that only the large-scale channel state information (CSI) at the transmitter is considered for reducing system overhead in addition to implementation complexity. This is to address the challenges of fairness-oriented precoding design through the formulation of a max-min optimization problem that is solved iteratively. The developed scheme shows improved performances in terms of minimum achievable rate in comparison to conventional precoding schemes such as full digital baseband precoding (FD-BP). A transmission mechanism that is based on block Markov superposition transmission (BMST) and spatial modulation (SM) is proposed in [81] for oceanic communications in order to improve the reliability of land-ship sea-water signal propagations based on distributed antennas. The transmission scheme (based on BMST and SM) is evaluated under Rician fading channel, where simulation results demonstrate that the proposed transmission mechanism will enhance maritime communication systems when the Rician factor is

lowered and the memory of the BMST system is increased. Furthermore, a cooperative multicast marine communication algorithm is developed in [82] based on joint beamforming optimization and relay design for extending over-sea signal coverage. The importance of relay-aided communications in the enhancement of sea-water communications cannot be over-emphasized since a wider signal coverage area can be provided for cooperative wireless networks in addition to the delivery of improved spatial diversity gain. The optimal non-convex optimization problem in this work is divided into a pair of subproblems which are solved using the feasible point pursuit successive convex approximation (FPP-SCA) approach, where an alternating optimization (AO) scheme is developed to yield near-optimal solutions for power minimization techniques. The proposed AO scheme demonstrates performances that show its superiority and efficiency in seafaring propagations since it offers considerable energy-efficiency in comparison with other existing optimization schemes.

The works in [3,4] made appreciable progress in the improvement of maritime communication systems by analysing the network performances of novel distributed antenna selection schemes which improved coastal communications using Wi-Fi and cellular links for data transmission. The author in [4] adopts the Rayleigh fading channel distribution for modelling the communication channel over signal transmissions involving various vessel-embedded MUE and the cluster head of specified vessels while the communication of the aggregated cluster head (CH) sensor information through the coastline mounted directional antenna to the remotely located cellular BS is modelled using the Rician fading channel distribution. It is important to state that this Rician distributed channel is known to be more applicable to propagation scenarios having a dominant line of sight (LoS) path between the transmitter and receiver. Finally, the works in [68] also made significant research in the marine industry by documenting state-of-the-art technical characteristics of viable high-speed maritime wireless networks, where the benefits of the fourth generation (4G) long term evolution (LTE) technology is exploited for the enhancement of network data rates over relatively large coverage areas. In addition, a testbed for the proposed LTE-maritime system as discussed in [68] is implemented, where documented experimental results show that the proposed LTE-Maritime system could be adopted as a reliable vessel-to-shore data communication network. Nonetheless, these works do not consider a systematised CE technique for enhancing maritime communication as it is assumed that full CSI is perfectly known at the receiving end of the cellular costal-mounted BS which is not always the situation in practice. As a result, the proposed systems may not optimally enhance the marine network coverage area in addition to system throughput especially in conditions where the channel experiences frequent heavy shadowing. This is because the actual CSI of the system is not well considered since the receiver detection techniques

cannot guarantee enhanced network performances. Based on the aforementioned, the need to develop efficient CE schemes in order to guarantee accurate decoding of transmitting packets over maritime communication networks is necessary considering the unstable environmental factors usually exhibited across marine habitats. To ensure the QoS requirements of marine users in addition to rendering improved QoE of nautical network users, we consider designing and evaluating two efficient CE schemes that take into veritable consideration, the actual fading characteristics of the CSI. To achieve this endeavour, the conventional ML and the adaptive RLS CE scheme are modified to improve the network performances of our developed oceanographic framework (in terms of outage probability and average data rate) for the overall improvement of maritime user QoE.

As previously mentioned, satellite communication networks are known for their high implementation cost. This stimulates the need for the development of more reliable and affordable coastal communication technologies where the benefits offered by routing protocols can be capitalized on for the operation of marine activities. For this reason, an overview of wireless mesh communication technologies and protocols is documented for maritime communication networks. Additionally, future research directions are outlined for deploying wide-area maritime wireless mesh networks. Interested readers are referred to [83] for more information in these developments in addition to the main multi-hop routing protocols established for marine wireless networks. These nautical wireless networks are designed based on the optimized link-state routing protocol (OLSR), ad-hoc on distance vector (AoDV) and ad-hoc on-demand multipath distance vector (AoMDV) protocols.

2.4 EMERGENT CONFIGURATIONS IN THE IIOT

IoT systems consist of distributed smart objects which are designed to be heterogeneous, effectively communicate with one another, autonomous, distributed, managerially and operationally independent. The concept of EC is presented in [84] for engineering the design of IoT systems. EC can be define as “a set of things with their functionalities and services that connect and cooperate temporarily to achieve a goal" [84–86]. A “thing” on the other hand, is defined as any smart connected device (or object) with its functionalities and services or applications.

Table 2.3. Summary of maritime communication project traits.Taken from [68], © 2020 IEEE.

System/Project	Communication Technology	Communication Coverage (km)	Maximum Data Rate (kb/s)	Cost
DSC-1	MF/HF	>463	0.1	Low
DSC-2	VHF	120	1.2	Low
AIS	VHF	120	9.6	Low
NAVDAT	MF	556	18	Low
VDES	VHF	120	307	Low
India Project	Low-rate Wi-Fi	52 (ship-to-shore)	3000	Low
WISEPORT	WiMAX (IEEE 802.16e)	15	5000	Medium
TRION	WiMAX (IEEE 802.16d)	14.2 (ship-to-shore)	6000	Medium
MariComm	LTE (ship-to-shore)	120	7600	Medium
BLUECOM+	IEEE 802.16e (air-to-surface)	30	5500	Medium
Inmarsat C	Geo Satellite	Global, except polar regions	0.6	High
Inmarsat GX	Geo Satellite	Global, except polar regions	50,000	High
VSAT	Geo Satellite	Global, except polar regions	46,000	High
Iridium	Leo Satellite	Global	134	High

For an EC network to be formed, operated and managed, four components must interact, collaborate and coordinate with one another. These components are user agent, emergent configuration manager (ECM), device manager (DM) and a set of things. The UA is usually an object that enables a user to express his/her goals. The UA makes interaction with the EC at runtime while the duty of an ECM is to form, operate and manage the EC at runtime in order to satisfy the goals of the user. The role of the DM in the EC is to register the smart connected devices/objects so as to ensure their connection to the internet for enhancement in communication and interaction. Additionally, the DM is also responsible for monitoring the availability of smart connected objects while informing the ECM in situations where the connected objects become faulty or are not reachable. Finally, the set of things are connected together so that they can cooperate and interact with one another under the supervision of the ECM for the actualization of the goals of the user through the formation of an EC. Based on the above description of an EC, it can be concluded that the UA, ECM and DM all constitute the logical layer of an EC network where they collaborate with one another to achieve a common user goal. Figure 2.2 presents a diagrammatic illustration of the physical and logical layer of an EC and the interactions between components that form these layers.

In section 2.2, a review of IoT architectures, technologies and applications is presented. It can be observed from the aforementioned section that IoT technologies find useful applications in industries

Table 2.4. Summary of contemporary research works in the maritime IoT.

Reference	Aim of research	Technological Approach	Methodology	Contributions	Conclusions
[68]	To develop High-speed maritime communication system based on LTE technology that is capable of supporting high data rate applications in the communication range of 100 km.	Connection of marine base stations to LTE-maritime testbed centres consisting of numerous servers, evolved packet core (EPC) equipment and entity management systems.	Implementation and performance evaluation of LTE-maritime test bed in addition to conduction of onboard experiments across South Korean sea waters.	Development of a maritime communication network architecture based on LTE technology using remotely mounted (high-altitude) multiple radio and digital units in addition to vessel embedded routers for the enhancement of nautical communication networks in terms of signal coverage and through-put.	LTE-Maritime communication networks can offer higher system data rates (in Mbps) in addition to the provision of longer network coverages in the order of about 100 km for oceanic propagations and activities.
[4]	To develop antenna selection technologies in application to maritime IoT.	Deployment of massive distributed antenna technologies for enhancing QoS-guaranteed communications during the management and operations of maritime activities.	Embedment of routers on marine vessels in addition to subsequent communication network performance evaluation considering numerous on-shore positioned directional antennas.	• Development of a user-centric communication model for marine communication systems based on distributed antennas. • Development of antenna selection schemes for coastal communication networks for user QoS enhancement.	Simulation results demonstrate that the probability of QoS enhancement in marine operations increases with increasing antenna service cloud size. It is shown that maritime operations can be enhanced using dynamic service cloud architecture consisting of accurate antenna selection methods.
[3]	To develop an antenna selection scheme for enhancing maritime IoT communication networks.	Use of MUEs and distributed antennas for communication with on-shore cellular base stations.	A variety of directional antennas are positioned to communicate between seashore base stations and vessel mounted MUEs.	• Development of a hierarchical architecture for uplink maritime radio communications. • Development of antenna selection algorithms for supporting QoS requirements in coastal networks.	The developed antenna selection algorithm is capable of complementing maritime operations by the provision of energy and cost-efficient oceanic communication networks.
[78]	To develop a maritime communication architecture capable of providing affordable and real-time broadband access by reducing the power consumption of shipborne base stations through resource allocation techniques.	• Development of a novel voyage-based resource allocation (VB-RA) algorithm for shipborne base station switching and cooperative downlink power adjustment. • Development of system architecture for serving sparse marine vessels beyond the coverage of on-shore LTE base stations for offloading the expensive satellite traffic.	• Use of voyage-based shipborne base station switching actions for recovering blocked user ships from link failures and inter-cell interference mitigation. • Power consumption reduction by considering the sailing positions of the farthest user ship of individual shipborne base station during adjustment of downlink power of the seaborne-base station.	• Design of a coordinated satellite and terrestrial architecture for marine broadband and real-time access. • Development of a voyage-based cooperative resource allocation algorithm for mitigating the inter-cell interference of shipborne base stations in addition to its power consumption management.	The developed algorithm demonstrated that the designed coordinated satellite and terrestrial architecture in addition to the voyage-based cooperative resource allocation scheme is capable of providing mobility robustness and efficient system power utilization for broadband maritime communication networks. The proposed VB-RA scheme offered system improvement as compared to classical allocation methods.

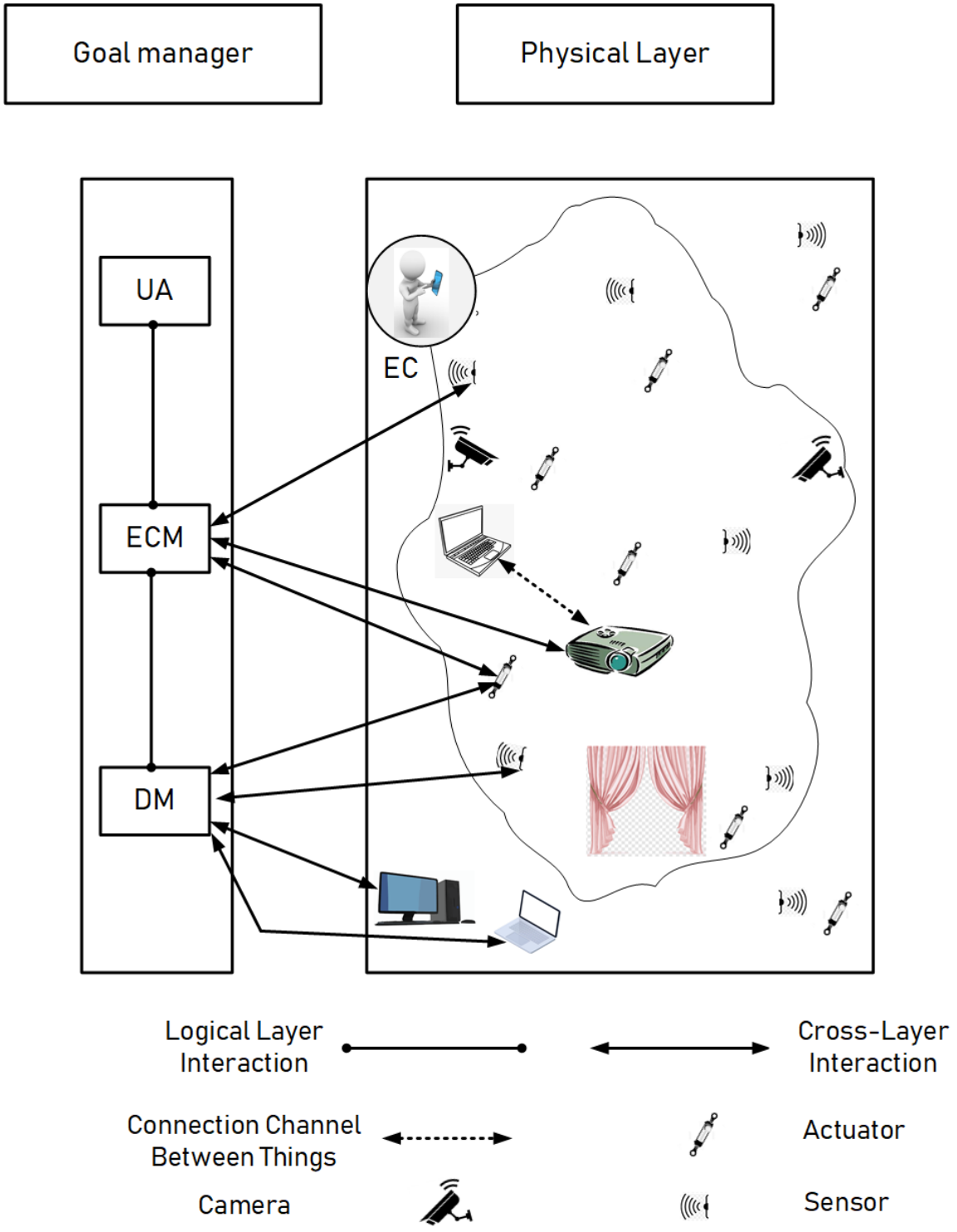

Figure 2.2. Illustration of the physical and logical layers of an EC.

Table 2.4. Summary of contemporary research works in the maritime IoT.

Reference	Aim of research	Technological Approach	Methodology	Contributions	Conclusions
[83]	A comprehensive review of wireless mesh communication technologies and protocols for maritime operations.	Development of a typical coastal mesh network and classification of marine communication protocols.	Classification of maritime mesh networks and systems in addition to numerous marine communication protocols.	• Review and documentation of coastal communications technologies and networks. • Overview of maritime wireless mesh network communication protocols and their operational mechanisms.	The research work presents information/guidelines to wireless service providers on the incorporation of the benefits of broadband terrestrial communications technologies with maritime operations.
[77]	To review and classify maritime communication technologies in addition to provision of radio engineering challenges for marine environments.	Enhancement of digital maritime communication systems using wide and narrowband access technologies.	Categorization of market pull and technology push marine communications.	• Classification and documentation of available digital marine communication technologies • Discussion of marine high north challenges and future trends.	Coastal regions can be sufficiently covered using terrestrial system technologies such as sub-GHz WiMAX and enhanced wireless narrowband access such as digital very high-frequency technologies.
[76]	To develop an improved OceanNet architecture that will enhance internet connectivity for marine users through coverage distances of over 60 km.	Collection of monitored data using underwater nodes and designing a wireless multi-hop backhaul network for extending signal coverage and connectivity improvement in maritime networks through a selection of the best path from marine user position.	Development of hardware testbed for analysing system performances in terms of throughput and signal coverage.	Development of a hybrid network architecture for coastal networks based on LTE technology for maritime overwater and underwater communication systems.	• The developed network architecture offers novel and efficient network potentials for coastal communication systems • Packet delivery ratio is significantly enhanced using the proposed path selection schemes for the benefits of fishermen and other marine users.

which may be in manufacturing, transportation, healthcare, agriculture, etc. One pre-eminent manufacturing industry that can exploit the merits of IoT and EC technology to boost production output is the oil and gas sector. In this section, the procedures for the formation of EC in addition to the architectural description of an EC process is highlighted. Furthermore, an overview of maritime operation activities during oil and gas exploration is discussed while the applications of EC in IIoT for maritime operation is as well propounded for further research developments.

2.4.1 Procedures for the formation of an emergent configuration

Two subprocesses are put into consideration in the formation of an EC in order to meet user goals. The first subprocess involves the collaboration of the three elements of the logical layer (i.e., UA,

ECM, and DM) towards actualizing the goals of the user whereas, in the second subprocess, the EC is continuously managed by a monitor, analyses, plan, execute, system knowledge base (KB) update (MAPE-K) loop. In the first subprocess, the user expresses his/her goals over a specified goal location boundary using a smart connected device (i.e., the user agent). Common examples of user agents include personal computers such as palmtops, laptops, desktops, electronic notebooks or smart mobile phones, etc. Once the user expresses the user goal through the aid of a user agent, an ECM then interprets the goals and then makes a subsequent analysis of the possibilities of actualizing the goal. For instance, the ECM can then decide if the boundary location intended for use by the user is available or not. If not available, the ECM may then suggest alternative boundary locations for the user in order to help the user to achieve his/her goals. The interaction between the DM and the ECM then takes place, where information of the current state of connected things are made known to the ECM through the aid of the DM. The ECM then analyses the entire system and ensure that all connected things work together to achieve a common goal for the user's satisfaction. The second subprocess of EC formation (MAPE-K loop) is explained in Subsection 2.4.2.

2.4.2 Architectural description of an EC process management

An architecture for the IoT process management consists of seven core components which can be used to describe the core components of an ECM. These components of an EC architecture include; goal manager, adaptation manager, context manager, enactment engine, business rules, domain ontology and system KB [84, 87–89]. The responsibilities of these components are explained subsequently.

Firstly, the primary role of the goal manager according to Figure 2.3 is to interpret the goals of the user and then specify suitable goal location boundaries. The goal manager is also responsible for analyzing available IoT objects/services while making efforts to exploit the functionalities of these objects towards the actualization of user goals. Furthermore, the goal manager is responsible for suggesting relevant and alternative services to the user in order to enable the user to achieve his/her goals, while also deriving subgoals for the EC to meet user needs. Moreover, the goal manager is responsible for connecting and coordinating the available IoT connected devices for the actualization of the user's expectations.

Secondly, the adaption manager is responsible for managing the MAPE-K loop which involves

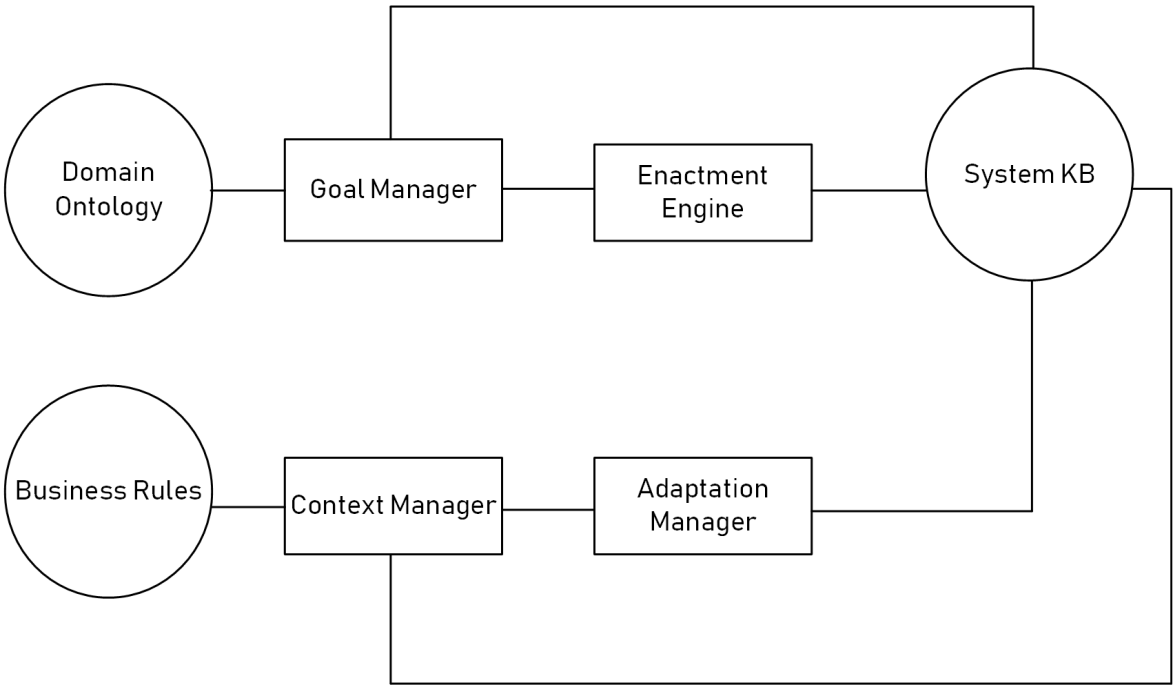

Figure 2.3. An architecture of an EC management process

monitoring of changes in the context, for instance, discovery of new connected devices and faulty devices by dynamically configuring and updating the EC system to meet the user goals. The adaptation manager also analyzes the effects of the system changes for the satisfaction of user goals while planning all changes to the subgoal model of the EC. Other roles of the adaption manager according to the MAPE-K loop involves execution of the planned changes by communicating with the enactment engine as depicted in Figure 2.3.

The context of the EC such as system KB update and detection of dynamic events in the environment is managed and maintained by the context manager. The primary context (which is the raw data) that made available from sensing is as well maintained by the context manager while inferring new business rules based on the context.

It is attention-worthy to note that the primary responsibility of the enactment engine is to give instructions to IoT connected devices while coordinating their activities and ensuring effective collaboration between the devices in order to satisfy user needs. The business rules component, on the other hand, is a central location that consists of domain related and theorize rules which are based on the context changes whereas the domain ontology host a classification of Semantic information about domains that

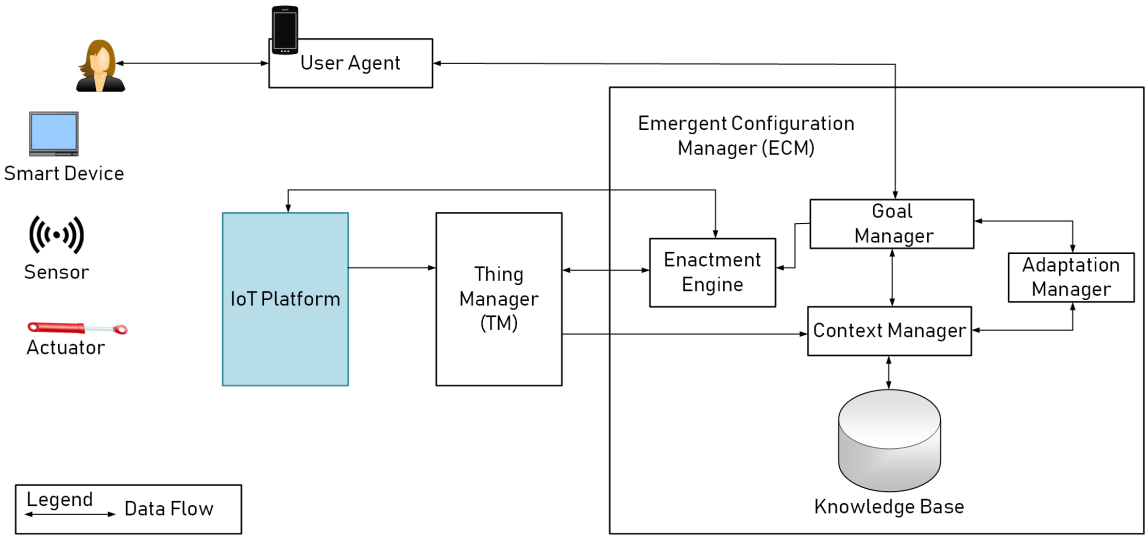

Figure 2.4. A refined architecture for realizing ECs. Adapted from [86], © 2020 Springer.

are employed for the derivation of the EC subgoals for example, “a smart room”. Finally, the system KB is a container that houses information of the EC context.

The architecture of an EC process is refined in [86] as diagrammatically illustrated in Figure 2.4. A detailed description is as well presented for all components in the refined architecture for realizing EC in the IoT (Eco-IoT), in addition to their interaction with the IoT platform. A first prototype is developed using Java programming language, while performance is evaluated to validate the feasibility of EC in some key components of the refined architecture. Interested readers are referred to [86], for more information on the refined Eco-IoT architecture.

2.4.3 Overview of Maritime Operations in Oil & Gas Extraction

Drilling of reservoir rocks is considered as a major objective of maritime operations with a goal of finding trapped hydrocarbons that are buried in the rocks, for several years. The processes of oil and gas explorations begin by building the oil rig in an exact and location with the aid of a satellite so that trapped hydrocarbons can be optimally explored using a vessel. A drill bit is connected to the sea floor (to a depth ranging between 2 to 11 km) through the aid of a conductor pipe, where the bit rotates to drills the rocks and sediments formed below the seabed. Drill pipes are then connected to a conductor pipe which runs down to sea floor after which the conductor pipe is installed into the rock. A casing pipe (with approx. diameter of 50 cm) is inserted into the hole through the conductor pipe to ensure

installation firmness. A cement is then poured in between the drilled hole and the inserted casing pipe in order to strengthen and firmly position the casing pipe. During drilling operations, a special mud is injected through the drill pipes to cool the drill bit and for mitigating the gushing of oil and gas from the drilled layers by stabilizing the pressure. The mud is a mixture of clay (for thickness) and fine ground rocks (for weight). This mud is also used for cleaning the bottom of the well by carrying rock fragments to the water surface as it travels through the pipes. When hydrocarbons are found, the oil and gas flow to the surface of the water through the calibrated hole at high pressure and are collected and stored in vessels, where they are transported onshore for further refining in the petrochemical refineries.

During oil drilling operations and transportation, there is a possibility of oil spillage occurring. The spillage constitutes a significant challenge for marine engineers during maritime operations [90]. Oil spillage in the context of maritime oil and gas extraction is described as an accidental release of the drilled petroleum hydrocarbons into the marine ecosystem which consequently pollutes the marine environment. Simple plankton organisms such as bacteria, plants, and animals are adversely affected by oil and gas spillages in the marine environment. Fishes, seabirds, marine mammals (such as dolphins and whales), marine reptiles, sea grasses, and mangroves are organisms that greatly suffer the harmful consequences of oil pollution. These organisms end up losing their habitat/shelter. Toxic chemicals released into seawater from marine oil spillages may cause impairment of cellular functions in these marine organisms which can result into a catastrophic mortality rate of marine lives [91].

Oil spillages are caused by two principal actions that may arise naturally or from anthropogenic activities. The spillage is naturally caused from oil and gas leakages that spring up from the bottom of seawater (or oceans). On the other hand, oil spillages may arise from human (anthropogenic) related activities such as accidental oil spills during oil drilling and refining processes including oil collection, storage and transportation. It can also be caused from intentional anthropogenic activities such as oil discharges through drains to the marine environment in a sewer system as well as through burning of fuels.

Oil on water locator (OWL) is a device that is adopted for sensing and detecting oil spillages in both seawater surfaces and sea depth [92]. Hyperspectral laser-induced fluorescence light detection and ranging (HLIF LIDAR) is the technology that is adopted by the OWL for detecting oil leakages in seawaters and oceans [92, 93]. Several remote oil sensing techniques such as radio detection and

ranging (Radar), ultraviolet (UV)/infrared (IR) scanners and spectral imaging can be employed for detecting oil spillages. The HLIF LIDAR technology detects oil leakages in water by using the intrinsic fluorescence of polycyclic aromatic hydrocarbons (PAH) present in the oil [92]. It receives the re-emitted light using an inbuilt telescope which is diffracted and thus detected by a 500 channel hyper-spectral detector which detects UV and visible light. To mitigate the deterioration of aquatic environments and to save the lives of marine animals as well as other living marine organisms as a result of oil spillages, the concept of EC can be deployed for the maritime IIoT. An application of the concept of EC is propounded in Section 2.4.6 for the maritime IIoT.

2.4.4 An SDN-based ubiquitous computing-aided EC for Oil & Gas Explorations

The maritime networks deplored for oil & gas deracination need to be carefully designed to deliver smarter, reliable, scalable and faster services in order to increase the output of ocean-going extractions. The merits of ubiquitous computing technology which is an embodiment of IoT networks can be adopted in cooperation with SDN technique in order to meet the above-stated needs of naval networks. In this Section, we present a succinct overview of SDN technology and successively propose a ubiquitous computing enabled SDN-based architecture for enhancing the production outputs (or throughputs) of nautical explorations.

2.4.4.1 Overview of SDN Architecture in Wireless Network Applications

As a result of the resource-constrained limitations of existing traditional network infrastructures due to pre-programmed application-specific integrated circuits, there is need to develop flexible network architectures that will efficiently adapt to changes in network conditions and operations in order to perform a dedicated task. Consequently, the SDN architecture is proposed in [94] where network control is decoupled from the conventional hardware devices [10]. In other words, the data plane (also known as forwarding plane) which is responsible for forwarding packets/frames from a given interface to another is separated from the control plane that is usually designed to manage network operations for decision-making procedures on traffic directions. The SDN technology is designed to consist of three distinct layers including infrastructure, control and application layers, where all the information housed in the data plane (infrastructure layer) are centrally managed and directed by the control plane.

The application layer consists of network applications that are deployed for managing the technical configuration of network devices while the control layer (control plane) fundamentally consist of one or a given combination of SDN controllers that may otherwise be described as the wholistic brain of the entire SDN architectural system. Application program interfaces (API) are often used for interfacing (or interacting) between the layers of the SDN structure and may be classified into four groups including northbound API, southbound API, east and westbound API respectively. The communication between the application and control layer is interfaced by the northbound API while the southbound API is required for communication between the control and infrastructure layers as depicted in Figure 2.5. Network communication protocols such as OpenFlow protocol are good examples of southbound API which is often conventionally deployed in SDN-based networks for interaction between the control plane and the infrastructure layer. Finally, the east and westbound API are used as network interfaces between controllers especially when multiple controllers are engaged for enhancing communication performances in the software-defined network. Few examples of open-source controllers for enabling SDN include OpenDaylight, Nox/PoX, Cherry, ONOS, OpenKilda and RUNOS etc.

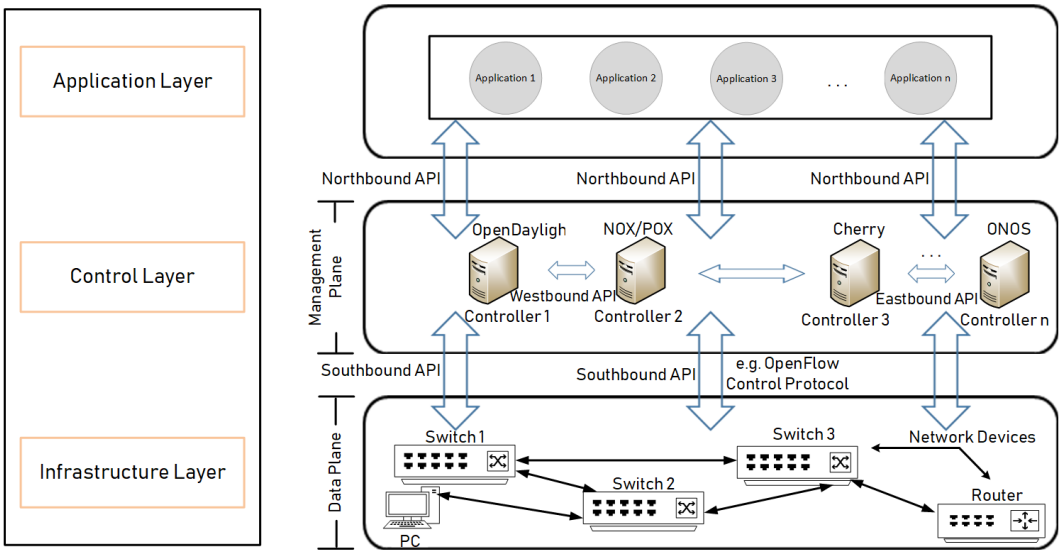

Figure 2.5. Diagrammatic illustration of an SDN architecture.

2.4.4.2 A Ubiquitous Computing SDN Architecture of EC for Maritime Operations

Ubiquitous computing (or simply "Ubicom") is simply described as a paradigm where computing can be made by various device users in any given location and at any given time. The user in this context is described to interact with the computer which could either be desktop computers, laptops,

electronic hardware, and terminals that are incorporated into everyday objects such as a pair of eye glasses, curtains, windows, doors and fridges. etc. This paradigm also known as ambient intelligence or pervasive computing is supported by some fundamental IoT enabling technologies such as sensors, actuators, microprocessors, internet connectivity and numerous specialised application layer protocols. Motivated by the works done in [86, 95], we propose an EC architecture for monitoring the operations of nautical explorations as illustrated in Figure 2.6 in such a way that the onshore marine users exploit the benefits of ubiquitous computing and SDN technology in order to satisfy user standards. In this architecture, the interaction between the seashore located marine user (i.e. UA) and an ECM is managed by an efficient ubiquitous computing service system (UCSS) that is based on matchmaking and rule-based algorithms, where the UA of the EC network tries to exchange dynamic information to perform network diagnosis and high-quality evaluations for improving the communication efficiency and throughput of the entire marine networks.

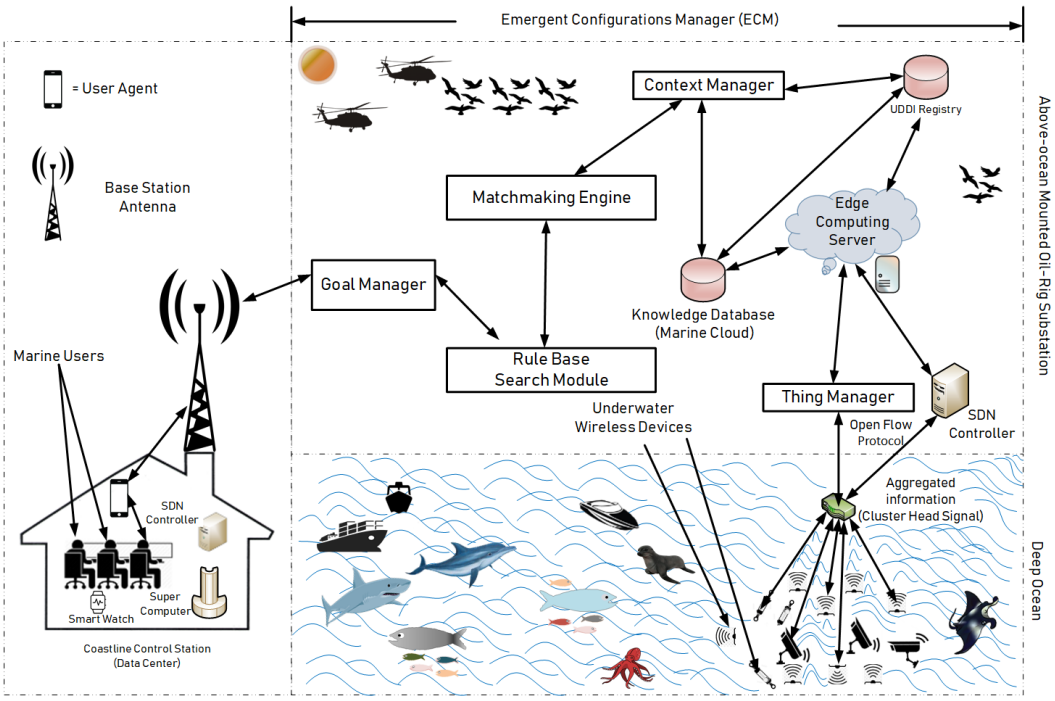

Figure 2.6. Proposed ubiquitous computing SDN-based EC architecture for maritime explorations

In the development of our proposed naval communication architecture, a littoral-based marine user expresses his/her desire to monitor the conditions and operations of the entire seafaring explorations then, the ECM tries to ensure meaningful and seamless communication between all ocean-embedded network devices and the seashore-located marine base station. The user can express his desire to request performance information through a UA that is made available through any electronic object that forms a part of any ubiquitous computing system. The goal manager then takes control of the

request and makes communication with other components of the EC process in order to meet the user requirements. Assuming an underwater-embedded sensor becomes faulty and the user intends to find out the faults in the nautical network after receiving some signals in the control room, the thing manager that is managed by the ECM and primarily configured to control all connected wireless devices of the network will then identify the faulty sensors and send the information to a knowledge database that is mounted on the ocean oil-rig substation. The communication interface between all aggregated sensor information through the cluster head (CH) and the control layer is managed by an SDN controller using the OpenFlow communication control protocol. Thus, the transmitted information which is stored in the marine cloud/universal description, discovery, and integration (UDDI) registry is then managed by the context manager whose general responsibility is to manage data within the maritime network. Imminently, the ECM retrieves the storage information through the context manager and contacts the matchmaking engine. The matchmaking engine consists of an extended defense advanced research projects agency (DARPA), agent markup language (DAML)/ UDDI translator whose responsibility is to construct an interpretation based on the information retrieved from the context manager as described by a DAML-S profile. More over, the reasoner contained in the matchmaking engine ranks the aggregated CH information retrieved from the context manager using a matchmaking algorithm and subsequently computes a match level to meet the user demand in accordance with the network architecture of a matchmaking engine represented in Figure 2.7.

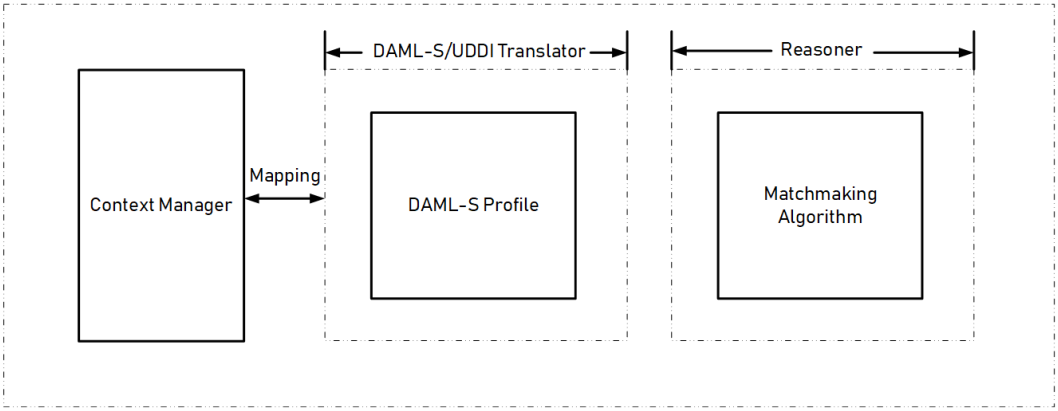

Figure 2.7. System architecture of a matchmaking engine.

After the computation and ranking of data is performed in the matchmaking engine, the required information is eventually sent for verification procedures through a rule-based module using appropriate QoS measurement algorithm to the goal manager who then interprets the information and conveys the requested message to the marine user for appropriate action procedures. The rule-based engine varifies the ranked information by comparing the computed data received from the matchmaking engine with

that of the context managed UDDI profile registry. A system architecture of the rule-based engine is represented as depicted in Figure 2.8. In this architecture, the search for rule-based information from the ECM can be implemented using SweetJess [96] which is then converted into Jess's rule language through an extensible stylesheet language transformer (XSLT). The Jess engine then converts the rules and information to form usable by a reasoner after which the results are subsequently concluded using the Jess engine for further actions by the goal manager.

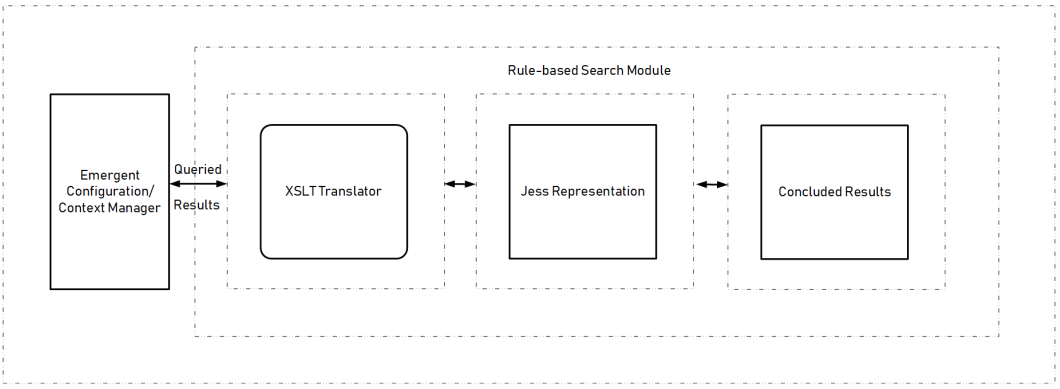

Figure 2.8. System architecture of a rule-based engine.

2.4.5 Communication Technologies for Facilitating EC in Oil and Gas Explorations

It is noteworthy to remember that some technologies are deployed for enhancing the performances of IoT applications. The merits of these technologies can be exploited to manage the EC process while they may either be classified as data-acquisition technologies or networking technologies according to their abilities to enhance the performances of IoT and EC systems. The traditional IoT architecture consists of three layers that include the perception, application, and network layers. Information that is obtained from the physical world is converted into electrical signals in the perception layer where the converted information is subsequently transmitted through the network layer to the application layer for exploitation and adequate utilization (by the IoT users) in order to enable meaningful decision makings. Several technologies can be deployed for assisting the performances and efficiencies of various layers of the propounded SDN-based EC architecture for oil and gas extractions according to Figure 2.6. These technologies and communication routing protocols are discussed subsequently.

Table 2.5. A comparison of existing IoT communication technologies for EC in Oil & Gas extractions

Communication Technology	Transmission Range	IEEE Standard	Data Rate	Power Consumption	Cost
WPAN (Bluetooth)	$8-10\,m$	802.15.1	1 - 24 mb/s	Low	Low
LR-WPAN (ZigBee)	10 - 100 m	802.15.4	40 - 250 kb/s	Low	Low
WiFi	$20-100m$	$802.11a/b/g/n/ac$	1 Mb/s - 6.75 Gb/s	High	High
WiMAX	Less than 50 km	802.16	1 Mb/s - 1 Gb/s (fixed)	Medium	High
Mobile Communication	Entire Cellular Region	4G-LTE based on CP-OFDM	100 Mb/s - 1 Gb/s	Medium	Medium

2.4.5.1 Data Acquisition Technologies for Enabling EC in Oil & Gas Extractions

The technologies adopted in the perception layer are mostly data acquisition technologies because this layer is responsible for obtaining information from surrounding objects/environmental conditions. Data acquisition devices such as quick response (QR) code, RFID, sensors and actuators are employed in this layer of the oil exploration phase. The obtained information is then converted into electrical signals, where the propagating information is transmitted from the perception (or infrastructure) layer through the network layer to the application layer. Networking technologies aid the transmission of information from one layer to another. These technologies that are capable of enabling EC in marine networks, whose properties are summarized and compared in Table 2.5 include; low-rate wireless personal area networks (LR-WPANs) e.g. ZigBee [97–99], wireless personal area networks (WPAN) e.g Bluetooth, IPv6 over low-power wireless personal area networks (6LoWPAN), wireless local area networks (WLAN) e.g wireless fidelity (WiFi), wireless metropolitan area network (WMAN) e.g. WiMAX and mobile communication technologies such as the current fourth generation (4G) - long-term evolution (LTE) based cyclic prefix orthogonal frequency division multiplexing (CP-OFDM) technologies.

2.4.5.2 Communication Routing Protocols for Realising EC in Oil and Gas Explorations

Application layer messaging protocols such as message queue telemetry transport (MQTT), constrained application protocol (CoAP), advanced message queuing protocol (AMQP) and extensible messaging and presence protocol (XMPP) can be adopted to aid the transportation of the sensed data across the marine communication network for meaningful decision making. Communication protocols constitute

the backbone of IoT systems as they enable the coupling and connectivity of IoT networks to the ubiquitous computing-assisted SDN based EC network architecture and its applications while allowing data devices to exchange information over the communication network. Data exchange formats and encoding are defined using communication protocols including routing of packets from the transmitter to the receiver. In addition, flow control, sequence control, and lost packet re-transmission are other functions performed by communication protocols. Table 2.6 presents a brief comparison of the afore-mentioned application layer protocols for IoT including CoAP, MQTT, XMPP, XMPP and WebSocket which are further discussed and classified in [34, 100] and may be deployed for communication in any suitable application of the propounded EC architecture. The security provided by these protocols are presented in [101, 102]. These protocols are deployed in constrained environments such as the described smart oceanic domains where the devices operate under constrained conditions including low memory and processing power situations. In [7], a classification of low-end (constrained) IoT devices is presented. CoAP on the other hand is an alternative application layer protocol to the hypertext transfer protocol (HTTP) [103] which is not suitable in resource-constrained environments. The CoAP uses the efficient extensible markup language interchange binary data format while supporting features such as automatic configuration, asynchronous message exchanges, congestion control and support for multicast message [5]. More so, four kinds of messages make up the CoAP namely; confirmable, nonconfirmable, reset and acknowledgment message [5, 100]. MQTT is a lightweight international business machines (IBM) created publish-subscribe message protocol that uses transmission control protocol/internet protocol (TCP/IP) in constrained environments such as low memory devices with limited processing capabilities. According to [100, 101], three QoS modes namely fire and forget mode, acknowledge delivery (or at least once) and assured delivery (or exactly once) are provided for message delivery according to the MQTT specification. It is documented in [103] that MQTT protocol outperforms CoAP in situations of high traffic networks. It is note worthy to mention that some sets of open technologies deployed for instant messaging, chat and voice calls as standardized by the internet engineering task force (IETF) is the XMPP where the exchange of data is made possible by the use of small pieces of extensible markup language (XML) structured data named *XML stanzas* [101] whose architecture is based on the client-server concept. Abstract layering of the XMPP is based on TCP, transport later security (TSLS) and simple authentication and application layer (SASL) [101]. Other application layer protocols are data distribution service (which is a publish-subscribe) protocol adopted to enhance the operation of high-performance device-to-device (D2D) communication), advanced message queuing protocol (AMQP) and WebSocket. In [104], the performances of three application layer protocols namely CoAP, WebSocket and MQTT are documented in a LAN and IoT scenario using

simple and affordable devices. The performances are evaluated in terms of protocol efficiency and average round trip time (RTT) in LAN and IoT scenario. Results obtained show that the protocol's efficiency does not change as the network changes however, RTT increases by a factor of two to three times in an IoT scenario as compared to LAN scenario. The results obtained also demonstrate that CoAP offers the highest efficiency in comparison to MQTT and WebSocket while MQTT offers the highest RTT as a result of the presence of both application layer acknowledgements and transport.

Network layer communication protocols such as optimised link-state routing protocol, ad hoc on-demand multipath distance vector, dynamic source routing and ad-hoc on distance vector have been proposed for configuring maritime wireless communication systems. However, none of these protocols has been found efficient [105] since they cannot provide optimal communication capability, sustained interoperability and guaranteed reliable communications. Because the sea-embedded network devices are not stationary and the underwater signal coverage is limited, there is a need to develop energy-efficient and energy balanced protocols that can be used as communication interfaces between submerged network devices. This is required because permanently installed under-sea sensors may be difficult to replace thus, prolonging the battery life of such nodes is necessary for the extremely harsh under-water atmospheric conditions which can be achieved either through clustering or load-balancing techniques. In such scenarios, load balancing schemes require multihop configuration approaches whereas, single-hop methods are adopted for implementing the clustering procedures. Thus, we propose the use of an energy-efficient and energy balanced routing protocol that attempts to balance the energy dissipation of the marine user equipment (MUE) during the formation of cluster networks in the aquatic communication system according to [39] named mobile sink selective-path priority table (MSPT). In this technique, a priority table is developed, where the two shortest paths to the CH are prioritised using some simple rules. The aforementioned rules are formulated to improve marine explorations by combining routing metrics including the transmission power and range of each sensor node in addition to the residual energy of each sensor. Likewise, two phases are involved in the formation of the MSPT routing protocol for maritime communication networks and these consist of the set-up and steady phases respectively. The former phase involves the election of CH nodes for the marine communication networks whereas, the latter phase primarily consists of the development of the data identification and transmission paths in order to optimise the seafaring network performances while considering the energy maximization of network devices.

Table 2.6. Comparison of adaptable application layer protocols for marine communication networks

Application Protocol	Key Features (Benefits)	Originator	Message Transition	Underlying Transport Protocol
MQTT	Efficient routing for small, cheap, low-power and memory devices	IBM and Circus Link	Publish/Subscribe	TCP/IP
COAP	Automatic configuration, multicast messaging, congestion control	IETF	Publish/Subscribe	UDP
AMQP	Provides flow controlled message-oriented communications.	JPMorgan Chase	Publish/Subscribe	TCP
XMPP	Secure and spam-free instant messaging, chat, video and voice calls.	IETF	Publish/Subscribe	TCP
WebSocket	Full-duplex communication for encrypted and unencrypted connections.	IETF	Request/Response	TCP

2.4.6 Application of EC in the IIoT for Maritime Operation

The fundamental concept of EC is presented in Section 2.4 of this chapter, whereas, an overview of maritime operations with specific application to oil and gas extractions is presented in Section 2.4.3. The propounded application of EC in combating oil and gas leakages during maritime oil and gas explorations is further highlighted in this Section. For this application, it is assumed that a ground station is positioned at some remote onshore location, where the entire oil and gas exploration processes are monitored as depicted in Figure 2.9. The control station consists of display management systems such as computer monitors and projectors, lighting systems including numerous shared IoT objects such as sensors and actuators. The oil rig (which is a platform that is built over the oil well) is designed to consist of a substation that receives instructions from the onshore control station. The oil exploration set up, and procedures is described as presented in Section 2.4.3. Stationed around the derrick are sensor objects, for instance, a helium-filled balloon (aerostat) carrying OWL IoT sensors. Positioned at the onshore control station are emergency mechanical devices built with OWL sensors such as helicopters and other unmanned aircraft systems for instance, remotely piloted aircraft systems (RPAS). Platform supply vessels (PSVs) are offshore kind of vessels that are adopted for transiting required equipment as well as additional manpower for oil explorations. Another name for PSVs is offshore supply vessels (OSV) and they are also useful during oil spillage cleaning operations. Other kinds of unmanned surface sensor carrying vessels are also well positioned onshore in preparation for oil spillage emergencies. At a depth of the sea are stationed unmanned underwater vehicles which are designed for monitoring the activities of the oil drilling and explorations. For instance, autonomous underwater vehicles (AUV) are robots that do not require human operations to monitor drilling operations several kilometers beneath the sea. Mobile non-autonomous underwater vehicles that require human control can also be employed for motoring/surveying drilling activities beneath the sea. A good example is the remotely operated underwater vehicle (ROV) that is linked through a tether to a host vessel on the water surface.

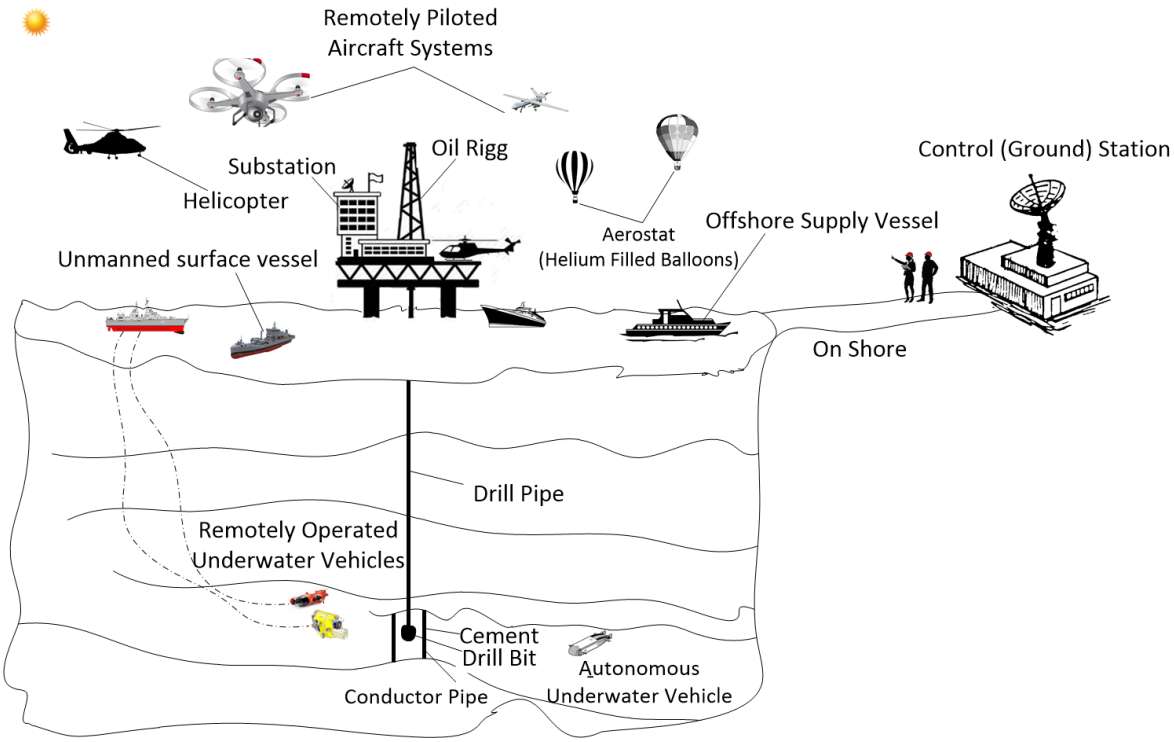

Figure 2.9. Application of EC in Oil & Gas explorations.

Marine environments can be polluted from accidental oil spillages. The pollution may occur from the depth of the sea or on the water surface. It can arise from the bottom of the seawater as a result of improper drilling operations that may occur from human errors. For instance, the ground rocks not being cemented appropriately when drilling operation commences as a result of the drilled ground rock diameter been greater than the diameter of the cemented conductor pipe. This may cause leakage of high-pressure hydrocarbons from the sides of the cemented conductor pipe consequently posing great environmental hazards to marine organisms. On the other hand, seawater pollution can also occur from the surface of the ocean especially during collection and storage of the drilled hydrocarbon as well as offshore to onshore oil transportation. Hydrocarbon transportation vessels with badly damaged tanks can be a chief reason for this kind of oil and gas spillages.

An onshore control system is built for monitoring and managing the installed surveillance devices as well as the drilling process taking place from the onshore station to the offshore ground rocks. An ECM is set up to handle the control processes during emergency operations such as oil leakages as well as during clean up operations. For instance, the ECM triggers an alarm to notify the users of an emergency. A simple application example is given as follows. It is assumed that the maritime

control engineers together leave the control room of the onshore station for a quick lunch few meters away. Suddenly, they hear an alarm indicating an emergency. The curious engineers move to the dark control room to find knowledge of the current emergency situation. Using a user agent (for instance, a computer), the engineers express their goal to “monitor the entire drilling process". An EC is set up which interprets the goals of the users and collaborates with selected resources to achieve this goal. The installed light sensors in the control room detect that the room is dark and the lights are automatically put on for improved visibility. Projectors, relevant sleeping monitors and other potential display media comes up to enable the users to monitor the entire drilling process. Suddenly, excessive sunlight comes into the room which makes it impossible for the screens to be viewed appropriately. The light sensors figure it out that there is too much light in the control room and the smart curtains are triggered to close automatically, and the perfect lighting is maintained in the room. The engineers can now visualize the cause of the alarm as it displays on the media that there is oil spillage occurring in the oil well. In the process, the temperature of the room is increased due to the incoming sun rays and the ECM triggers an actuator that puts on the air conditioners. This is a brief application of EC in the control room working in collaboration with IoT devices to meet the user goal. For the engineers to appropriately visualize the cause of the emergency, they need to have accurate knowledge of the ongoing processes in the oil rig as well as on the sea floor. The ECM contacts the EC set up in the oil rig substation. The setup oil rig EC subsequently contacts the device manager so as to obtain first-hand information of the current state of seawater surface and submerged surveillance devices. Unmanned underwater vehicles carrying OWL in addition to ROVs detects an oil leakage gushing from the bottom of the sea floor. The substation ECM is notified which sends the information to the onshore ground station. IoT sensor objects positioned on the sea surface like the aerostats become more vigilant in sensing for oil spillages while the ECM instructs sensor carrying mechanical devices such as helicopters and RPAS to patrol and survey the oil exploration area. The PSVs are notified, and they move towards the oil rig platform in preparation for cleaning processes. The onshore control engineers monitor and analyze the entire process while making efforts to minimize the detrimental effects of the oil pollution to the marine environment. They could see that the cause of the oil spillage is due to improper installation of conductor pipes beneath the sea floor and they express their goal of sending more cement and mud through the conductor pipes to firmly seal the drilled hole beneath the seafloor. The ECM instructs the substation which automatically sends cement and mud to appropriately seal of the drilled well beneath the sea floor, while oil that floats to the sea surface is cleaned using the PSVs.

2.4.7 Limitations of IoT for Maritime Operation & Possible Research Directions

The effective implementation of EC and IoT technologies for the operation and management of maritime activities is encountered by numerous limitations including data management challenges, resource constraints, security and privacy challenges, mobility management and cost-effective communication systems. Firstly, the sensor-based MUE embedded to marine devices can generate large volumes of data which needs to be processed and stored for accurate maritime decision-making procedures. The generated data during the processes of EC needs to be accurately processed in order to guarantee high system performance, efficiency and scalability. Hence, it is required that certain preprocessing procedures be performed where the collected information can be arranged to form clusters by splitting the collected data into smaller groups for more reliable transmission and data processing actions. The development of clustering evolutionary algorithms for the collection and processing of the transmitted IoT-enhanced data for maritime decision-making processes is still an open research area. Secondly, it is worthy to mention that the sensor nodes deployed for EC activities during oil and gas explorations are usually resource-constrained by energy, memory and processing resources. As such, the optimal allocation of network resources for marine oil & gas explorations is still an open research issue. Additionally, developing traffic engineering techniques and energy-efficient protocols for monitoring the EC procedures in oil and gas explorations is required for the optimal exchange of data during maritime communications. Furthermore, scalable and dynamic SDN and NFV-based architectures/frameworks can still be developed to guarantee the efficient management of limited cloud memory in addition to mobility management procedures and optimal utilization of system energy for seamless operation of maritime activities. Thirdly, another challenge of realizing IoT technologies for the explorations of oil and gas in the marine environment as mentioned earlier is data security and privacy. This is because the integrity, authentication and confidentiality of the MUE collected data during EC-based oil and gas explorations requires to be given priority as the wireless interactions of different devices can result to unwanted third user activities such as network tapping, tampering and forgery since most network components will be left unattended due to self-configurations. As such, developing novel security enhancement techniques that will prevent denial of service (DOS) and distributed DOS challenges is an open research problem for the IIoT in application to maritime environments. Finally, a significant challenge of maritime operations is cost-effective communications. Satellite communication technologies are usually deployed for the operation of marine activities [105]. Nonetheless, these technologies are known for their high cost despite their rapid developments. To minimize the high communication cost of satellite systems in addition to achieving high-datarate, reliable and lower latency QoS requirements

in maritime IoT-based communication technologies, alternative communication techniques such as EC, SDN, NFV, mobile and cloud computing as well as use of multiple directional coastline-mounted directional antennas can be deployed and connected together for monitoring and improving the operation of seashore maritime activities. Hence, the development of novel frameworks and models that are in line with the above-mentioned communication techniques for the extraction of oceanic oil and gas explorations is an open research area awaiting contributions from researchers and practitioners in this field for meaningful decision-making procedures based on application requirements.

2.5 CHAPTER SUMMARY

In this chapter, a comprehensive review of the concept of IoT is presented. A general overview of the concept of IoT is reviewed as applicable to the industrial environment. The concept of ubiquitous computing SDN-assisted EC is propounded for managing emergency situations as applicable to the maritime IIoT, in order to mitigate the detrimental effects of oil and gas spillages onto marine environments for higher throughput and gain maximization in offshore oil and gas explorations. Marine ecosystem can also be preserved from safe offshore oil and gas exploration which can be enhance by the technology of ubiquitous computing assisted SDN-based EC in the IIoT for maritime operations. The concept of EC can also be deployed to preserve lives in maritime environments during explorations of hydrocarbons from quick responses to emergency situations. This novel concept (EC) can be extended in future research works to other industrial applications of IoT technologies such as manufacturing, health care, transportation, smart energy and agriculture etc. In addition, WSN-based technologies such as SDN and routing protocols etc., can be further developed to enhance the drilling of marine operations. The benefits of EC technology can also be exploited for onshore oil and gas production. Thus, keeping in view the coverage of this chapter, it is presumed that this thesis will spring up possible research directions in improving the autonomous extraction procedures of oil & gas across deep waters using contemporary IoT-based communication technologies. For future works, we consider to present a detailed comparative data analysis that compares the output performances of an SDN-aided EC-enabled oil and gas extraction technology in comparison to exploration scenarios where the EC process is not aided. A comparative analysis of existing maritime routing protocols such as the MAC-based routing protocol for TRITON (MRPT), OLSR, AoDV and AoMDV protocols etc in comparison with our MSPT routing protocol for oil and gas explorations will be elaborately provided. Finally, we intend to also develop energy balanced protocols that would mitigate the energy-hole problem of marine sensor

networks.

CHAPTER 3 CHANNEL ESTIMATION FOR NAUTICAL RADIO NETWORKS

3.1 CHAPTER OVERVIEW

Similarly to terrestrial communication networks, wireless communication systems within the marine environment can be affected by severe environmental conditions such as extreme temperatures, deep-water waves, ship movements, inconsistent weather conditions including rain, snow and fogs etc. The seaside territories usually consist of constricted infrastructures that eventually overwhelm the quality of transmission between the ocean-going vessels and the outlying shore-positioned base station (BS) whereas, marine users (identical to terrestrial users) require high-quality broadband communication services such as ship rescue, voice and data services in addition to video monitoring services for the operations of maritime ministrations. These environmental conditions and obstacles could result in obnoxious effects such as signal attenuation and multipath propagation. To overcome these challenges accordingly, there is a need to design cost-effective and energy efficient network architectures in addition to suitable communication techniques that will eventually enhance the communication quality and extended signal coverages across ocean-water surroundings. One such worthwhile technique that can enhance the proficiency of marine communications is channel estimation (CE). Channel estimation is a useful communication technique that can be exploited for maritime exploration in order to enable the receivers of deep-sea networks to efficiently approximate the channel impulse response (CIR) of the wireless communication channel so that, the effects of the communication channel on the transmitted packets can be understood and predicted for useful decision-making procedures [45]. Thus, the concept of signal attenuation, multipath propagation and channel estimation is tersely presented in this chapter.

The rest of this chapter is structured as follows. Section 3.2 discusses the mechanism of propagation in general wireless communication networks where the concepts of multipath propagation and fading in scenarios that are applicable to both terrestrial and nautical radio networks are described. Thereafter, the concept of CE is abruptly explained in Section 3.3 while the formulation of the considered standard estimators which will be analysed and compared to the proposed methods developed in Chapter 4 is presented in Section 3.4. Finally, Section 3.5 summarises the chapter.

3.2 MECHANISM OF PROPAGATION IN WIRELESS CHANNELS

In the design of typical terrestrial mobile-radio systems, the information to be transmitted across the wireless channel as waveforms require efficient modulation techniques, where the properties of a periodic carrier signal are varied with a modulating signal and subsequently transmitted in waveforms over a wireless communication channel. As the modulated signals propagate over the wireless medium to a receiver, terrain objects such as mountains, hills, buildings, cars, trees, etc, interfere with the LoS path of transmission. This interference could result in undesirable effects on the transmission network. Consequently, the propagating signals may then experience the unwanted effects of reflection, diffraction and scattering (as shown in Figure 3.1) which makes the symbols to return to the receiver side with multiple reflective paths with characteristic time delays, fluctuating amplitudes and different phases in a phenomenon known as multipath propagation [45]. Additionally, due to multipath propagation, the received signals further experience attenuation as they encounter various environmental obstacles in the wireless radio channel which accordingly results in fading of the transmitted symbols. A brief description of the concept of multipath propagation and signal attenuation (fading) is presented in this section which both corresponds to terrestrial and thalassic transmission conditions.

3.2.1 The Concept of Multipath Propagation

As shown in Figure 3.1, propagation phenomena such as reflection, diffraction and scattering can make the propagating symbols arrive at the receiver of both terrestrial and nautical radio networks through numerous paths in a phenomenon termed multipath propagation. In mobile radio networks, reflection is described as a fundamental propagation mechanism which is known to have disastrous impact on transmitting signals and are known to occur when the transmitting electromagnetic waveform strikes on

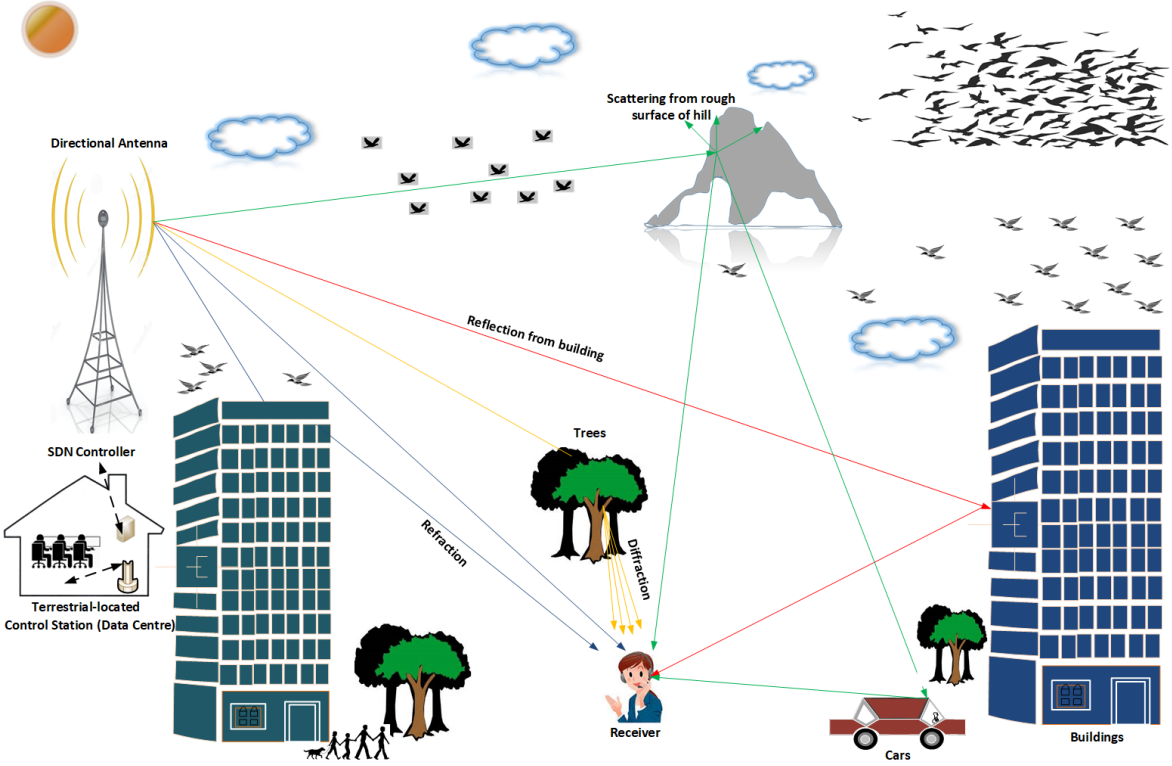

Figure 3.1. Illustration of multipath propagation effects on transmitting symbols.

terrain objects with huge dimensions as compared to the wavelength of the travelling waves [106]. This phenomenon frequently occurs when the travelling signal strikes the ground surface, walls and furniture etc. Thus, reflection is known to result in partial refraction of the transmitting symbols. On the other side, diffraction is simpley described as phenomenon that takes place when the paths of transmission between both transmitter and receiver are obstructed by sharp-edged surfaces. In this propagation phenomenon, the transmitting waveforms are bended around their impediment even in situations where there is no LOS path between the transmitter and the receiver. Thus, resulting in the formation of secondary waves behind the encumbering body as illustrated in Figure 3.1. Scattering of propagating packets take place when transmitting radio signals encroach upon massive rough surfaces (i.e. when number of impediments per unit volume is colossal). Scattering is bound for occurrence when the communication medium consists of objects that posses extremely small dimensions in comparison to the wavelength of the wave which results in the spread out of the reflected energy in all directions. Environmental objects such as street signs, lamppost, foliage and and hills can cause transmitting symbols to scatter in urban and maritime centres.

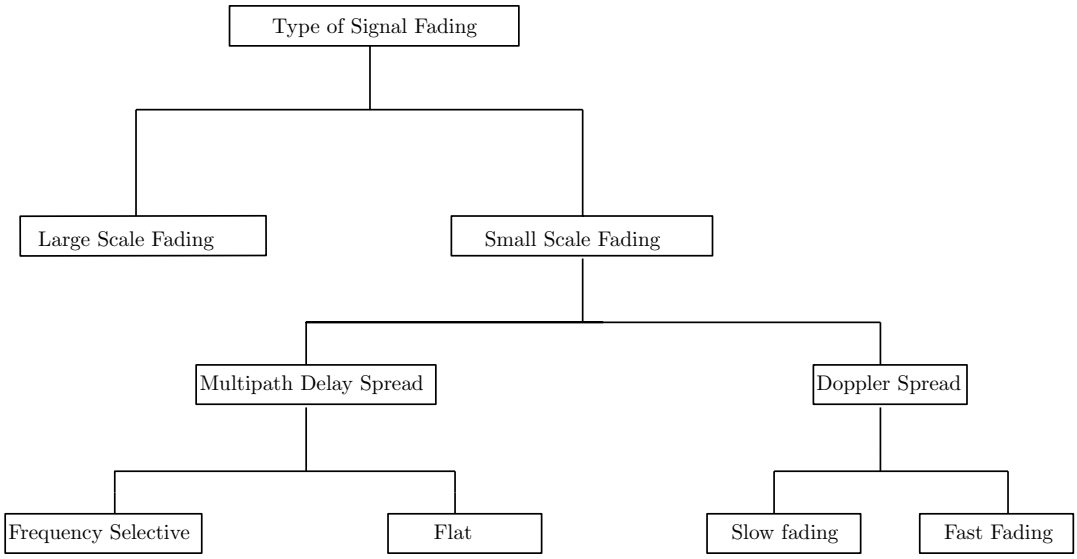

Figure 3.2. Taxonomy of fading types in mobile radio networks.

3.2.2 Fading in Terrestrial and Nautical Radio Networks

Several kinds of fading may be encountered in both terrestrial and nautical radio systems. The type of fading felt by the propagating packets depend on the characteristics of the medium of propagation in addition to the nature of the travelling packets. Based on the aforestated, fading can either be classified as large scale or small scale.

Large scale fading types usually occur as a result of the average attenuation (or path loss) of the power of the transmitting packets because of the propagating motion over large areas. Prominent terrain contours including forests, hills, buildings, bill boards etc. which find position between the transmitting base station and the communication receiver are common factors affecting this kind of fading. The obstructions from these physical objects leads to a phenomenon known as shadowing of the transmitting signals. In this effect, the power of the received signal oscillates haphazardly because of these obstructions that reduce the LoS path between the base station transmitters and receivers. Notwithstanding, small scale fading occurs as a result of changes in the amplitude and phase of the transmitting waveforms due to small changes in the spatial separation between the transmitter and receiver. The various kinds of fading that may be experienced in both terrestrial and maritime networks are classified according to Figure 3.2. From this figure, small scale fading type may result from

either due to multipath delay spread or from Doppler spread. The former fading type arise from time spreading of the transmitting symbols in what is termed signal dispersion while in the latter, fading occurs due to time variation of the transmission medium (or channel).

When the transmitting signals disperse due to multipath delay spread, two fading types may arise which could either be frequency selective or flat fading. Frequency selective fading is felt by the received signal when the bandwidth of the propagating symbol is greater than the bandwidth of the communication channel at constant gain and linear phase response [107]. When frequency selective fading occurs, the received signals become scattered, attenuated and time delayed. The signal will then consist of several other versions of the transmitted symbols which results to a phenomenon known as ISI. Conversely, the signal received will experience flat fading when the bandwidth of the propagating signal is less than the bandwidth of the transmission medium at constant gain and linear phase response. This is the most common fading type experienced in practice as the signal strength changes with time due to fluctuations in the channel gain. Flat fading is primarily caused from the undesired effects of multipath propagation.

As mentioned earlier, a transmitting signal can also experience fading due to Doppler spread (or time variation of the channel). The channel in this condition is time variant since there are variations in the path of propagation that occurs due to motion between the base station transmitter and the moving receiver thus, leading to either slow or fast fading. In other words, Doppler spread is subject to how fast or slow the transmitting baseband signal varies in comparison to the time rate of change of the channel. Fast fading channels are distinguished by a swift change in channel impulse response within symbol duration. In essence, fast fading conditions involve the rate of change of the channel due to motion. In this fading type, the symbol period of the travelling symbols is essentially greater than the coherence time of the channel. This condition inevitably results in distortion of the propagated signal. The maritime radio network designed in this study considers the performances of channel estimation assuming both slow and fast changing channel conditions when the aggregated sensor information ts propelled to travel to the remotely mounted onshore BS. The CIR for Doppler spread slow fading channel conditions varies at a much slower rate when compared to the symbol period of the transmitting packet. Thus, the Doppler spread of the entire communication medium is considered to be far less than the bandwidth of the transmitted information when viewed in the frequency domain.

3.2.3 Summary of Channel Models for Terrestrial and Nautical Networks

Several channel models find application in the design and evaluation of wireless communication networks in general. Considering the varieties of fading environments, a considerable number of channel models have been proposed in the literature to statistically describe the wireless transmission medium assuming short-term, long-term and mixed (hybrid) fading scenarios. The Rayleigh, Rice, Nakagami-*m*, Weibull and Hoyt models are well known models applicable to short-term (small) fading propagation scenarios while the well-known lognormal distribution is accepted for modelling long-term (large) fading conditions particularly in terrestrial communication networks. Mixed channel models including Nakagami-lognormal, Rice-lognormal and Suzuki etc, are used for modelling wireless channel propagations when short and long-term fading scenarios coexist in the wireless transmission medium.

3.3 CHANNEL ESTIMATION FOR MARITIME IOT

Since the propagation of transmitting signals across the marine environment can be perniciously affected by multipath-induced fading and Doppler spread resulting from reflection, diffraction, scattering and interference particularly in severe weather scenarios, the need for accurate estimation of the channel conditions is consequently necessary in order to guarantee excellent transmission and reception of propagating signals across the wireless maritime environment so as to make well-informed decisions. CE is thus, a worthwhile signal processing technique that is required at the receiver for combating the varying nature of the fading communication channel in order to ensure accurate detection of the propagating signals. At this point, it is important to remember that CE techniques can be broadly classified (according to Figure 3.3) into three main categories including non-blind, semi-blind and blind CE. Non-blind CE can be further classified into two categories which are training-based (also referred to as pilot-assisted or data-aided) and decision directed estimation schemes.

The pilot-based CE scheme adopts the use of receiver known training sequences named pilot signals for the estimation of the channel properties. When the density of the pilot signals deployed in a radio network is high, the accuracy of the system CE tremendously improves. Nonetheless, the spectral efficiency of the communication network will decrease considerably as a result of the introduction of system overhead by the introduced pilot symbols. In decision directed CE (DDCE) methods,

training symbols are usually adopted for estimation of the communication channel in addition to the re-modulated detected message signals [108]. In these CE techniques, the CE of previous symbols is employed for detecting the data of the current channel estimates thereafter, the newly detected data is adopted for estimating the current channel. Data detection in DDCE can be achieved either using soft or hard decision where bitwise detection may be employed for soft decision wheras, a specific constellation is forced for hard decision methods [109].

In semi-blind methods, information from the transmitted signal's statistical properties as well as training sequences is incorporated to estimate the CIR of the channel. This implies that semi-blind schemes are hybridization of the training based and blind methods. The blind estimation schemes require enormous amount of data and this approach is well-known for exploiting the statistical and mathematical properties of the transmitted data [108]. When blind estimation method is considered for CE in wireless media, two techniques named deterministic and statistical blind CE can be incorporated. The deterministic CE schemes offer improved system performances when compared to statistical CE methods at the expense of extremely high computational complexities that further increases in direct proportion to the order of constellation in the transmitter's modulator. Blind CE techniques are generally known to be bandwidth efficient because they do not need pilot signals to perform CE. On the contrary, they are known to have tremendous high computational complexities. These estimators only offer superior performances in slow time-varying channels conditions and this trait makes them not suitable for fast fading channels. Interested readers are referred to [108, 110] for more information on the taxonomy of CE schemes.

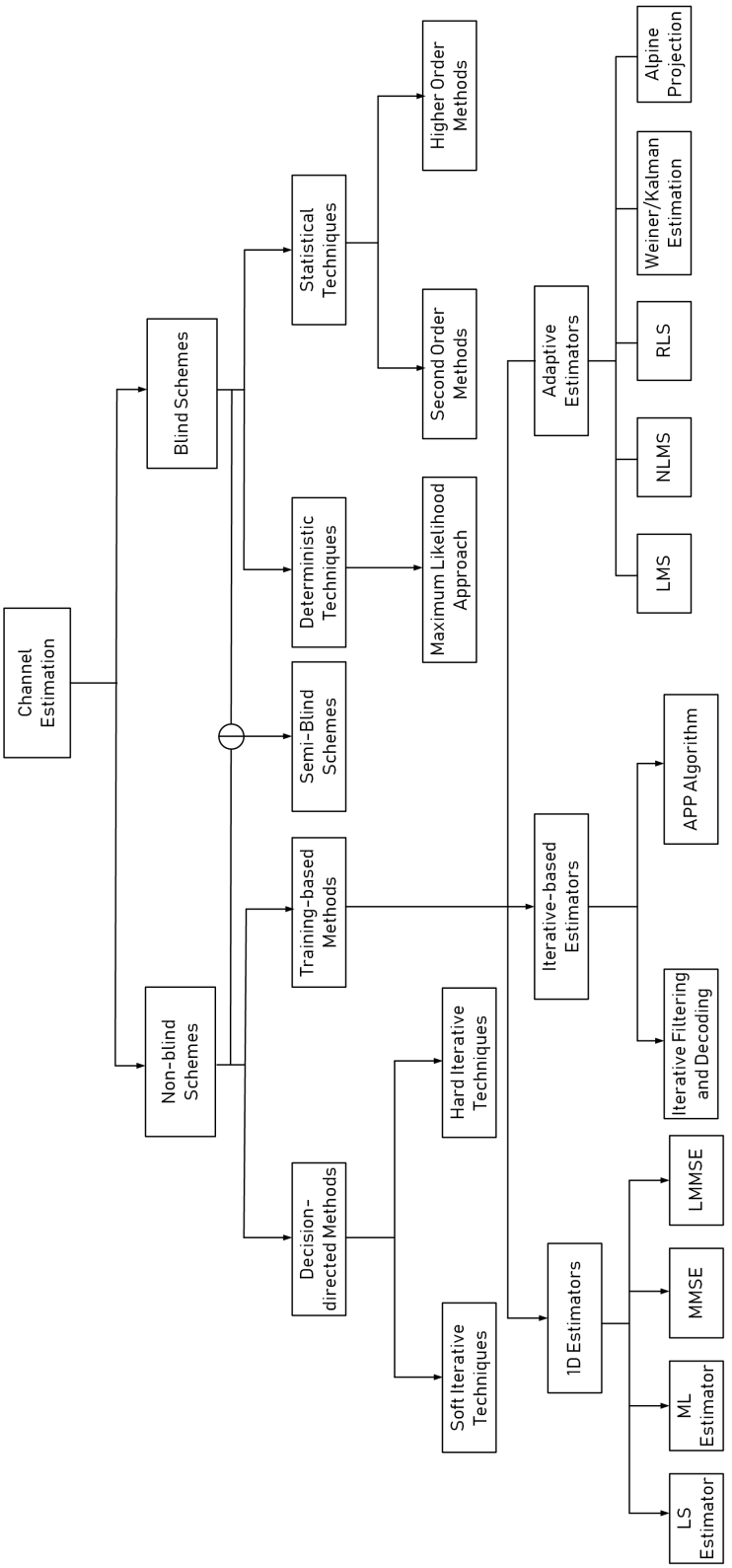

Figure 3.3. Classification of CE techniques [45]

3.4 DESCRIPTION OF THE CONVENTIONAL ESTIMATORS

In this thesis, two linear and two adaptive conventional estimators are considered, analysed and compared with the proposed methods which are described in Chapter 4. These traditional estimators are LS, LMMSE, NLMS and RLS CE methods. Simple step by step procedures for deriving these marine-based estimators are elaborately documented for the benefits of intending readers in Addendum A of this thesis and are summarised as follows:

3.4.1 Conventional LS Channel Estimation

The least square channel estimate $\left(\hat{\mathbf{C}}_{LS}[D_i,i]\right)$ for estimating the oceanic transmission channel is given as [111]:

$$\hat{\mathbf{C}}_{LS}[D_i,i] = \left[\hat{\mathbf{C}}[1],\hat{\mathbf{C}}[2],...,\hat{\mathbf{C}}[d]\right] = \left[\frac{\mathbf{y}[1]}{\mathbf{g}[1]},\frac{\mathbf{y}[2]}{\mathbf{g}[2]},...,\frac{\mathbf{y}[d]}{\mathbf{g}[d]}\right] \tag{3.1}$$

where $\mathbf{y}[d]$ represents the received training signal as elaborated in 4.15 whose aggregated sensor information to be transmitted across the wireless maritime channel is denoted by $\mathbf{g}[d]$. The symbol $[D_i,i]$ is the set of DAs serving vessel i as fundamentally elaborated in Chapter 4 while d is the total number of DAs serving vessel i.

3.4.2 Linear MMSE Channel Estimation

The LMMSE channel estimate $\left(\hat{\mathbf{C}}_{LMMSE}[D_i,i]\right)$ can be generally expressed as [111, 112]:

$$\hat{\mathbf{C}}_{LMMSE}[D_i,i] = \mathbf{A}_{cy}[D_i,i]\mathbf{A}_{yy}^{-1}[D_i,i]\mathbf{y}[D_i,i] \tag{3.2}$$

where $\mathbf{A}_{cy}[D_i,i]$ represents the cross-covariance matrix between the channel $\mathbf{C}[D_i,i]$ and $\mathbf{y}[D_i,i]$ while $\mathbf{A}_{yy}[D_i,i]$ is the auto-covariance matrix of $\mathbf{y}[D_i,i]$. The above-mentioned matrices can be mathematically expressed as:

$$\mathbf{A}_{cy}[D_i,i] = \mathbb{E}\left[\mathbf{C}[D_i,i]\mathbf{y}^H[D_i,i]\right] = \mathbf{A}_{cc}[D_i,i]\mathbf{G}^H[D_i,i] \tag{3.3}$$

$$\mathbf{A}_{yy}[D_i,i] = \mathbb{E}\left[\mathbf{y}[D_i,i]\mathbf{y}^H[D_i,i]\right] = \mathbf{G}[D_i,i]\mathbf{A}_{cc}[D_i,i]\mathbf{G}^H[D_i,i] + \sigma_w^2\boldsymbol{I}[m] \tag{3.4}$$

where $\mathbf{G}[D_i,i] = \text{diag}\left[\mathbf{g}[D_i,i]\right]$ and σ_w^2 represents the variance of the zero mean complex white Gaussian noise $\mathbf{w}[D_i,i]$. Substituting (3.3) and (3.4) into (3.2) gives the LMMSE channel estimate as:

$$\hat{\mathbf{C}}_{LMMSE}[D_i,i] = \frac{\mathbf{A}_{cc}[D_i,i]\mathbf{y}[D_i,i]}{\mathbf{G}[D_i,i]\left[\mathbf{A}_{cc}[D_i,i] + (\mathbf{G}^H[D_i,i]\mathbf{G}[D_i,i])^{-1}\sigma_w^2\boldsymbol{I}[m]\right]} \tag{3.5}$$

3.4.3 NLMS Channel Estimation

To obtain improved CE performances based on the NLMS scheme, a cost function is deployed for minimizing the MSE of the maritime fading channel. This cost function is expressed as [113]:

$$\mathbf{J}_{cf}[D_i,i] = \mathbb{E}\left[|\boldsymbol{e}_r[D_i,i,i]|^2\right] = \mathbb{E}\left[\boldsymbol{e}_r[D_i,i]\ \boldsymbol{e}_r^*[D_i,i]\right] \tag{3.6}$$

where $\mathbb{E}$ signifies the expectation operator and $*$ represents complex conjugation. In this expression (3.6), $\boldsymbol{e}_r[D_i,i]$ denotes the CE error given in (3.7) where H represents the Hermitian transpose operator, while $\mathbf{J}_{cf}[D_i,i]$ signifies the cost function to be minimized.

$$\boldsymbol{e}_r[D_i,i] = \mathbf{y}[D_i,i] - \mathbf{C}^H[D_i,i]\mathbf{g}[D_i,i] \tag{3.7}$$

Furthermore, the term $\mathbf{C}^H[D_i,i]\mathbf{g}[D_i,i]$ is the inner product of the CH-aggregated sensor signal $\mathbf{g}[D_i,i]$ and the corresponding LS estimate as obtained from (3.1). Substituting the expression in (3.7) into (3.6), the cost function can then be written as the expression in (3.8),

$$\mathbf{J}_{cf}[D_i,i] = \mathbb{E}\left[(\mathbf{y}[D_i,i] - \mathbf{C}^H[D_i,i]\mathbf{g}[D_i,i])(\mathbf{y}^*[D_i,i] - \mathbf{C}[D_i,i]\mathbf{g}^H[D_i,i])\right] \tag{3.8}$$

where the expression $\boldsymbol{e}_r^*[D_i,i]$ as used in (3.6) is given as:

$$\boldsymbol{e}_r^*[D_i,i] = \mathbf{y}^*[D_i,i] - \mathbf{C}[D_i,i]\mathbf{g}^H[D_i,i] \tag{3.9}$$

To obtain the NLMS CE for the maritime communication, the LMS CE is first obtained after which it is then normalized using the power of the input signal according to (3.11). Hence, the LMS channel estimate of the marine communication network is given as:

$$\hat{\mathbf{C}}_{LMS}[D_i+1,i] = \mathbf{C}[D_i,i] + \mu\boldsymbol{e}_r^*[D_i,i]\mathbf{g}^H[D_i,i] \tag{3.10}$$

where μ is defined as a fixed positive step size parameter that is responsible for controlling the steady-state behaviour of the adaptive CE scheme which is designed to satisfy the condition $0 < \mu < 1$. The derivation of the LMS CE scheme is shown in Addendum A.3. If the expression $\mu\boldsymbol{e}_r^*[D_i,i]\mathbf{g}^H[D_i,i]$ as given in (3.10) is normalized by the power of input signal $\left(||\mathbf{g}^H[D_i,i]||^2\right)$ then the NLMS CE for the maritime communication system can be obtained as:

$$\hat{\mathbf{C}}_{NLMS}[D_i+1,i] = \mathbf{C}[D_i,i] + \frac{\mu\boldsymbol{e}_r^*[D_i,i]\mathbf{g}^H[D_i,i]}{||\mathbf{g}^H[D_i,i]||^2} \tag{3.11}$$

3.4.4 The Customary RLS Channel Estimation

The conventional RLS CE where the cost function to be minimized for the channel estimate is given as [45, 113]:

$$\mathbf{J}_{cf}[D_i,i] = \sum_{i=1}^{D_i} \mathbb{F}[D_i,i]|\boldsymbol{e}_r[D_i,i]|^2 \tag{3.12}$$

The symbol $\mathbb{F}[D_i,i]$ in (3.12) is the forgetting factor also known as weighting factor which assumes values in the range $0 << \mathbb{F}[D_i,i] < 1$. If λ is a positive constant chosen in the range $0 << \lambda < 1$, then the weighting factor can be expressed as:

$$\mathbb{F}[D_i,i] = \lambda^{D_i-1} \tag{3.13}$$

If $\bar{\boldsymbol{\Upsilon}}_{RLS}[D_i,i]$ is expressed as the inverse autocorrelation matrix of the transmitting signal, then the gain vector of the RLS maritime channel estimate is given as:

$$\vec{\eth}[D_i,i] = \frac{\lambda^{-1}\bar{\boldsymbol{\Upsilon}}^{-1}_{RLS}[D_i-1,i]\mathbf{g}[D_i,i]}{1+\mathbf{g}^H[D_i,i]\lambda^{-1}\bar{\boldsymbol{\Upsilon}}^{-1}_{RLS}[D_i-1,i]\mathbf{g}[D_i,i]} \tag{3.14}$$

where $\bar{\boldsymbol{\Upsilon}}^{-1}_{RLS}[D_i-1,i]$ is given as :

$$\bar{\boldsymbol{\Upsilon}}^{-1}_{RLS}[D_i-1,i] = \lambda^{-1}\bar{\boldsymbol{\Upsilon}}^{-1}_{RLS}[D_i-1,i] - \lambda^{-1}\vec{\eth}[D_i,i]\mathbf{g}^H[D_i-1,i]\bar{\boldsymbol{\Upsilon}}^{-1}_{RLS}[D_i-1,i] \tag{3.15}$$

Thus, the RLS channel estimate for the maritime communication system as derived in AddendumA.5 is given as:

$$\hat{\mathbf{C}}_{RLS}[D_i,i] = \hat{\mathbf{C}}_{RLS}[D_i-1,i] + \vec{\eth}[D_i,i]\boldsymbol{e}^*_r[D_i,i] \tag{3.16}$$

3.5 CHAPTER SUMMARY

As signals transmit over a wireless communication channel, they are likely t experience the unwanted effects of phenomena such as multipath propagation and signal attenuation (fading). In this chapter,

the concept of multipath propagation has been explicitly described. An incisive explanation and classification of the fading types that could be encountered in both terrestrial and nautical radio networks have been presented. More so, the channel models that could be adopted to statistically describe fading scenarios in both terrestrial and nautical radio networks is concisely presented while the rudiments and taxonomy of CE are presented for the IoMT. Finally, the customary estimators that have been adopted to validate the proposed methods of this study are mathematically described which includes the orthodox LS, LMMSE, NLMS and RLS estimation methods.

CHAPTER 4 SYSTEM MODEL DESCRIPTION

4.1 INTRODUCTION

It is worthy to mention that ten key enabling and contemporary technologies have been identified for the enhancement of the emerging fifth generation (5G) networks and beyond [114]. Some of these technologies include; D2D communications, big data & mobile cloud computing, millimetre wave communications, radio access techniques, wireless software-defined networking and the IoT. From the above-mentioned technologies, IoT technology can be described as a fascinating system of interconnected computing devices with crucial application scenarios in the fast emerging 5G networks and beyond. It is a well-known fact that IoT-based technologies are modelled to build a connected world by the incorporation of non-electronic everyday objects such as household appliances, buildings, roads, vehicles, cargoes etc., in such a manner that these objects communicate with one another and with the internet using embedded sensors, actuators and microprocessors [6, 10, 115–118]. As such, this indispensable technology (IoT) is essential in applications ranging from smart societies, industrial applications and security. In order to yield higher throughput while minimizing the cost of production/operation, the benefits of IoT technology can be exploited in the industries which consequently gives birth to the concept of Industrial IoT (IIoT). In the industries, IoT is deployed in sectors such as manufacturing, transportation, healthcare, smart energy and food production. Applications of IoT in the transportation sector include smart self-driving cars and parking, aviation management and maritime operations etc. Maritime transportation in particular is considered as a major conduit of international trade as over 80 % of intercontinental trade is transacted on the sea [119]. It is worth mentioning that the maritime industry (especially within African seaports) is faced with numerous binding constraints which may arise from either anthropogenic or naturogenic conditions such as delivery and traffic clearance delays, environmental degradation (oil and toxic waste spillages), congestion control management, insecurity, inefficient road networks and inadequate per-crane hours

etc [120]. The effects of these maritime limitations can be mitigated by deploring the IoT technology in what is know as the IoMT, where sensors are positioned at strategic locations to enhance the monitoring of maritime environments in addition to the prevention of disaster occurrences that may result from congestion/collision through assisted navigation while facilitating oceanographic data collection and analysis. Nevertheless, the realization of IoMT is limited by factors such as wide area coverages, efficient allocation/optimization of network resources, cost-effective communication, mobility management and secure signal transmission [121]. As such, reliable and high-speed devices with efficient data services are required in order to meet wide network coverage needs.

Satellite communication are reliable communication systems that provide high network data rate applications in addition to wide area networks. Be that as it may, these communication systems are not cost effective. Hence, there is need for developing alternative cost-effective sensor-based IoMT network technologies for improved operation of maritime activities as considered in this research work. When sensors are adopted to implement low-cost communication networks for maritime operations, extra efforts must be but in place to improve the communication quality in order to offer improved QoS and QoE to marine explorers. Since the aggregated sensor information to be transmitted over the maritime channel are low cost, low speed and low powered, especially due to the absence of carrier signal transmission, the transmitting CH information in an IoMT network is most likely to experience the effects of severe multipath propagation and fading. To mitigate these effects and to improve the communication quality, efficient CE technique is required in the pelagic network. Motivated by these reasons, the research work in this thesis proffers an IoT-based working solution to the challenges of network transmission and traffic management in the maritime environment by describing an IoT-enabled network architecture, where two CE techniques named RER CE and ISI/ANR CE are carefully proposed and evaluated for improving the QoS and QoE requirements of sea-going users. In the proposed ISI/ANR CE technique, we consider the effects of possible ISI that may arise from maritime transmissions in such a way that transformation using a low-pass filter is incorporated for eliminating the effects of channel noise in addition to the overall mitigation of the reverberations of multipath propagation. For realising the proposed RER technique, we normalise the Manhattan distance of the CIR and introduce a variable leakage factor controlled log-sum penalty function whose responsibility is to provide stability to the developed RER technique over existing techniques in all considered fading scenarios. A reweighting attractor is then added to further shrink the CE which then gives this scheme a performance advantage over all analysed estimators that generally find applications in terrestrial communication networks. As such, the contributions of this chapter are outlined as follows:

- An IoT-based framework is designed for improving the QoS requirements in application to maritime operations and management where off-shore navigating vessels are equipped with environmental sensing equipment in communication with a cluster head user equipment that transmit aggregated seawater sensor information via the marine channel to a shoreward located central BS.
- We propose two novel CE techniques for improving the performances of maritime communication systems named RER and ISI/ANR CE that both attempt to improve the performance of conventional schemes such as maximum likelihood (ML) based estimation and recursive least squares (RLS) techniques in order to reduce the CE error of the maritime communication network using combinational techniques that involve summing the instantaneous square error with a log-sum penalty which is subsequently realised by the normalisation of the Manhattan distance of the system CIR.
- We evaluate and document the QoS performance in terms of system data-rate, outage probability and QoS-guaranteed probabilities for improved nautical user QoE over signal transmission in both heavy frequent and light infrequent shadowing conditions of oceanic signal propagations.

The rest of this chapter is structured as follows. A system model description of our IoMT framework is described in Section 4.2 while the proposed CE methods are elaborately described in Section 4.3. The QoS requirements for nautical radio networks are expounded in Section 4.4 thereafter, the summary of this chapter is finally presented in Section 4.5.

4.2 SYSTEM MODEL DESCRIPTION OF PROPOSED MARITIME SYSTEM

The shore side of maritime environment as considered in our system is illustrated in Figure 4.1, where marine vessels are designed to effectively exploit the innumerable benefits of IoT technology in such a way that various varieties of sensors/MUE are embedded on vessels for monitoring diverse environmental and control system conditions. This is achieved by sending sensor information from well-positioned CH through coastline mounted DAs to a remotely located control station for essential analysis and decision making procedures. A description of the clustering process of the MUE that can propagate through Rayleigh fading channel to an on-shore mounted BS is described in this session.

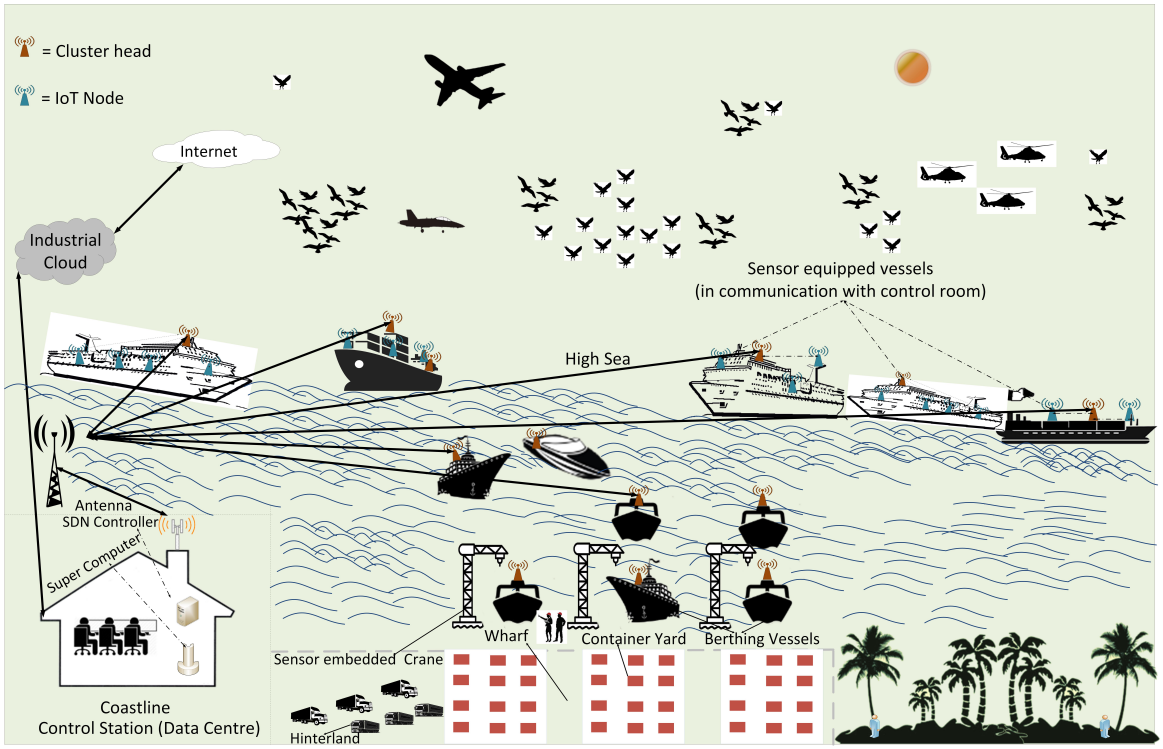

Figure 4.1. Framework structure of IoT-based Maritime Environment

4.2.1 Description of the Clustering Process

It is earlier mentioned that efficient and reliable communication methods such as sensor-based IoT technologies can be deployed during maritime operations for minimizing the blameworthy effects of maritime congestions in order to avoid ship-dock delays and marine accidents so that the QoE of marine users can be improved. The installation and exploitation of sensor networks around maritime vessels and the surroundings will alleviate the possibility of sudden/frequent occurrences of maritime queue formations, congestions and accidents since the sensor information can be configured to give maritime users early signals so as to make informed and early decisions for prevention of disaster occurrences. Consequently, relevant information such as the position, size, arrival time, unloading and departure time of individual ship can be predicted and collected for transmission to the seashore-located control station for processing in order to guarantee safe marine operations. Taking these points into consideration, there is a need to design suitable models for the transmission of the aggregated sensor information to the control station for decision making. As previously stated, individual vessels contain MUE known as cluster members (CM), where a CH is located in the centre of the vessel for signal transmission through the DA to the control station. If the set of oversea user type of equipment (i.e.

MUE) is represented as $E_i = \{1,2,3,...,e\}$ (where e is the total number of MUE on vessel i), while the set of DAs serving vessel i is represented as $D_i = \{1,2,3,...,d\}$ (where d is the total number of DAs serving vessel i), then the distribution of the maritime wireless sensor nodes can be modelled using a poison-based modified *Neyman-Scott* cluster process. This clustering process generally consists of a union of clusters having a parent point in addition to numerous offsprings, where the parent process is characterised by homogeneous and poison-distributed processes (with intensity λ_p) while the offspring processes (MUE) are independently dispersed (with intensity λ_o) around their parents [122–124]. Two special cases of the Neyman-Scott cluster processes are *Matérn* and *Thomas* cluster processes. The former cluster process can be deployed for delineating the operational activities of the sensor-based maritime environment if the sensors are uniformly distributed to form a ball of dimension d and radius R whose density function is represented as:

$$f_{U_M}(\boldsymbol{u}) = \begin{cases} \frac{dr^{d-1}}{R^d} & \|\boldsymbol{u}\| \leq \mathrm{R} \\ 0 & \text{otherwise} \end{cases} \tag{4.1}$$

where $\boldsymbol{u}$ in (4.1) represents the position (or location) of the MUE while r is a random variable that denotes the distance between a parent and offspring point in the Mat*é*rn cluster. On the other hand, if the clustering of the MUE is in accordance with a symmetric normal distribution (with variance σ^2), then the clustering process exhibits the characteristics of a Thomas cluster distribution. The Thomas cluster process is a more realistic distribution for simulating IoMT since the sensors are assumed to be scattered at various positions on individual vessels for environmental monitoring. Hence, if l_v and σ_n respectively represents the length of the vessel and the MUE clustering intensity, then the location of the MUE can be expressed using the Thomas cluster distribution as:

$$f_{U_T}(\boldsymbol{u}) = (2\pi\sigma_n^2)^{-\frac{d}{2}} \exp\left(-\frac{1}{2\sigma_n^2}\|\boldsymbol{u}\|^2\right) \quad \|\boldsymbol{u}\|^2 \leq l_v \tag{4.2}$$

Thus, sequential procedures for implementing the Thomas process for IoMT is presented as shown in Algorithm 4.1 while Figure 4.2 illustrates a bubble plot of the Poisson distributed Thomas cluster process for $\lambda_p = 5$ and $\sigma = 0.02$.

Algorithm 4.1 Sequential Procedures for Implementing Thomas Cluster-based Aggregated MUE

Input: $\{\lambda_p, \lambda_o, \sigma_n^2\}$

Output: $\{\mathbf{g}\}$

1: Generate area (size) of the extended maritime vessel.

2: Obtain parent-point stationary poison process using (λ_p) and the marine vessel size.

3: Generate random Poisson-based offspring process using (λ_o) and the number of Poisson point processes.

4: **for** $i = 1, 2, \ldots e$, **do**

5: Initiate relative positions/distribution of MUEs according to (4.2).

6: **end for**

Return: $\{\mathbf{g}\}$

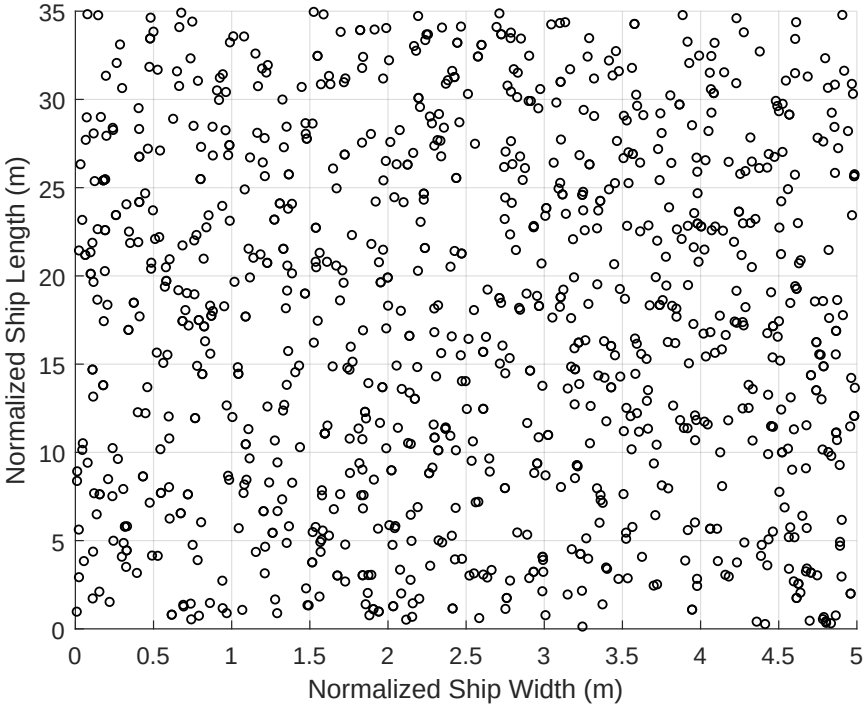

Figure 4.2. Thomas cluster-based distribution of MUE for IoMT with $(\lambda_p, \sigma) = (5, 0.02)$.

4.2.2 Channel Description

It is worth mentioning that physical obstacles such as trees, buildings and mountains are limited across the open ocean which consequently enables a LoS path to be present across transmitter and receiver. Even if the effects of shadow fading on transmitting signals is minimal on oceanic wave propagations, the attenuation of propagating symbols across maritime environments can still be adversely affected by the effects of multipath-induced fading, particularly in situations of extreme weather conditions since the network performances can be influenced by factors such as rain, fog, oceanic waves and ship movements. As a result of this territorial variability, the Nakagami-*m* fading channel distribution will be most appropriate for modelling such environmental channel-fading scenarios since it offers remarkable flexibility attributes by altering two positive-valued parameters namely *shape factor* (m) and *spread controlling parameter* (Ω). In this Nakagami-based channel model, the shape factor (sometimes referred to as *fading parameter*) is adopted for varying the shape of the channel distribution in accordance with the gravity of the fading signal such that ($m \geq \frac{1}{2}$). On the other hand, the spread parameter is utilized for manipulating the delay spread, where $(\Omega \geq 0)$. It is useful to note that the probability density function (PDF) of a Nakagami-*m* distribution is equal by definition to a Rayleigh fading distribution (where there is no LoS path) if $m = 1$. Whereas, this distribution will become a single-sided Gaussian distribution if $m \geq \frac{1}{2}$ and a uniform distribution in extreme scenarios when $m \rightarrow \infty$, thus confirming the flexibility of this channel model. Consequently, the Nakagami-*m* channel based on these parameters can be configured to enhance adaptive signal transmission over the communication channel in multipath fading environments. Nevertheless, n order to analyse, validate and document results in the performance analysis of the considered estimators, we consider the worst case Rayleigh fading scenario where $m = 1$.

Since it is required that the collected vessel sensor information be propagated across the high sea to the remotely mounted seashore DAs, if N is used to describe the multiplicative fading properties of the channel, then the overall distribution of the CIR with $\hat{\mathbf{c}}[D_i, i]$ random CIR is given as:

$$\mathbf{c}[D_i, i] \stackrel{\Delta}{=} \prod_{j=1}^{N} \hat{\mathbf{c}}_j[D_i, i] \tag{4.3}$$

The communication channel will exhibit the characteristics of a double Rayleigh fading channel

[125–127], when $N = 2$ as the received signals at DAs are generated by multiplying the numerous reflected sensor signals that are obtained when the coastline mounted antennas are in motion while communicating with the CHs of the nonstationary vessels. Furthermore, it is assumed that the coastline DAs are mounted thus stationary in position. Hence, the signal propagation can be modelled (in its worst-case scenario) as a Nakagami-*m* based single Rayleigh fading channel where the moment generating function (MGF) of $\mathbf{c}[D_i, i]$ is generally expressed as:

$$M_h(s) = \frac{1}{\sqrt{\pi}\prod_{j=1}^{N}\Gamma(m_j)} \times G_{2,N}^{N,2}\left(\frac{4}{s^2}\prod_{j=1}^{N}\left(\frac{m_j}{\Omega_j}\right)\middle|\begin{matrix}0.5, 1\\ m_1, m_2, \ldots, m_N\end{matrix}\right) \tag{4.4}$$

In (4.4), $G(.)$ is the *Meijer's G-function* as described in [128] while m is the shape factor that usually assume values but not limited to the range $0.5 < m \leq 1$. Furthermore, Ω in (4.4) represents the *spread controlling* parameter while $\Gamma(.)$ is the *gamma function* as defined in [128]. Taking the inverse Laplace transform (ILT) of the expression in (4.4) (i.e. $\mathscr{L}^{-1}(M_h(s))$, the PDF of $\mathbf{c}[D_i, i]$ in accordance with the Nakagami-*m* distribution is given as [129, 130]:

$$f_G(\boldsymbol{g}) = \frac{2}{\prod_{j=1}^{N}\Gamma(m_j)} G_{0,N}^{N,0}\left(\boldsymbol{g}^2\prod_{j=1}^{N}\left(\frac{m_j}{\Omega_j}\right)\middle|\begin{matrix}-\\ m_1, m_2, \ldots, m_N\end{matrix}\right) \tag{4.5}$$

where $\boldsymbol{g}$ is the transmitted sensor information. Using the expression in [131] given that $N = 1$ while bearing in mind that $e^{-x} = G_{0,1}^{1,0}\left(x\middle|\begin{matrix}-\\ 0\end{matrix}\right)$, the conditional PDF of the Nakagami-*m* fading channel is expressed as [132–134]:

$$f_G(\boldsymbol{g}) = \frac{2m^m}{\Omega^m\Gamma(m)}\boldsymbol{g}^{2m-1}\exp\left(-\frac{m}{\Omega}\boldsymbol{g}^2\right) \tag{4.6}$$

Two properties can be used to describe the characteristics of the Rayleigh fading channel. These properties are power spectral density (PSD) and the autocorrelation function (ACF). The PSD of the Rayleigh fading channel coefficients is given as [45]:

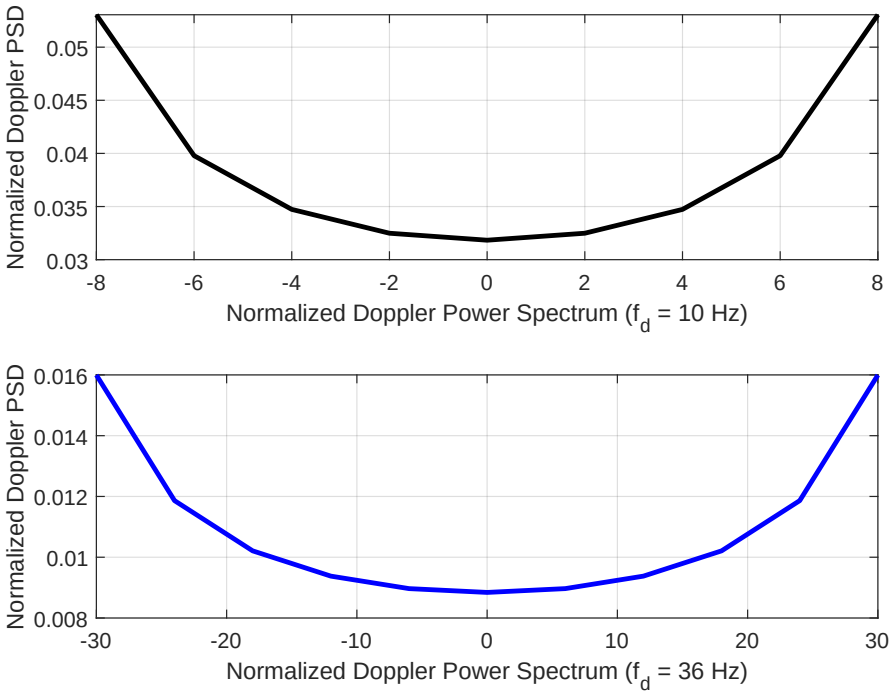

Figure 4.3. u-shaped Jakes spectrum corresponding to $f_d = 10$ Hz and 36 Hz respectively

$$s|f| = \begin{cases} \frac{1}{\pi f_d \sqrt{1-\left(\frac{f}{f_d}\right)^2}} & |f| \leq f_d \\ 0 & otherwise \end{cases}$$

while the corresponding autocorrelation function is represented as:

$$a[D_i, i] = J_0(2\pi f_d T_s |D_i|) \tag{4.7}$$

Equation (4.7) represents the u-shaped band-limited Jakes spectrum as shown in Figure 4.3, where information is provided about the PSD of the propagating signal at a range of frequencies given that the Doppler frequencies are 10 Hz and 36 Hz respectively. The corresponding Bessel function-based ACF of the channel is represented in Figure 4.4. In the expression in (4.7), f_d is the maximum Doppler frequency of the variable channel given as $f_d = \frac{v}{\lambda_w}$, where v is the velocity of the mobile CH while λ_w is the wavelength of the propagating symbols. Furthermore, $J_0(\cdot)$ is described as the zeroth-order Bessel function of the first kind while the symbol period and the normalized Doppler frequency (i.e.

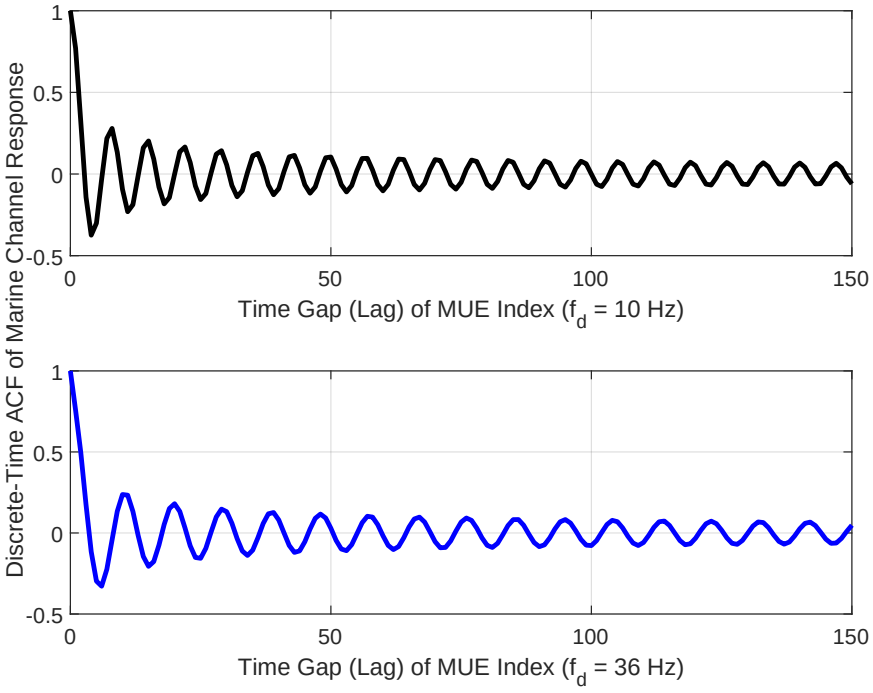

Figure 4.4. Plot of channel ACF corresponding to $f_d = 10$ Hz and 36 Hz respectively

Doppler rate) is respectively given as T_s and $f_d T_s$. The correlation coefficients obtained from (4.8) can be used to form a correlation matrix $\mathbf{A_{cc}}$ whose expanded form as a function of the ACF is represented as:

$$\mathbf{A_{cc}}[D_i] = \begin{bmatrix} a[1] & a[2] & \dots & a[d] \\ a[2] & a[1] & \dots & a[(d-1)] \\ \vdots & \vdots & s & \vdots \\ a[d] & a[(d-1)] & \dots & a[1] \end{bmatrix} \tag{4.8}$$

The channel fading coefficients can be realized using a complex recursive dth-order time-domain autoregressive process in the order of $AR(d)$ given as:

$$\mathbf{c}[D_i] = \sum_{i=1}^{d} \mathbf{z}[i]\mathbf{c}[D_i - i] + \boldsymbol{\vartheta}[D_i] \tag{4.9}$$

where $\boldsymbol{\vartheta}[D_i]$ is a zero mean additive white Gaussian noise process with variance given as σ^2_{ϑ} while $\mathbf{z}[i]$ is mathematically formulated as:

$$\mathbf{z}[i] = -\boldsymbol{\rho}[i] \tag{4.10}$$

If T represents the transpose operator, then the symbol $\boldsymbol{\rho}[i]$ as used in (4.10) is define as:

$$\boldsymbol{\rho}[i] = [\rho[1], \rho[2], \ldots, \rho[d]]^T \tag{4.11}$$

besides, the variance of the noise process (σ^2_{ϑ}) can be represented as:

$$\sigma^2_{\vartheta} = a[1] + \sum_{i=1}^{d} \boldsymbol{\rho}[i]\boldsymbol{a}[i] \tag{4.12}$$

The coefficients of the AR model parameters $\boldsymbol{\vartheta}[D_i]$ can be obtained using the Yule-walker equation [113] define as:

$$\boldsymbol{\rho}[i] = -\mathbf{A_{cc}}^{-1}[i]\mathbf{b}[i] \tag{4.13}$$

where,

$$\mathbf{b}[i] = [a[1], a[2], \ldots, a[d]] \tag{4.14}$$

A sequential procedure for implementing the maritime channel assuming Rayleigh fading is demonstrated using Algorithm 4.2.

4.2.3 Receiver Description

It has been earlier mentioned that as marine vessels navigate across the high sea to the dock areas, the CHs in this IoMT system attempt to communicate with numerous seashore-mounted DAs as shown in Figure 4.5. A set of the coastal-mounted DAs configured to serve a particular vessel (or cluster) is known as a service cloud and the signals received at the cloud serving vessel i is given as:

$$\mathbf{y}[D_i, i] = \mathbf{C}[D_i, i]\mathbf{g}[D_i, i] + \mathbf{w}[D_i, i] \tag{4.15}$$

where $\mathbf{C}[D_i, i]$ is a $d \times d$ diagonal matrix containing the channel coefficients that is obtained resulting

Algorithm 4.2 Implementation of the Maritime Channel assuming Rayleigh Fading ($m = 1$).

Input: $\{f_d, T_s, d\}$

Output: $\{\mathbf{c}\}$

1: Generate autocorrelation vector of (4.3) as follows:
2: **for** $d = 0 : 1 : d - 1$, **do**
3: $a = bessel\,j(2\pi f_d T_s d)$.
4: **end for**
5: Then formulate Toeplitz autocorrelation matrix ($\boldsymbol{A}_{cc}$) according to (4.8).
6: Calculate the marine channel fading coefficients as follows:
7: **Step 1**: Obtain vector **b** using (4.14) and solve the resulting Yule-Walker equation using (4.13). Then compute **z** using (4.10).
8: **Step 2**: Calculate the variance of the noise process (σ^2_{ϑ}) by initializing Sum = 0,
9: **for** $i = 2 : 1 : length(\mathbf{z})$, **do**
10: $U_\rho = \boldsymbol{\rho}(i).a(i)$
11: Sum = Sum + U_ρ
12: **end for**
13: $\sigma^2_{\vartheta} = \mathbf{b}(1,1) + \text{Sum}$ % variance of the Gaussian white noise process.
14: **Step 3**: Generate zero mean AWGN ($\boldsymbol{\vartheta}$) according to (4.9) using the value of σ^2_{ϑ} obtained above.
15: **Step 4**: Initialize the channel coefficients as follows:
16: $c = \text{zeros}(1, d+1)$,
17: $c(1,1) = \text{randn}(1,1) + j*\text{randn}(1,1)$

Algorithm 4.2 Implementation of the Maritime Channel assuming Rayleigh Fading ($m = 1$).

Step 5: Calculate the CIR as follows:
for $ii = 2:1:d+1$, **do**
    $b_1 = []$, % initialization (empty matrix)
    for $k = 1:1:ii-1$, **do**
        $b_2 = z(k).c(ii-k)$,
        $b_3 = [b_1 \;\; b_2]$, % concatenate vectors
        $b_3 = sum(b_1(1,:))$,
        $b_4 = b_3 + \vartheta(ii-1)$
    end for
$c(ii) = b_4$
end for
$c = c(2{:}end)$
Return: {**c**}

from fading effects while $\mathbf{g}[D_i, i]$ denotes the transmitted information signal vector that is received at the DAs. Lastly, $\mathbf{w}[D_i, i]$ represents the zero mean complex white Gaussian noise with a variance σ_w^2 such that $w \sim \mathcal{N}(0, \sigma_w^2)$ while the received signal at service cloud i is given by $\mathbf{y}[D_i, i]$ such that $y \sim \mathcal{N}(\mathbf{C}\,\mathbf{g}[D_i, i], \sigma_w^2)$. If the distance between the coastline-based DA a_k and vessel i is denoted as $z_{ak,i}$ while the path loss due to this distance from antenna is represented as $z_{ak,i}^{-\alpha}$, then the noise variance σ_w^2 is expressed as:

$$\sigma_w^2 = \frac{\overline{E}_p \sum_{k=1}^{d} \|\mathbf{C}_{ak,i}\|^2 z_{ak,i}^{-\alpha}}{\gamma_i} \tag{4.16}$$

where the symbol α is regarded as the path loss exponent that takes value from 2 (free space propagation) to 6 (no LoS Propagation) [135]. In (4.16), $\overline{E}_p$ represents the power of the CH-aggregated signal given as $\mathbb{E}\left[\mathbf{g}^2[D_i, i]\right]$, where $\mathbb{E}$ denotes the expectation operator and $\|.\|$ signifies Euclidean norm while γ_i is the SNR at the receiver side.

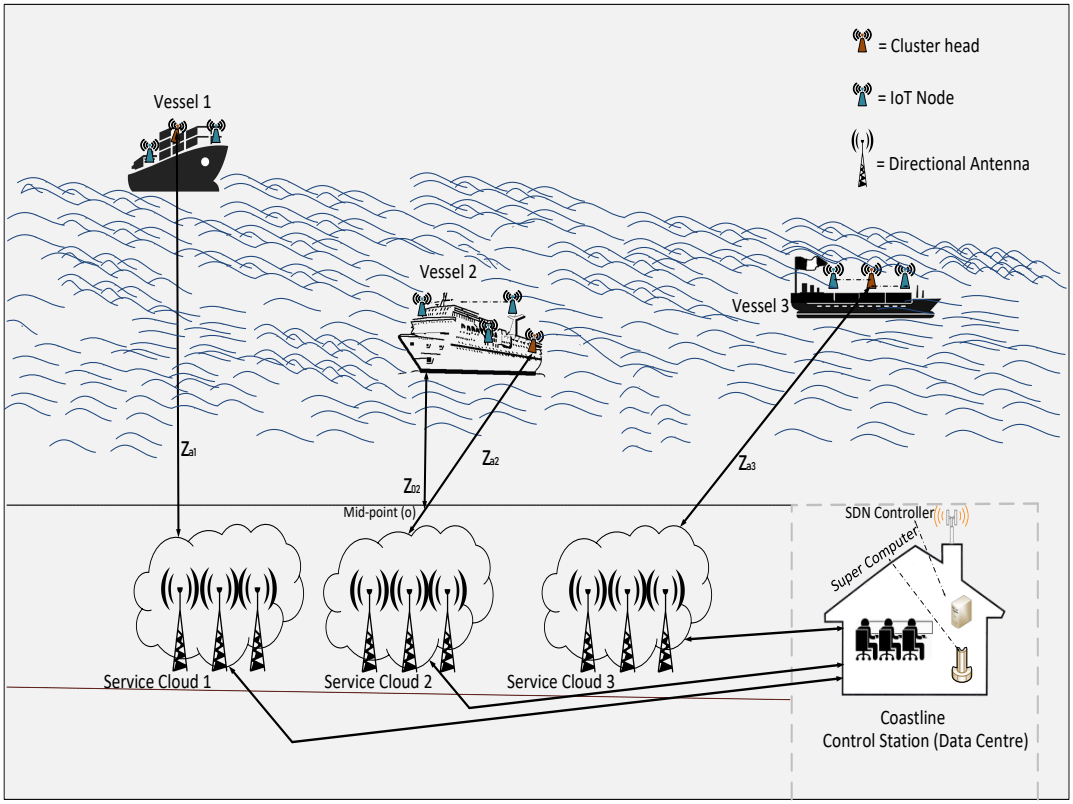

Figure 4.5. Illustration of cluster head communication with service clouds

4.3 DESCRIPTION OF PROPOSED ESTIMATORS

In this thesis, two channel estimators are proposed for estimating maritime transceivers which are based on improving the performances of conventional ML and RLS-based CE schemes for estimating the maritime fading channel conditions, where their performances are compared with conventional CE schemes such as normalised least mean squares (NLMS) and linear minimum mean square error (LMMSE) estimators. This is achieved by designing the estimators in such a manner that extra stability is given to enhance the quality of marine signals that are received over situations of both severe and non-severe environmental setups. The proposed estimation schemes are named ISI/ANR and RER channel estimators respectively and all estimators considered for implementation and comparison in our nautical communication framework are described in Chapter 3.

4.3.1 Proposed ISI/ANR Channel Estimator for Maritime Communication

The PDF of receiving a CH signal over the wireless fading channel is given as:

$$f_Y(\mathbf{y}[D_i,i]) = \frac{1}{\sqrt{2\pi\sigma_w^2}} \exp\left(-\frac{1}{2\sigma_w^2}\Big(\mathbf{y}[D_i,i] - \mathbf{C}[D_i,i]\mathbf{g}[D_i,i]\Big)^2\right) \tag{4.17}$$

whereas, the joint PDF of the received signal vector (also referred to as the likelihood function of the channel estimate $\Lambda_L[\mathbf{y}[D_i,i],\mathbf{C}]$) is given as the product of the PDFs of the individual received signals which is represented as:

$$\Lambda_L[\mathbf{y}[D_i,i],\mathbf{C}] = \left(\frac{1}{\sqrt{2\pi\sigma_w^2}}\right)^d \exp\left(-\frac{1}{2\sigma_w^2}\sum_{k=1}^{d}\Big(\mathbf{y}[k] - \mathbf{C}[k]\mathbf{g}[k]\Big)^2\right) \tag{4.18}$$

The natural logarithm of the above-expressed likelihood function is represented as:

$$\Lambda_{\log L}[\mathbf{y}[D_i,i],\mathbf{C}] = d\ln\left(\frac{1}{\sqrt{2\pi\sigma_w^2}}\right) - \left(\frac{1}{2\sigma_w^2}\sum_{k=1}^{d}\Big(\mathbf{y}[k] - \mathbf{C}[k]\mathbf{g}[k]\Big)^2\right) \tag{4.19}$$

Thus, the maximum likelihood estimate of the fading channel which is explicitly proven in AddendumA.4. is obtained by maximizing the log-likelihood function given as:

$$\hat{\mathbf{C}}_{ML}[D_i,i] = \frac{\sum_{k=1}^{d} y[k]g[k]}{g^2[k]} \tag{4.20}$$

When the maritime communication channel experiences frequent heavy shadowing, there is a possibility that ISI may likely occur which is capable of degrading the reliability of maritime communication systems since propagating signals can face unpleasant distortions. To avoid spreading successive symbols beyond their assigned intervals, there is a need for CE procedures to re-consider the effects of possible ISI that may occur during transmission of sensor information in the maritime communication network. To minimize the effects of ISI in addition to channel noise during operation of coastal

networks, the use of low-pass filtering can be incorporated for estimating the channel transfer function in order to significantly reduce the detrimental effects of these undesired phenomena. Inspired by the work in [136], we propose a novel CE technique that aims to improve the performances of conventional ML CE scheme, where the repercussions of the channel noise in addition to possible ISI that may result from multipath propagation are put into consideration. Our proposed improved ML-based CE scheme is named ISI/ANR channel estimation. Here, we reduce the upshot of noise by averaging the estimated channel parameters that are obtained from the ML estimation already established in (4.20). Consequently, the resulting ISI/ANR CE technique obtained by averaging the noise variance of the channel using the number of distributed antennas for augmenting the marine channel, provided that the expression in (4.15) is substituted into (4.20) is represented as:

$$\hat{\mathbf{C}}_{ML_{AV}}[D_i,i] = g^{-2}[k]\left[\sum_{k=1}^{d}\left[\left(C[D_i,i]g[D_i,i]+d^{-1}w[D_i,i]\right)g[k]\right]\right] \tag{4.21}$$

Since the noise variance of the conventional ML-based channel estimate has been averaged to $\left[d^{-1}\sigma_w^2\right]$, the damaging consequences that can be potentially introduced by the noisy components of the maritime system are sequentially reduced. Taking the possibilities of signal distortions due to ISI into account, we further consider designing the maritime channel to meet the Nyquist ISI criterion by normalizing the combined ramifications of the channel noise and the ISI components using the Frobenius norm of the noise reduced ML-based channel estimate according to (4.21). As such, the noise-reduced transfer function of the maritime channel is given as:

$$\hat{\mathbf{C}}_{ANR}[D_i,i] = g^{-2}[k]\left[\sum_{k=1}^{d}\left[\left(C[D_i,i]g[D_i,i]+\frac{1}{\|\mathbf{C}_{ML}[D_i,i]\|_F}\left(\vec{I}[D_i,i]+d^{-1}w[D_i,i]\right)\right)g[k]\right]\right] \tag{4.22}$$

where $\|.\|_F$ is the Frobenius norm operation while the expression $\left[\frac{1}{\|\mathbf{C}_{ML}[D_i,i]\|_F}\left(\vec{I}[D_i,i]+d^{-1}w[D_i,i]\right)\right)\right]$ consisting of the ISI component is a zero mean random Gaussian noise process. Because the channel conditions are known to change rapidly over time especially when the system experiences heavy shadowing/fading, the need to create system stability is inevitably required. As such, transformation using lowpass filtering is needed such that the modified ML-based channel transfer function for the maritime communication for noise reduction and ISI mitigation is written as:

$$\hat{\mathbf{C}}_T[t] = \sum_{k=1}^{d} \hat{\mathbf{C}}_{ANR}[k] \exp\left(-j\frac{2\pi}{d}kt\right) \tag{4.23}$$

where t is the transformation index that takes values from $t \in [1,d]$ and reflects the variation speed of the frequency selective fading channel. To achieve lowpass filtering, the signals at high-frequency regions are zero-padded since the noise and ISI components are spread over this region while the vessel propagating sensor signal component is located at the lower frequency region.

4.3.2 Description of the Proposed RER Channel Estimator

In this section, a description of our proposed RER CE algorithm is presented. Motivated by the concepts presented in [137, 138], we develop the proposed RER CE technique for our maritime communication system by formulating a new heuristic approach where the cost-function of the traditional RLS-based CE according to (3.12) is modified. In this modification, the aforementioned cost function is combined with a log-sum penalty presented as.

$$\mathbf{J}_{cf_p}[D_i,i] = \sum_{i=1}^{D_i} \lambda^{D_i-1} |\boldsymbol{e}_r[D_i,i]|^2 + \hat{\varepsilon} \sum_{i=1}^{D_i} \log\left(1 + \ddot{\varepsilon}^{-1} \left\|C[D_i,i]\right\|_1\right) \tag{4.24}$$

In the formulation of our RER heuristic, the Manhattan (or $L1$ norm) distance of the CIR is taken, which is subsequently normalised by a stability constant $(\ddot{\varepsilon})$ whose responsibility is for correcting any potential numerical system instability that may arise during the updating stages of the CIR. In order to decrease the received signal error, the log-sum penalty function is eventually multiplied by an adjustable leakage factor $(\hat{\varepsilon})$ that provides additional stability to the oscillating channel behaviour in addition to minimizing the stalling of the channel coefficients under different marine fading conditions. This leakage factor takes value in the range $0 \leq \hat{\varepsilon} \ll 1$ and can be made adaptive using the variable leakage factor technique presented in [139] expressed as:

$$\hat{\varepsilon}[D_i+1] = \hat{\varepsilon}[D_i] - \mu\Upsilon \boldsymbol{e}_r^*[D_i,i]\mathbf{C}[D_i,i]\mathbf{g}^H[D_i,i] \tag{4.25}$$

where $\left[\Upsilon = \frac{\mu\hat{\varepsilon}}{\ddot{\varepsilon}}\right]$. If $\varepsilon = \ddot{\varepsilon}^{-1}$, then the proposed RER channel estimate for maritime communication networks is then given as:

$$\hat{\mathbf{C}}_{RER}[D_i+1,i] = \mathbf{C}[D_i,i] - \Upsilon[D_i,i]\frac{\text{sgn}\mathbf{C}[D_i,i]}{1+\varepsilon\mathbf{C}[D_i,i]} + \mu\vec{\eth}[D_i,i]\boldsymbol{e}_r^*[D_i,i] \tag{4.26}$$

In (4.26), the expression $\left[-\Upsilon[D_i,i]\frac{\text{sgn}\mathbf{C}[D_i,i]}{1+\varepsilon\mathbf{C}[D_i,i]}\right]$ is a reweighting attractor that is adopted for shrinking (or reducing) the CE error. Additionally, the sgn function as used in this expression is the signum function which is defined as:

$$\text{sgn}(\hat{C}) = \begin{cases} \frac{\hat{C}}{|\hat{C}|} & \text{if } \hat{C} \neq 0 \\ 0 & \text{if } \hat{C} = 0 \end{cases} \tag{4.27}$$

4.4 QOS REQUIREMENT ANALYSIS AND EVALUATION

The performance of the proposed maritime architecture according to Figure 4.1 can be described and analysed for the CH-DA links in terms of data rate, outage probability and the QoS-guaranteed probability. The aforementioned performance indices are for our maritime communication system as follows:

4.4.1 Average Data Rate Requirement for ship-DA link

Since the conditions of the wireless transmission channel of the marine environment fluctuates over time and can be adversely affected by multipath propagation and heavy shadowing, we model the average capacity of the IoMT network while exploiting the flexibility of the Nakagami-fading channel model in such a manner that situations of frequent heavy and infrequent light shadowing conditions are considered. As a result, the average data rate requirement of a ship navigating over Rayleigh fading conditions (where there is no LoS path between the aggregated CH signal and the BS-mounted DA) is analysed in addition to the Rician-fading scenarios where there is often a LoS component between

DA-vessel transmission for maritime decision-making procedures as respectively presented in Sections 4.4.1.1 and 4.4.1.2.

4.4.1.1 Average Capacity under Rayleigh fading Channel

The maritime communication network is diagrammatically described in Figure 4.5. In this figure, multiple offshore-positioned vessels are in communication with the seashore-mounted service cloud DAs. The achievable data rate (or capacity) of vessel i (denoted as $\vec{\mathring{R}}_i$) is mathematically given as [140]:

$$\vec{\mathring{R}}_i = \mathbb{E}_{\mathbf{C}[D_i,i]}\left[\log_2\left(1+\gamma_i\right)\right] \tag{4.28}$$

where the SNR (γ_i) can be obtained from the expression in (4.16). As such, the expression in (4.28) becomes:

$$\vec{\mathring{R}}_i = \mathbb{E}_{\mathbf{C}[D_i,i]}\left[\log_2\left(1+\frac{\overline{E}_p\sum_{k=1}^{d}\|\mathbf{C}_{ak,i}\|^2 z_{ak,i}^{-\alpha}}{\sigma_w^2}\right)\right] \tag{4.29}$$

From (4.29), let $\hat{\tau}_h$ be represented as:

$$\hat{\tau}_h = \sum_{k=1}^{d}\|\mathbf{C}_{ak,i}\|^2 z_{ak,i}^{-\alpha} \tag{4.30}$$

For simplicity, if $\zeta_k = z_{ak,i}^{-\alpha}$ then, the PDF of the generalized Erlang random variable according to the expression in (4.30) can be represented as:

$$f_{\hat{\tau}_h}(\mathbf{g}) = \sum_{k=1}^{d}\varpi_k(0) z_{ak,i}^{-\alpha}\exp(-z_{ak,i}^{-\alpha}g) = \sum_{k=1}^{d}\varpi_k(0)\zeta_k\exp(-\zeta_k g) \tag{4.31}$$

where $\varpi_k(0)$ is the *Lagrange* basis polynomial in relation to ζ_k given as:

$$\varpi_k(0) = \prod_{\substack{0 \le \dot{m} \le d \\ \dot{m} \ne k}}^{d} \frac{\zeta_{\dot{m}}}{\zeta_{\dot{m}} - \zeta_k} \tag{4.32}$$

Thus, the data rate of vessel i as derived in Addendum B.1 can be formulated as:

$$\vec{\mathring{R}}_i = -\frac{1}{\log_e(2)} \sum_{k=1}^{d} \varpi_k(0) \left[\left(e^{-\zeta_k g} \log_e \left(1 + \frac{\overline{E}_p g}{\sigma_w^2} \right) \right) + \left(e^{\frac{\zeta_k \sigma_w^2}{\overline{E}_p}} E_1 \left(\zeta_k g + \frac{\zeta_k \sigma_w^2}{\overline{E}_p} \right) \right) \right] \tag{4.33}$$

4.4.1.2 Average Capacity assuming shadowed-Rician fading

The average data rate of vessel i over the maritime communication network assuming shadowed Rician fading is expressed as [3, 141]:

$$\vec{\mathring{R}}_i = \frac{1}{\ln 2} \int_0^{\infty} \ln(1 + \bar{\gamma} g) \, f_{\|\mathbf{C}[D_i,i]\|^2}(g) \mathrm{d}g \tag{4.34}$$

where $\bar{\gamma}$ can be obtained from (4.16) as the ratio of the power of the CH-aggregated information to the noise variance. In the expression (4.34), the PDF $f_{\|\mathbf{C}[D_i,i]\|^2}(g)$ can be obtained for shadowed Rician fading by taking the ILT of the MGF of $\|\mathbf{C}[D_i,i]\|^2$, where the MGF of $\|\mathbf{C}[D_i,i]\|^2$ is given as:

$$M_{\|\mathbf{C}[D_i,i]\|^2}(s) = \frac{\eta (s+1)^{(1-\min[|D_i|,\varphi])}}{(2P_E)^{(2-\min[|D_i|,\varphi])} (s+\eta)^{m|D_i|}} \tag{4.35}$$

The notations m and Ω are as define in Section 4.2.2 while η and φ are mathematically expressed as $\eta = \frac{m}{2mP_E + \Omega}$ and $\varphi = max[|D_i|, \lfloor m|D_i| \rfloor]$ respectively. Furthermore, the greatest of the two positive integers is chosen for the $max[.,.]$ operation while the smallest is chosen for the $min[.,.]$ operation. Finally, the symbol $\lfloor . \rfloor$ is the floor operation which represents the largest integer not greater than the expression $(.)$ while $2P_E$ is the average power of the multipath component. Taking the ILT of (4.35), the PDF of the SNR (γ_i) given that $(\gamma_i) > 0$ is expressed as:

$$f_{\gamma_i}(g) = \sum_{\hat{l}=0}^{\xi} \binom{\xi}{\hat{l}} .(2P_E)^{((m-1)|D_i|)} \Big(\mathcal{F}(g,\hat{l},\varphi,\bar{\gamma}_i) + \eta\phi\mathcal{F}(g,\hat{l},\varphi+1,\bar{\gamma}_i)\Big)dg \tag{4.36}$$

where $\xi = (\varphi - |D_i|)^+$ and $(g)^+$ shows that if $g \leq 0$ then use $g = 0$. In addition, the function $\mathcal{F}(g,\hat{l},\varphi,\bar{\gamma}_i) = \frac{\eta^{(m|D_i|-\varphi)}}{\bar{\gamma}_i^{\frac{1}{2}(\varphi-\hat{l})}\Gamma(\varphi-\hat{l})} .g^{\frac{1}{2}(\varphi-\hat{l})-1} \exp(-\frac{\eta}{2\bar{\gamma}}g) \left[M_{\frac{1}{2}(\eta+\hat{l}),\frac{1}{2}(\varphi-\hat{l}-1)}\left(\frac{\eta}{\bar{\gamma}g}\right)\right]$, while $M_{a,b}(.)$ is the Whittaker function bearing in mind that the symbol ϕ in (4.36) is given as $\phi = \frac{\omega(m|D_i|-\varphi)}{2mP_E}$. Converting the expression in (4.36) to its Kummer's function equivalent and simplifying further as derived in AddendumB.3 gives the average data rate expression (assuming shadowed Rican fading) presented as:

$$\vec{\mathring{R}}_i = \frac{1}{\ln 2}(2P_E)^{\left((m-1)|D_i|\right)} .\eta^{(m|D_i|-\varphi)} \sum_{\hat{l}=0}^{\xi} . \left[\left(\frac{\eta^{-(\varphi-\hat{l})}}{\Gamma(\varphi)}\right) G_{4,3}^{2,3}\left(\frac{-\bar{\gamma}}{\eta}\middle| \begin{matrix} -\varphi+\hat{l}+1,1,1,0 \\ \hat{l},1,0 \end{matrix}\right) \right.$$
$$\left. + \left(\frac{\phi.\eta^{\varphi-\hat{l}-1}}{\Gamma(\varphi+1)}\right) .G_{4,3}^{2,3}\left(\frac{-\bar{\gamma}}{\eta}\middle| \begin{matrix} -\varphi+\hat{l},1,1,0 \\ \hat{l},1,0 \end{matrix}\right) \right] \tag{4.37}$$

4.4.2 QoS Requirement Evaluation for ship-DA link

In this section, the outage probability and the QoS-guaranteed probability evaluation for CH-DA communication is formulated.

4.4.2.1 Outage Probability for CH-DA Communication

A certain minimum signal level (or threshold) is required for acceptable performance of maritime communication networks. If excellent communication techniques are not well developed for the maritime communication systems, then the CH-DA transmission processes may experience outages that may result from the devastating effects of environmental fading conditions. Outage probability (P_{out}) is a useful metric (or parameter) that is required for the characterisation of network performances in communication systems and can simply be described as the probability that the received information rate falls below a certain required threshold, which further describes the probability that a system outage will take place over a specified period. For the described maritime communication system, the

outage probability of the vessel-DA transmission is symbolically defined as $\left[P_{out}(\gamma_i) \triangleq P_{out}(\gamma_i \leq \gamma_i^{th}) = P_{out}(\vec{R}_i \leq \vec{R}_i^{th}) = F_{\vec{R}_i}(\vec{R}_i^{th})\right]$,where $Pr(.)$ denotes probability and $F_{\vec{R}_i}(.)$ represents the cumulative density function (CDF) such that $\left[F_{\vec{R}_i}(g) = \int_0^g f_{\vec{R}_i}(g)dg\right]$ and $f_{\vec{R}_i}(.)$ is the PDF as previously described.

It can be observed from (4.29) that the data rate for the clustered maritime communication system assuming Rayleigh fading scenarios is given as $\vec{R}_i = \left[\log_2\left(1+\frac{\overline{E}_p\hat{\tau}_h}{\sigma_w^2}\right)\right]$. From this expression, if $\hat{\tau}_h$ is expressed in terms of the data rate, then the outage probability of the vessel- DA link can easily be computed bearing in mind that $P_{out}(\gamma_i) = F_{\hat{\tau}_h}(\hat{\tau}_h)$. Thus, after simple mathematical analysis, it can easily be deduced that $\left[\hat{\tau}_h = \frac{\sigma_w^2}{\overline{E}_p}\left(e^{\vec{R}_i \log_e 2} - 1\right)\right]$. Consequently, the outage probability of the maritime system under non-LoS (NLOS) propagations can be simply be expressed as:

$$P_{out}\left(\vec{R}_i^{th}\right) = F_{\hat{\tau}_h}(\hat{\tau}_h) = F_{\hat{\tau}_h}\left(\frac{\sigma_w^2}{\overline{E}_p}\left(e^{\vec{R}_i \log_e 2} - 1\right)\right) \tag{4.38}$$

Solving the expression in (4.38) yields the Rayleigh fading outage probability given as:

$$P_{out}\left(\vec{R}_i^{th}\right) = \frac{1}{\log_e(2)}\sum_{k=1}^{d}\varpi_k(0)\left[-\left(e^{-\zeta_k\left(\frac{\sigma_w^2}{\overline{E}_p}\left(e^{\vec{R}_i\log_e 2}-1\right)\right)}\log_e\left(1+\frac{\overline{E}_p\left(e^{\vec{R}_i\log_e 2}-1\right)}{\sigma_w^2}\right)\right.\right.$$
$$\left.\left.+\left(e^{\frac{\zeta_k\sigma_w^2}{\overline{E}_p}}E_1\left(\zeta_k\left(e^{\vec{R}_i\log_e 2}-1\right)+\frac{\zeta_k\sigma_w^2}{\overline{E}_p}\right)\right)\right)\right] \tag{4.39}$$

Since the CDF of the outage probability is expressed as $F_{\vec{R}_i}(g) = \int_0^g f_{\vec{R}_i}(g)dg$ and the data rate requirement of the ith vessel according to (4.28) is generally related to the SNR as $\vec{R}_i = \left[\log_2\left(1+\gamma_i\right)\right]$, then the outage probability assuming Rician fading channel can be obtained if γ_i (in the above data rate expression) is made the subject of the relation. Hence,

$$P_{out}\left(\vec{\delta}_i^{th}\right) = F_{\gamma_i}(\exp(\log_e 2.\vec{\delta}_i^{th}) - 1) = \sum_{\hat{l}=0}^{\xi} \binom{\xi}{\hat{l}} .(2P_E)^{((m-1)|D_i|)} \Big(\mathcal{G}(g,\hat{l},\varphi,\bar{\gamma}_i) + \eta\phi\mathcal{G}(g,\hat{l},\varphi+1,\bar{\gamma}_i)\Big) dg \tag{4.40}$$

where $g = (e^{(\log_e 2.\vec{\delta}_i^{th})} - 1)$ while from the expression shown in (4.40), $\mathcal{G}(g,\hat{l},\varphi,\bar{\gamma}_i)$ is given as:

$$\mathcal{G}(g,\hat{l},\varphi,\bar{\gamma}_i) = \int_0^g \mathcal{F}(g,\hat{l},\varphi,\bar{\gamma}_i) = \int_0^g \mathcal{F}(g,\hat{l},\varphi,\bar{\gamma}_i) = \left[\frac{\eta^{(m|D_i|-\varphi)}}{\bar{\gamma}_i^{\frac{1}{2}(\varphi-\hat{l})}\Gamma(\varphi-\hat{l})} . \left(e^{\left(\log_e 2.\vec{\delta}_i^{th}\right)} - 1\right)^{\frac{1}{2}(\varphi-\hat{l})-1} .\exp\left(-\frac{\eta}{2\bar{\gamma}}.(e^{\left(\log_e 2.\vec{\delta}_i^{th}\right)} - 1)\right)\right] \times \left[M_{\frac{1}{2}(\eta+\hat{l}),\frac{1}{2}(\varphi-\hat{l}-1)}\left(\frac{1}{\bar{\gamma}}\right).\left(\frac{\eta}{(e^{(\log_e 2.\vec{\delta}_i^{th})} - 1)}\right)\right] \tag{4.41}$$

The equation in (4.40) is thus, the outage probability expression of ship i in relation to the rate threshold $\vec{\delta}_i^{th}$.

4.4.2.2 QoS-guaranteed probability Evaluation

The QoS-guaranteed probability for a marine vessel i is the probability requirement that satisfactory services are provided by the communication network of vessel i. This service probability can be generally expressed for both frequent heavy shadowing and infrequent light shadowing conditions. When the transmission channel experiences Rayleigh fading, the QoS-guaranteed probability is given as [4]:

$$P_{QoS}\left(\vec{\delta}_i^{th}\right) = Pr\left\{\vec{\delta}_i \geq \vec{\delta}_i^{th}\right\} = Pr\left\{\log_2\left(1+\frac{\overline{E}_p\hat{\tau}_h}{\sigma_w^2}\right) \geq \vec{\delta}_i^{th}\right\} = 1 - F_{\hat{\tau}_h}(\hat{\tau}_h) = 1 - F_{\hat{\tau}_h}\left(\frac{\sigma_w^2}{\overline{E}_p}\left(e^{\vec{\delta}_i \log_e 2} - 1\right)\right) \tag{4.42}$$

On the other hand, the QoS requirement assuming infrequent light shadowing is given as:

$$P_{QoS}\left(\vec{\mathring{R}}_i^{th}\right) = Pr\left\{\vec{\mathring{R}}_i \geq \vec{\mathring{R}}_i^{th}\right\} = Pr\left\{\log_2\left(1+\gamma_i\right) \geq \vec{\mathring{R}}_i^{th}\right\}$$
$$= 1 - F_{\gamma_i}(\gamma_i) = 1 - F_{\gamma_i}\left(e^{\vec{\mathring{R}}_i \log_e 2} - 1\right) \tag{4.43}$$

4.4.3 Sequential Procedures for Performance Evaluation and Comparison

Simple simulation procedures for evaluating and analysing the system performances of the above-described maritime system in terms of QoS requirements are summarized as presented in Algorithm 4.3.

Algorithm 4.3 Procedures for Network Performance Evaluation and Analysis

Input: $\{\mathbf{g}, \zeta_k, m, P_E\}$

Output: $\{\vec{\mathring{R}}_{\text{Ray}}, \vec{\mathring{R}}_{\text{Rice}}, P_{NLoS}, P_{LoS}\}$

1: **for** $i = 1$: Number of Iteration, **do**
2: **for** $E_b/N_o = 1$: length(γ_j) **do**
3: Compute the path loss based Lagrange basis polynomial $\left(\varpi_k(0)\right)$ using (4.32).
4: Evaluate the power of aggregated CH-signal $\left(\mathbb{E}\left[\mathbf{g}^2[D_i, i]\right]\right)$.
5: Calculate the data rate $\left(\vec{\mathring{R}}_{\text{Ray}}\right)$ over Rayleigh fading scenario using (4.33).
6: Evaluate the data rate $\left(\vec{\mathring{R}}_{\text{Rice}}\right)$ over Rician fading scenario using (4.37), considering the parameter definitions described in Section 4.4.1.2.
7: Compute the outage probability $\left(P_{NLoS}\right)$ over NLoS propagtion using (4.39).
8: Evaluate the outage probability $\left(P_{LoS}\right)$ over infrequent light shadowing based on (4.40).
9: **end for**
10: **end for**

Return: $\{\vec{\mathring{R}}_{\text{Ray}}, \vec{\mathring{R}}_{\text{Rice}}, P_{NLoS}, P_{LoS}\}$

4.5 CHAPTER SUMMARY

In this chapter, the framework of the considered marine radio network is comprehensively described. First, the clustering processes of the vessel-implanted MUE is carefully outlined where the MUE-CH communications are modelled by the well-known Thomas cluster (Neyman-Scott) process after which a comprehensive description of Rayleigh fading in addition to the Rician fading channel models are

presented in relation to our described maritime communication network. Secondly, an introduction to the underlying foundations of CE is succinctly demonstrated thereafter, the mathematical model description of all proposed CE methods are given. In the proposed adaptive RER CE technique, the cost function of the orthodox RLS technique is modified by in introduction of a log-sum penalty that contains the stability constant normalised Manhattan distance of the CIR obtained from traditional RLS CE methods. The responsibility of the stability constant is to correct potential numeric system instability when the CIR of this proposed adaptive technique is been updated. Thereafter the log function is subsequently multiplied by an adaptive leakage factor in order to reduce the MSE of the proposed RER method. In the proposed ISI/ANR scheme, the effects of possible ISI in the transmission channel is considered, where the use of low-pass filtering is incorporated to minimise the channel noise and any possible occurrence of ISI. This is achieved by averaging the channel noise component using the number of DA employed to aid the reception of the aggregated transmitted information. Afterwards, the interference component is normalised by the Frobenius norm of the channel estimate obtained from the classical ML method. Finally, the QoS requirements of nautical radio networks are analysed in terms of average data rate and outage probabilities for vessel-DA communications. The QoS evaluations are analysed for both Rayleigh and Rician channel fading scenarios. As such, in the next chapter, performance evaluation through computer-based simulations is exhaustively expounded and reported where the proposed CE methods in this research offer a significant improvement in average transmission data rate and outage probabilities in nautical radio networks.

CHAPTER 5 RESULTS AND DISCUSSIONS

5.1 CHAPTER OVERVIEW

The simulation results obtained by computer software-based implementation of our proposed CE algorithms in comparison to other accustomed CE techniques in the literature (classified as linear and adaptive) is extensively discussed in this chapter. The proposed CE algorithms are RER and ISI/ANR methods. The performance evaluations of these estimators are recorded assuming both slow and fast fading maritime channel conditions respectively corresponding to Doppler rates of 0.012 and 0.036. Generally, during higher Doppler rate transmissions, there is a tendency that the transmitting symbols may experience NLoS propagation. Thus, fast fading channel scenarios are synonymous with NLoS propagations as the variations of the channel responses would fluctuate rapidly in comparison to slow fading conditions. Furthermore, the QoS requirements in terms of signal outage probability and network data rate are evaluated assuming different DA values and SNR ranges in nautical radio communication systems. The QoS performances are evaluated in Rayleigh and Rician fading environments where the second hypothesis of this thesis is verified because it becomes evident that CE techniques can be adopted to boost the data rates and network outage probabilities of marine networks.

The rest of this chapter is structured as follows. The results obtained from simulating our proposed CE schemes in comparison to conventional techniques are discussed in Section 5.2 while Section 5.3 extensively presents the results obtained from the QoS evaluations of pelagic communication networks. A summary of simulation results and research findings is presented in 5.4.

5.2 SIMULATION AND DISCUSSION OF RESULTS FOR CE SCHEMES

This section evaluates and documents the CE performances of the considered customary techniques in comparison to our proposed techniques for the IoMT whose model has been comprehensively formulated as discussed in Chapter 4. A sequential procedure for realising the proposed estimators in addition to other conventional schemes is presented in this section. Furthermore, a discussion of the simulation parameters and obtained results are also reported in this section.

5.2.1 Sequential Procedures for Performance Evaluation and Comparison

Simple simulation procedures for evaluating and analysing the system performances of the above-described maritime system in terms of QoS requirements are summarized as presented in Algorithm 4.3. The coefficient of the perfect channel is simulated using (4.9) after which the proposed CE estimates are implemented using (4.23) and (4.26) respectively. The traditional schemes are realised using (3.1), (3.5),(4.20), (3.11) and (3.16) thereafter, the MSE can be computed where each estimate (C_{chan}) is compared with that of the known channel ($C[D_i,i]$) according to (5.1).

$$MSE = C[D_i,i] - C_{chan}[D_i,i] \tag{5.1}$$

5.2.2 Simulation Parameters for Realising the Considered Estimators

As earlier mentioned, simple simulation procedures for evaluating and analysing the system performances of the proposed CE techniques for IoMT are summarized as presented in Algorithm 5.1, where simulations were implemented using MATLAB programming language according to the table parameters shown in Table 5.1.

In these simulations, the MUEs are assumed to be embedded at random positions on the individual marine vessels in such a way that their distribution can be modelled by the well-known Thomas cluster processes. To prepare the maritime communication system for resilience in times of adversities such as multipath-induced fading, the Nakagami-m fading model is considered for the marine model in

order to checkmate the effects of frequent heavy, average and infrequent light showing conditions over the maritime environment. In the period when the oceanic surroundings battle the effects of

Algorithm 5.1 Procedures for realizing the proposed maritime CE schemes.

Input: $\{\mathbf{g}, \mathbf{c}, \sigma_w^2, \gamma_{\text{dB}}, d, t, \hat{\varepsilon}, \ddot{\varepsilon}, \mu\}$

Output: $\{\boldsymbol{C}_{ANR}\}$

1: Generate random AWGN with zero mean and variance (σ_w^2) as given in (4.16), where γ_{dB} can be converted to linear scale using the expression $\left[\gamma_{\text{j}} = 10^{\frac{\gamma_{\text{dB}}}{10}}\right]$. Then compute the $d \times d$ diagonal matrix of CIR using the channel response obtained as described in Algorithm 4.2.

2: From the generated Thomas cluster-based MUE and the simulated channel according to Algorithm 1 and 2 respectively, calculate the received signal at service clouds using (4.15).

3: **for** $j = 1$: Number of Iteration, **do**

4: Evaluate the channel estimates as follows:

5: **for** $E_b/N_o = 1$: length(γ_{j}) **do**

6: % Evaluating LS channel estimate

7: Compute diagonal matrix of transmit vectors given as $\left[\mathbf{G} = diag(\mathbf{g}, 0)\right]$

8: Obtain the LS CE using (3.1).

9: Compute the MSE of the LS channel estimate.

10: % Evaluating LMMSE channel estimate

11: Compute sensor information matrix $\left[\mathbf{G} = diag(\mathbf{g}, 0)\right]$

12: Evaluate $\boldsymbol{A}_{cy}$ and $\boldsymbol{A}_{yy}$ using (3.3) and (3.4) respectively.

13: Generate the LMMSE maritime channel estimate using (3.5).

14: Compute the MSE of the LMMSE channel estimate.

15: % Evaluating the NLMS channel estimate

16: $\hat{\mathbf{C}}_{NLMS} = zeros(1, d)$ % Initializing NLMS channel estimate.

17: **for** $i = 1$: Number of Iteration, **do**

18: $\hat{\mathbf{C}}_{NLMS}(1, 2{:}\text{end})$ = $\hat{\mathbf{C}}_{NLMS}(1, 1{:}\text{end} - 1)$. % Shifting frame coefficients of NLMS

19: $\hat{\mathbf{C}}_{NLMS}(1, 1) = \hat{\mathbf{C}}_{LS}(i)$

20: Choosing suitable step size parameter, evaluate the instantaneous error using (3.9) and compute the NLMS CE using (3.11).

21: **end for**

22: **end for**

23: **end for**

Algorithm 5.1 Procedures for realizing the proposed maritime CE schemes.

% Evaluating ISI/ANR channel estimate

Create an empty cluster head product vector ($\boldsymbol{p}_{CH}$) in addition to empty transmitter-receiver vector signal ($\boldsymbol{p}_{tr}$).

for $j = 1 : d$, **do**

$\mathbf{a}_1 = \mathbf{y}(j).\mathbf{g}(j)$;

$\mathbf{a}_2 = (\mathbf{g}(j).^2)$;

$\boldsymbol{p}_{tr} = \left[\boldsymbol{p}_{tr}, \mathbf{a}_1\right]$

$\boldsymbol{p}_{CH} = \left[\boldsymbol{p}_{CH}, \mathbf{a}_2\right]$

end for

Compute the ML estimate of the marine channel using (4.20).

Minimize noise upshot by averaging the noise variance of the maritime channel using d according to (4.22).

Enhance the channel stability by implementing the transformation expression given in (4.23).

% Evaluating the RER channel estimate

$\hat{\mathbf{C}}_{RER} = zeros(1, d)$

$\bar{\boldsymbol{\Upsilon}}_{RLS}(i,i) = inv(\lambda)$ % λ = regularization factor.

for $i = 1$: Number of Iteration, **do**

$\hat{\mathbf{C}}_{RER}(1, 2{:}\text{end}) = \hat{\mathbf{C}}_{RER}(1, 1{:}\text{end}-1)$.

$\hat{\mathbf{C}}_{RER}(1,1) = \hat{\mathbf{C}}_{LMMSE}(i)$

Compute the instantaneous error using (3.9).

Calculate inverse autocorrelation matrix using (3.15) and evaluate gain vector using (3.14).

To compare, compute the traditional RLS CE using (3.16).

Evaluate the variable leakage factor using (4.25).

Using the reweighting attractor expression, calculate the adaptive-based RER CE using (4.26).

end for

Return: {**c**}

burdensome shadowing, the Rayleigh fading channel model is best applicable (in worst-case scenarios) for evaluating the signal propagation performances where the fading parameter of the Nakagami-m channel equals unity. On the contrary, the Rician channel model is applicable under LOS CH transmissions whose average data rate requirements have been elaborately described in Chapter 4.4.1.2.

Marine vessels are conventionally assigned speed limits as they sail through the ocean. Various intercontinental seaports assign specific speed limits across seawater harbours which substantially depends on the kind of ship deployed. The allocated average speed limit ranges from 10 (18.52 km/hr) - 30 (55.56 km/hr) knots. It is worthy to remember that the channel transfer function is more likely to experience slow fading when ships travel at the lower speed limits. Conversely, coastal communication systems will experience fast fading channel behaviours when marine vessels propagate their signals at the upper-speed limit. If the Doppler frequencies corresponding to slow and fast fading maritime channels is chosen as 10 Hz and 36 Hz respectively, then complementary wavelength for the afore-mentioned channel conditions will be 0.431 m. More so, if the Doppler frequencies are normalized by a sampling period (T_s) of 10^{-3} sec, then the normalized Doppler frequencies corresponding to slow and fast maritime channel fading with bandwidth of $1000Hz$ will correlate to 0.0119 and 0.0358 respectively.

Table 5.1. Simulation parameters

Parameter	Specification
Step-size Parameter	0.50
RER Stability Constant	0.1
Cluster Intensity	0.3
Path Loss Exponent	2.4 (LoS), 4.68 (NLoS) [135]
Average Power	1.29 (LoS), 8.97×10^4 (NLoS) [141]
Shape Factor	19.4 (LoS), 1 (NLoS)
Doppler Rates	0.012 (Slow Fade), 0.036 (Fast Fade)
Channel Type	Rayleigh/Rician Fading

5.2.3 MSE Simulation Results Obtained for the Considered Estimators

In order to analyse and validate our proposed CE methods, comparative graphical results are presented where the performances of RER and ISI/ANR CE schemes are evaluated in terms of MSE in evaluation against other prevailing estimation techniques at various levels of SNR. Figures 5.1 - 5.9 show graphical illustrations of the CE performances of our proposed algorithms in comparison to other customary CE techniques as can be deployed in the operation of maritime communication networks. The performances of the estimators are analysed through Monte-Carlo simulations with 100,000 trials per SNR. First, we evaluate and compare our proposed CE schemes with existing techniques given that the communication between offshore navigating vessels and the seashore positioned BS occurs under slow fading and fast fading conditions respectively.

As shown in Figure 5.1 and 5.2, the performances of the proposed ISI/ANR estimator significantly improves the characteristics of conventional ML estimator. This is due to the fact that this estimator, in particular, considers the effects of marine channel noise in addition to possible effects of ISI that could arise during signal transmissions. Here, the noise variance of the nautical channel is averaged in order to reduce the possibility of noise upshoot, where the Frobenius norm of the estimated CSI obtained from ML technique is used to normalise possible ISI component of the propagating maritime signal. The resulting channel estimate is then transformed using lowpass filtering in order to further suppress unwanted channel noises and interference. More so, simulation results further demonstrate (as presented in Table 5.2 and 5.3) that improved system CE can be achieved for the operation of nautical networks using the ISI/ANR estimator in comparison with other linear estimators such as the orthodox LS and LMMSE CE schemes under both slow and fast fading channel conditions due to the aforementioned reasons.

Figure 5.3 presents a comparative analysis of the CE performances of all considered estimators when the Doppler rates correspond to both 0.0119 and 0.0358 respectively. It is observed from this figure that the channel properties can be better trailed during slow fading propagation since the effects of environmental obstacles on the propagating signals are much lower in comparison to the harsh fading habitats of the fast fading scenarios.

Results obtained from Figure 5.1 and 5.2 further show that the proposed RER CE method offers superior MSE performances in comparison to the conventional RLS in addition to the proposed

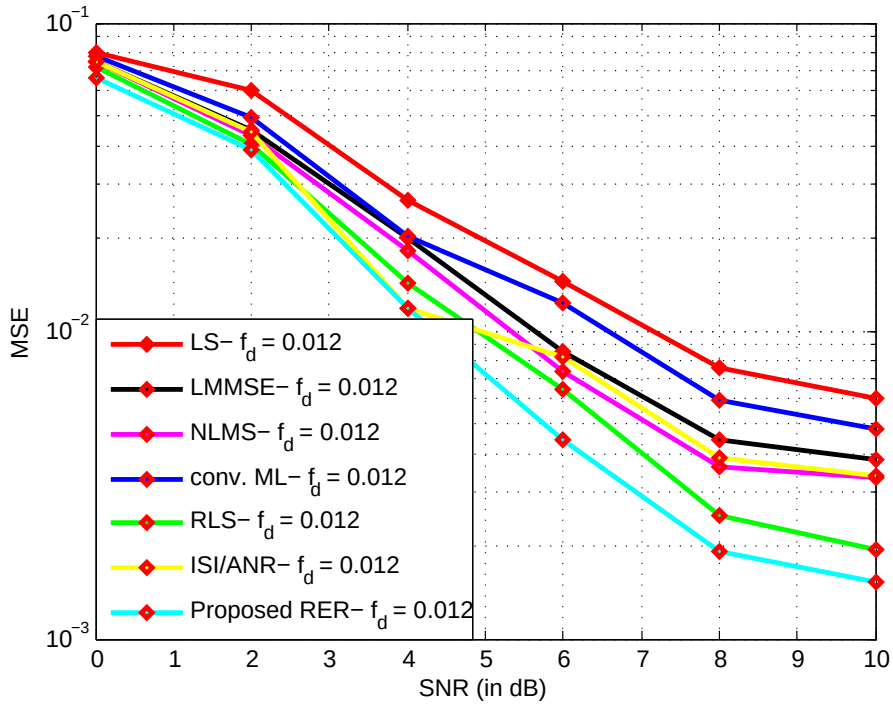

Figure 5.1. MSE performance of estimators versus SNR given $f_d T_s = 0.0119$ for IoMT

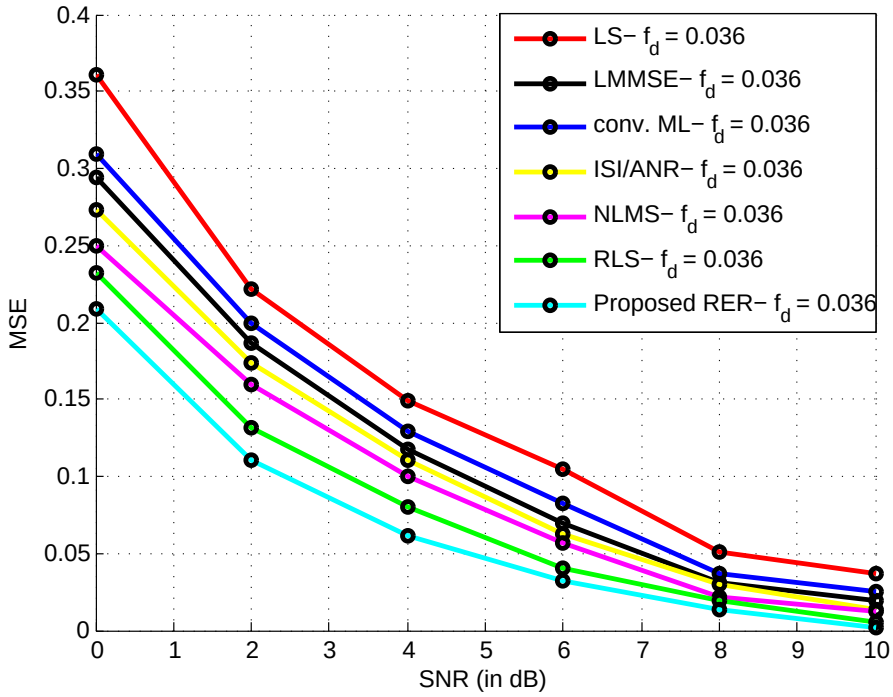

Figure 5.2. MSE performance of estimators versus SNR given $f_d T_s = 0.0358$ for IoMT

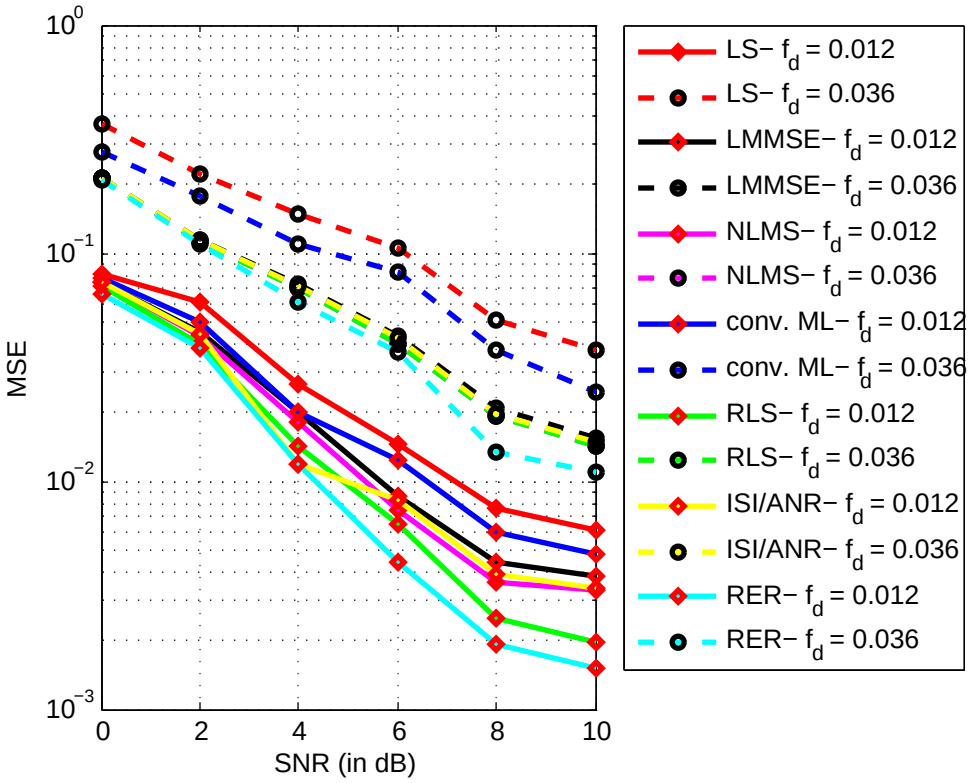

Figure 5.3. Combined MSE performance of estimators versus SNR given $f_d T_s = 0.0358$ and $f_d T_s = 0.0358$ for IoMT

ISI/ANR CE schemes. This superlative performance of RER technique is because this method introduces system stability (under both slow and fast fading environment scenarios) by the Manhattan distance normalisation of the CIR using a stability constant during the updating phase of the CIR as compared for both fading environmental conditions demonstrated in Figure 5.3.

It is noted from the formulation of the RER technique that the addition of a re-weighting attractor is adopted for providing additional network stability which offers the proposed adaptive RER technique the advantage to converge faster in comparison to other considered adaptive schemes including the customary RLS technique and the static step-size based NLMS method (as shown in Figure 5.4) at an SNR of 10 dB. This is further demonstrated as shown in Table 5.4 and 5.5 that the proposed RER technique offers significant improvement in MSE for both heavy frequent and light infrequent channel fading scenarios as compared with the traditional adaptive RLS and NLMS estimators for all levels of SNRs.

Table 5.2. Comparison of linear estimator MSE vs proposed ISI/ANR assuming slow fading channels

SNR (dB)	MSE-LS	MSE-LMMSE	MSE-ML	MSE-ISI/ANR
0	0.0805	0.0753	0.0778	0.0748
2	0.0603	0.0449	0.0493	0.0442
4	0.0264	0.0198	0.0201	0.0186
6	0.0144	0.0086	0.0122	0.0082
8	0.0076	0.0044	0.0059	0.0038
10	0.0060	0.0038	0.0048	0.0035

Table 5.3. Comparison of linear estimator MSE vs proposed ISI/ANR assuming fast fading channels

SNR (dB)	MSE-LS	MSE-LMMSE	MSE-ML	MSE-ISI/ANR
0	0.3713	0.2138	0.2789	0.2133
2	0.2211	0.1146	0.1795	0.1135
4	0.1490	0.0727	0.1086	0.0712
6	0.1047	0.0429	0.0827	0.0421
8	0.0504	0.0207	0.0373	0.0197
10	0.0372	0.0155	0.0246	0.0148

5.2.4 Effects of Estimator Parameters on Estimating Marine Channels

Changing the parameters of the estimators may have significant effects on the estimation performances for the operation of maritime communication systems. This section discusses the effects of changing the step-size parameter in estimation the adaptive NLMS and RER technique in addition to the effects on stability constant on the proposed RER method.

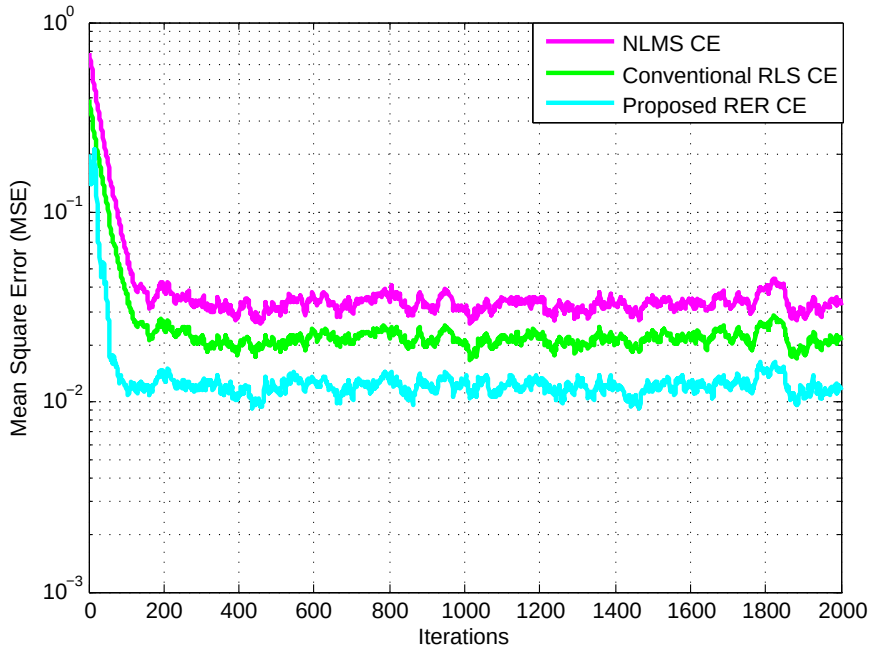

Figure 5.4. Convergence behaviour of proposed RER CE in comparison to RLS and NLMS under slow fading conditions.

5.2.4.1 Effects of Step-size Parameter on Estimating Marine Channels

For IoMT applications, the positive step size parameter of the adaptive NLMS CE scheme is chosen as 0.50 in order to provide an intermediate concession between nautical signal propagations assuming heavy frequent marine channel shadowing scenarios and LOS signal transmissions. In other words, appreciable system stability is offered using this value. More so, this research shows that the estimation scheme becomes unstable outside the optimal range of $0.40 \leq \mu \leq 0.50$ since the formidable convergence and steady-state behaviour of the algorithm cannot be easily administered outside this region. Furthermore, it is demonstrated that choosing a higher value of μ within this optimal range will guarantee better system stability for the adaptive NLMS and RER algorithms as shown in Figure 5.5.

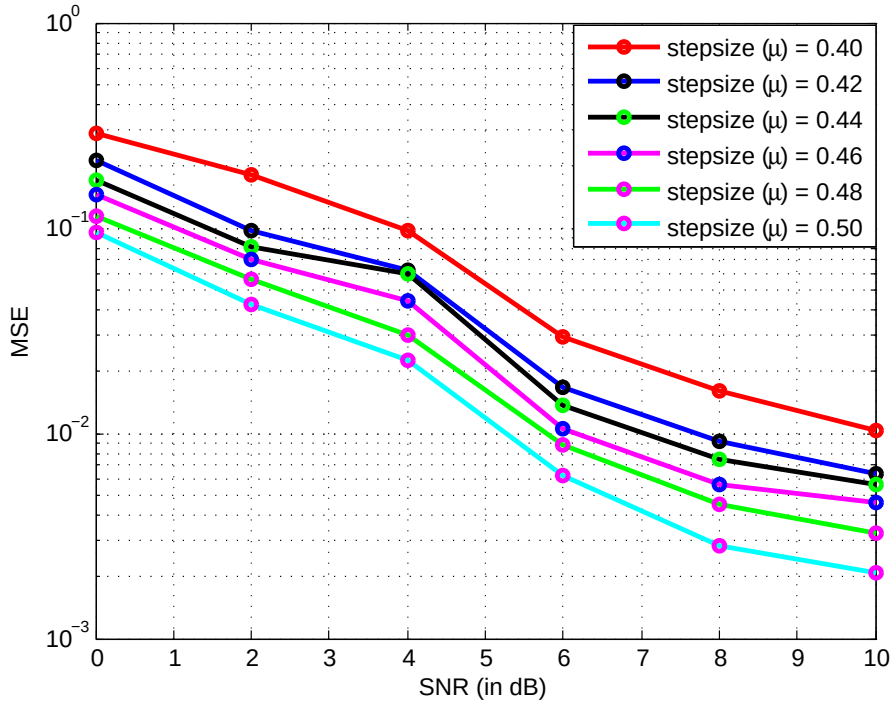

Figure 5.5. A comparison of MSE versus SNR at different step size for IoMT-based adaptive NLMS and proposed RER CE schemes.

Table 5.4. Collation of adaptive estimator MSE vs proposed RER assuming slow fading channels

SNR (dB)	MSE-NLMS	MSE-RLS	MSE-RER
0	0.0745	0.0723	0.0663
2	0.0430	0.0401	0.0385
4	0.0181	0.0142	0.0118
6	0.0073	0.0064	0.0044
8	0.0036	0.0025	0.0019
10	0.0033	0.0019	0.0015

5.2.4.2 Effects of Stability Constant of RER on Estimating Marine Channels

In realising the proposed adaptive RER CE scheme, a forgetting factor of 0.998 is used because it is shown in [142–144] that this value yields good results for customary RLS estimators. Additionally, a regularization factor of 0.001 is used for initializing the inverse autocorrelation matrix of the RER

Table 5.5. Collation of adaptive estimator MSE vs proposed RER assuming fast fading channels

SNR (dB)	MSE-NLMS	MSE-RLS	MSE-RER
0	0.2126	0.2126	0.2093
2	0.1119	0.1119	0.1101
4	0.0697	0.0697	0.0611
6	0.0401	0.0401	0.0364
8	0.0194	0.0194	0.0134
10	0.0142	0.0142	0.0109

estimate according to (3.15) while it is shown from this research that this algorithm achieves optimal stability when the stability constant offers extra sturdiness to the variable leakage factor in the range of $0.06 \leq (\ddot{\varepsilon}) \leq 0.1$. Hence a better MSE is obtained as $(\ddot{\varepsilon})$ increases within the stability region under both heavy frequent shadowing propagation and steady fading channel scenarios as depicted in Figure 5.6 and 5.7 respectively.

It can also be generally observed from simulation and results obtained that the maximum constant within the stability region yields superlative CE for the maritime signal transmissions while constants with magnitude above this region impacts negatively on the steady-state behaviour of this RER estimation algorithm. As depicted in Table 5.7 and 5.6, the MSE of the proposed RER adaptive estimator decreases swiftly as the SNR values increase. Similarly, the MSE of the estimator under consideration reduces as the stability constant $(\ddot{\varepsilon})$ increases. This behaviour continues until the optimal stability for the algorithm is achieved when $(\ddot{\varepsilon} = 0.10)$. Values above this region begin to show depreciation in MSE performances and this is achieved under both LoS and NLoS propagation scenarios as illustrated in Figure 5.6 and 5.7, where the combined simulated results under both channel characteristic is presented in Figure 5.8.

Finally, the simulation results for the estimators show that the higher the Doppler spread, the poorer the estimation performance as delineated in Figure 5.9, where the adaptive estimator performances are analysed for different values of Doppler spread at an SNR of 5 dB. In other words, the CE performances are directly proportional to the magnitude of the normalized Doppler frequency. Hence, when the maritime channel experiences slow fading with Doppler rate of 0.0119, all considered adaptive estimators will demonstrate superior performances in comparison to situations where the

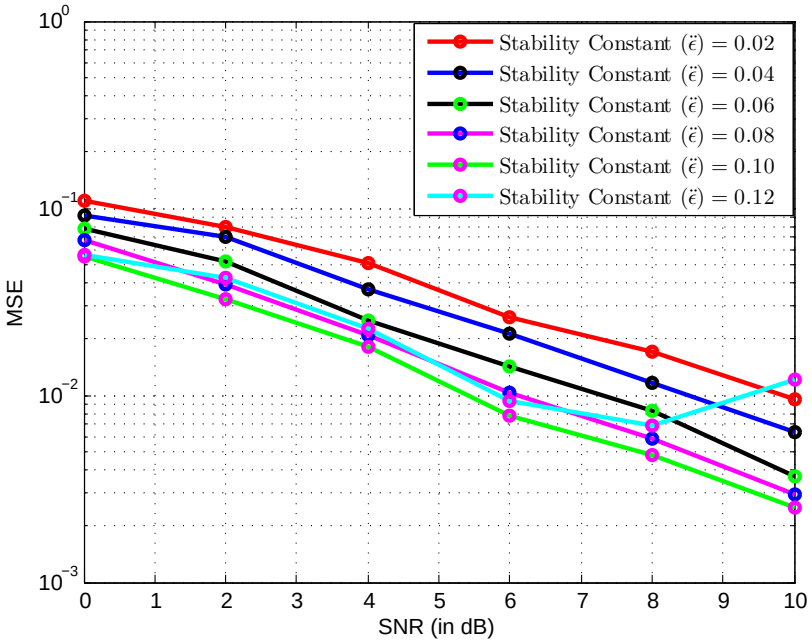

Figure 5.6. Comparative analysis of CE MSE versus SNR at different stability constants for proposed adaptive RER assuming slow fading NLoS propagations.

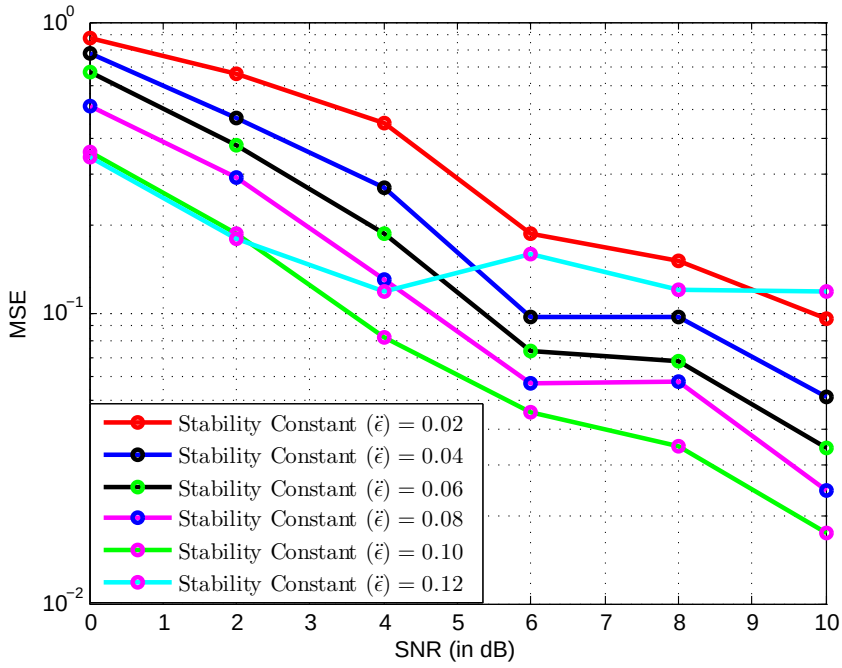

Figure 5.7. Comparative analysis of CE MSE versus SNR at different stability constants for proposed adaptive RER assuming fast fading NLoS propagations.

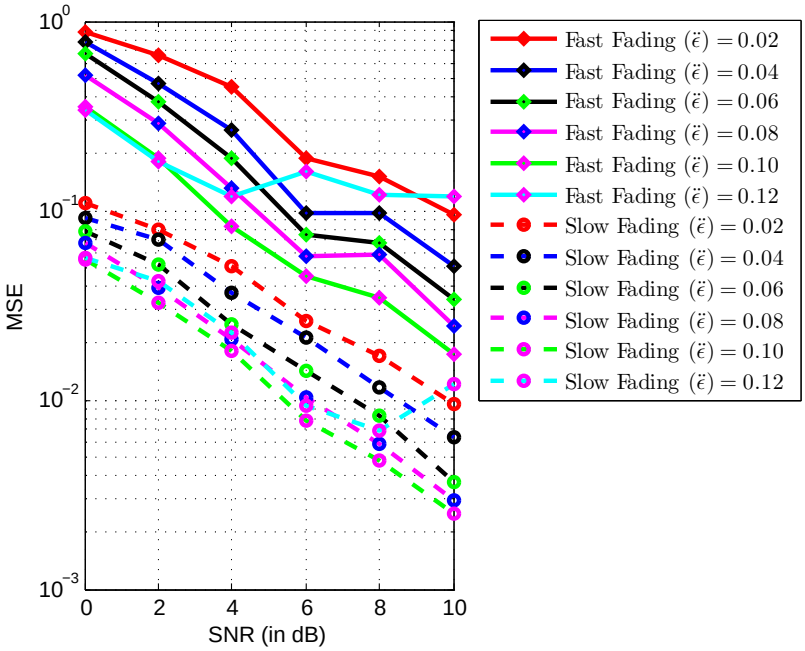

Figure 5.8. A comparative illustration of MSE versus SNR for adaptive RER estimator under different stability constants assuming both slow and fast fading channels.

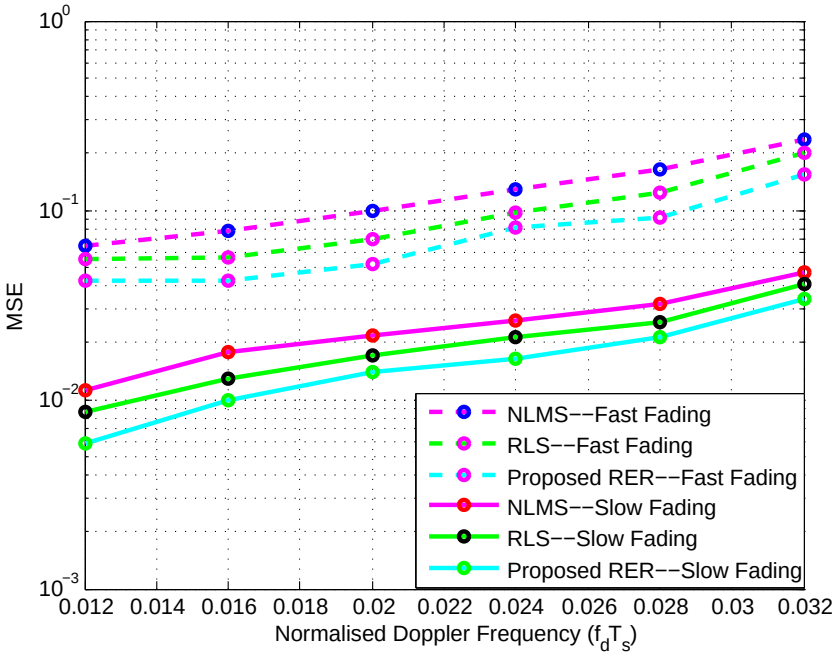

Figure 5.9. A comparative illustration of MSE versus Normalised Doppler frequency at SNR = 5 dB for adaptive estimators assuming slow and fast fading channels.

Table 5.6. RER CE MSE vs SNR assuming different stability constants for slow fading channels

SNR (dB)	MSE ($\ddot{\varepsilon} = 0.04$)	MSE ($\ddot{\varepsilon} = 0.06$)	MSE ($\ddot{\varepsilon} = 0.08$)	MSE ($\ddot{\varepsilon} = 0.10$)	MSE ($\ddot{\varepsilon} = 0.12$)
0	0.0921	0.0783	0.0675	0.0547	0.0568
2	0.0707	0.0522	0.0390	0.0323	0.0424
4	0.0370	0.0251	0.0208	0.0181	0.0226
6	0.0212	0.0141	0.0102	0.0077	0.0092
8	0.0117	0.0082	0.0058	0.0048	0.0069
10	0.0064	0.0037	0.0030	0.0025	0.0121

Table 5.7. RER CE MSE vs SNR assuming different stability constants for fast fading channels

SNR (dB)	MSE ($\ddot{\varepsilon} = 0.04$)	MSE ($\ddot{\varepsilon} = 0.06$)	MSE ($\ddot{\varepsilon} = 0.08$)	MSE ($\ddot{\varepsilon} = 0.10$)	MSE ($\ddot{\varepsilon} = 0.12$)
0	0.7846	0.6733	0.5153	0.3547	0.3424
2	0.4686	0.3751	0.2899	0.1873	0.1808
4	0.2681	0.1874	0.1308	0.0822	0.1186
6	0.0969	0.0741	0.0575	0.0453	0.1599
8	0.0964	0.0679	0.0580	0.0346	0.1201
10	0.0513	0.0342	0.0245	0.0174	0.1185

channel fades rapidly when the Doppler rate is 0.0358. Nonetheless, the proposed RER technique shows superior performances in both fading situations in comparison to conventional estimators.

5.3 SIMULATION AND DISCUSSION OF RESULTS FOR QOS PROVISIONS

In this thesis, the QoS requirements of CH-BS link in nautical radio communication networks are also evaluated in terms of average data rate and outage probability as a performance metric where a sequential procedure for realising this evaluation is described as presented in Algorithm 4.3. The network outage probability is simply described as the probability that a system outage will occur over a specified period, where the received information rate falls below a required threshold.

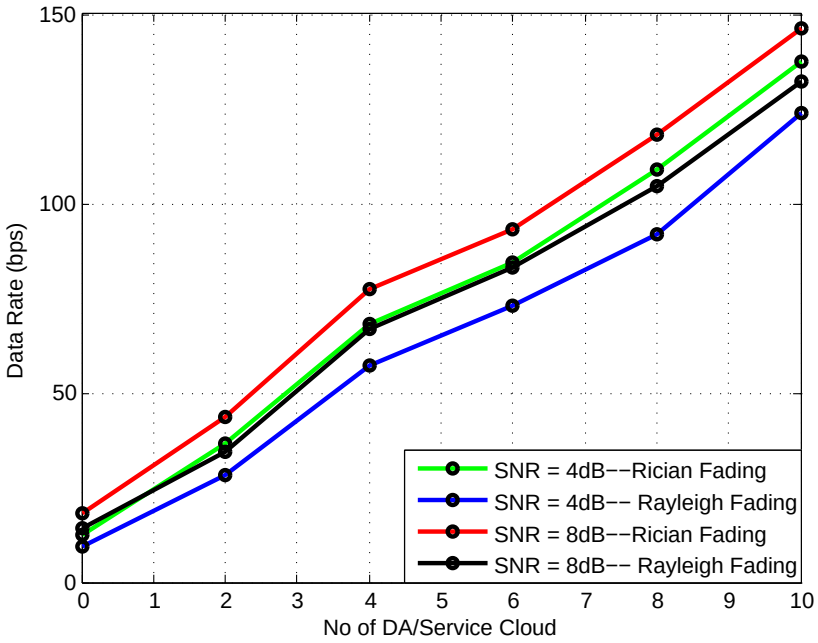

Figure 5.10. A juxtaposition of average maritime data rate vs number of DA per service cloud over Rician and Rayleigh propagation for SNR values of 4 and 8 dB.

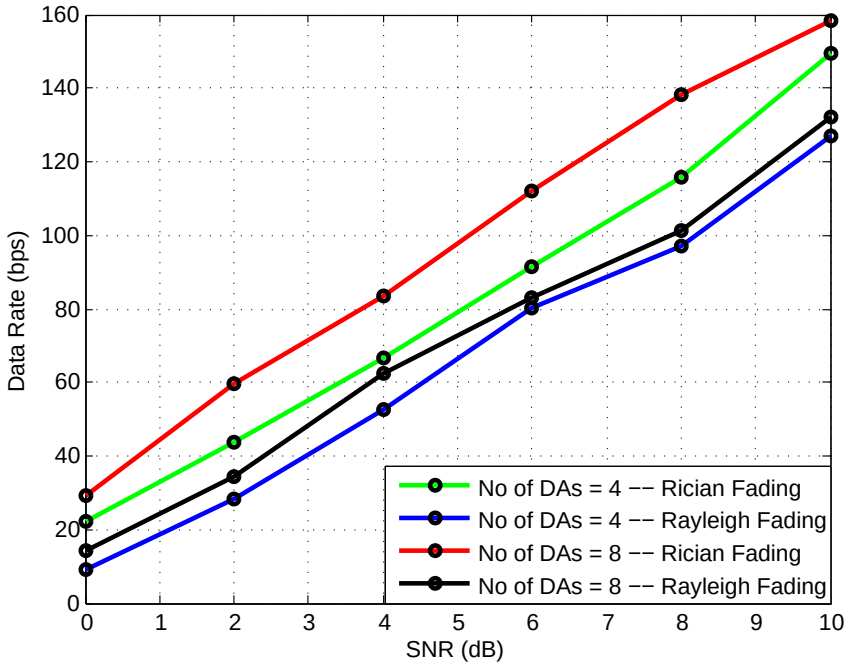

Figure 5.11. A juxtaposition of average maritime data rate vs SNR over Rician and Rayleigh propagation for 4 and 8 DA per service cloud.

As stated, the performances of the described nautical network framework according to Figure 4.1 are then evaluated in terms of average data rate and QoS requirements for the offshore navigating vessel to sea-shore mounted DA communications. The data rate requirements of the maritime communication system are principally evaluated assuming LoS and NLoS propagations (which correspond to a Nakagami shape factor of $m = 19.4$ [141] and $m = 1$ respectively). More so, the average power (Ω) of both the LoS and NLoS communication, corresponds to 1.29 and 8.97×10^{-4} respectively [141]. On the other side, the outage probability and QoS guaranteed probability is evaluated for both frequent heavy and infrequent light shadowing conditions of CH-DA communications.

The results obtained from computer-based simulations as illustrated in Figure 5.10 and 5.11 show that the average data rate increases as the SNR of transmission increases and vice-versa. Also, the marine network will offer a higher data rate over Rician fading channel scenarios in comparison to Rayleigh fading propagations. We can also deduce from these figures that as the number of DAs is increased in the service cloud, the average system data rate increases directly. For example, it is noted from Figure 5.10 that as the SNR value rises from 4 dB to 8 dB under Rician fading conditions, there is a significant increase in the data rate output. To be more specific, it is observed that when 5 DAs are employed for the marine communication network per service cloud, the data rate increases from a just a little over 75 bps to about 82 bps when SNR values change from 4 dB to 8 dB respectively. A similar trend is also achieved under the Rayleigh fading channel propagation scenario. More so, it is deciphered from Figure 5.11 that as the number of DA increases in the coastal communication network, the system data rate increases proportionally. Also, it is crearly read from this curve that the system data rate increases in magnitude at an SNR value of 9 dB in comparison to 8 dB or any other lower region.

The data rate characteristics are further analysed and expanded as represented in Figure 5.12 for SNR values ranging from 4 to 10 dB over both LoS and NLoS communication systems. It can be seen from the bar graph that the data rate improves when there is a LoS path along the marine communication network in comparison to when there is no LoS propagation. Another visible observation from this chart shows that increasing the number of DA over the maritime communication system will consequently result in improved system throughput. This occurs because of the antenna selection diversity and power where the propagating signals are more appropriately directed to the receiver end under the cooperation of more antenna applications.

To validate the hypothesis drawn from this research work in addition to answering the main research

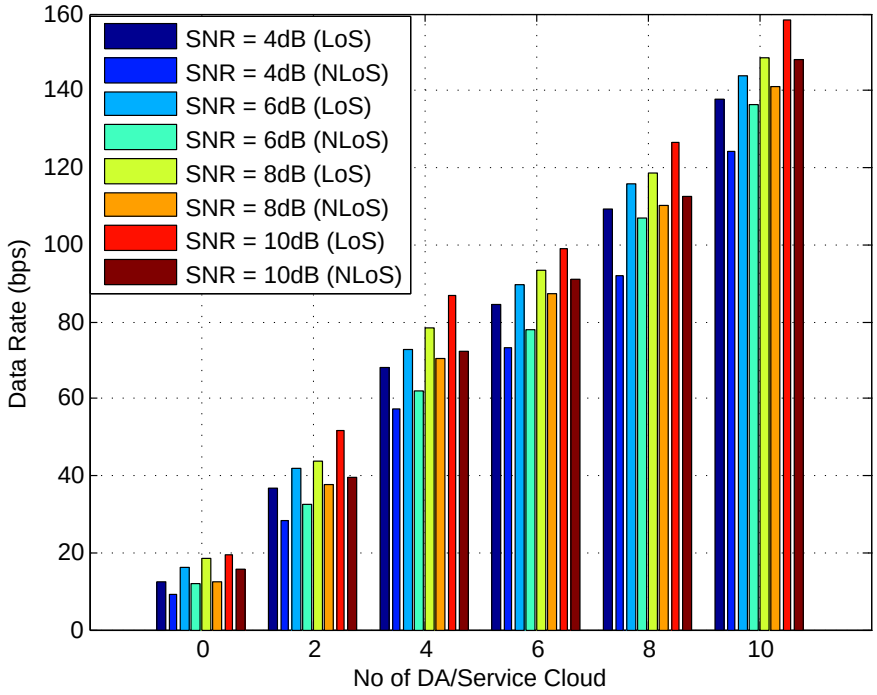

Figure 5.12. A plot of average data rate vs number of DA per service cloud over LoS and NLoS propagation at different SNR values.

question presented in Chapter 1, the performances of the estimators are further evaluated over Rayleigh and Rician fading channel conditions across the maritime radio network, where the data rates analysed over both channel conditions are presented as shown in Figure 5.13 and Figure 5.14 respectively. According to the results obtained from Figure 5.13, it is certainly observed that the proposed RER technique can better track the CIR of maritime radio networks for meaningful decision-making procedures over the receiving end of the network. This is because higher data rate transmissions can be achieved using this algorithm in comparison to other techniques while it has been previously shown that this method offers a lower MSE in comparison to other counterparts.

In this simulation, the performances of the other adaptive and linear estimators are also evaluated using the perfect channel and no CE scenarios as benchmarks in order to validate the performances of all proposed estimators in the maritime network. The estimators demonstrate a similar comparative pattern in a Rayleigh fading environment as in the Rician channel environment. However, it is substantiated from Figure 5.14 that the data rates will reduce in a Rayleigh fading environment in contrast to Rician fading scenarios because of the immense obstructions of transmission paths across a Rayleigh fading

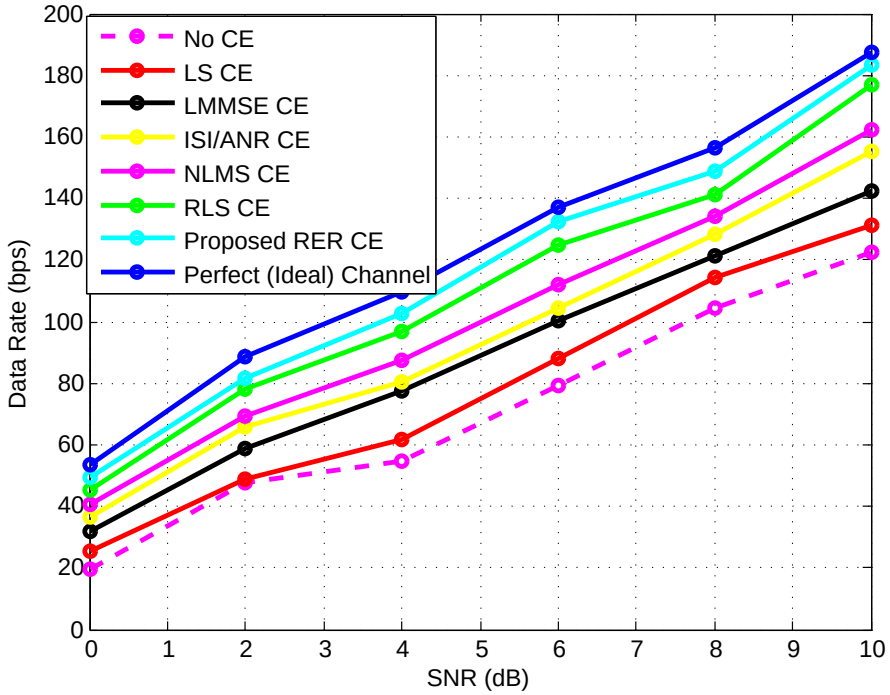

Figure 5.13. A plot of average data rate performance vs SNR over Rician fading marine channel environment for different channel estimators.

channel surrounding. To finalise, because of the lower MSE of the proposed ISI/ASN technique in comparison with other classical linear estimators, this technique consequently offers a higher data assurance in a nautical radio network over other linear estimation procedures.

The marine QoS can be evaluated based on the outage probability and the QoS-guaranteed probability at various SNR ranges considering the effects of massive antenna deplorations over service clouds to enhance the QoE of thalassic users. The outage probability of transmission from ship to coastline BS is evaluated in application to oceanographic communications as shown in Figure 5.15 for different values of SNRs and DAs per service cloud over Rayleigh and Rician fading channel propagation. Results obtained demonstrate that the transmission outage probability increases as the SNR values decreases and as the number of DAs serving the pelagic communication system decreases. It is also shown from this curve that the transmission of marine signals over Rayleigh fading channels increases the transmission outage probabilities due to the unpropitious effects of the environmental conditions thereby, leading to poorer signal reception at the coast-line BS during decision-making procedures. To further elaborate these claims, it is seen from this figure that the outage probability converges

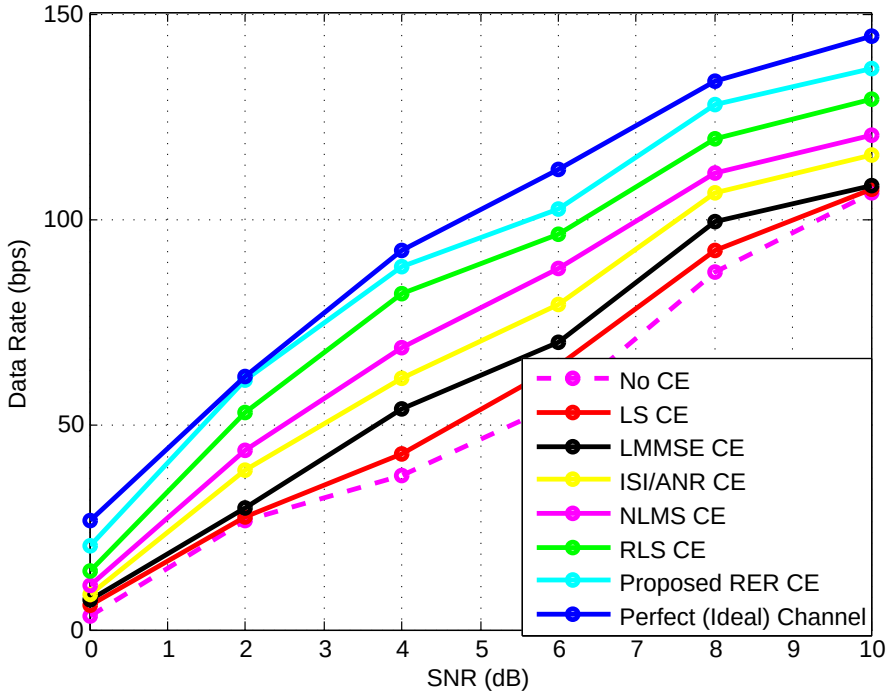

Figure 5.14. A plot of average data rate performance vs SNR over Rayleigh fading marine channel environment for different channel estimators.

faster under Rician fading propagation scenarios since there is an LoS path between communication networks especially when the number of DAs employed to aid the maritime communication network are higher in number. For example, the outage probability converges when SNR equals 8 dB under Rician channel when 8 DAs are employed as compared to that when 4 DAs are employed under similar channel conditions which converges to zero at almost 10 dB SNR value. It is also seen from this figure that when there is no LoS path between transmitter and receiver as applicable to the Rayleigh fading scenario, there is no convergence of outage probability within the simulated SNR ranges while the outage probability assuming this channel condition is very high at all levels of SNR. Nonetheless, employing more numbers of DAs in the maritime communication system will help the system performance of the network when the symbols travel over frequency heavy fading channel conditions. Thus, in such conditions where communication occurs in NLoS transmissions,

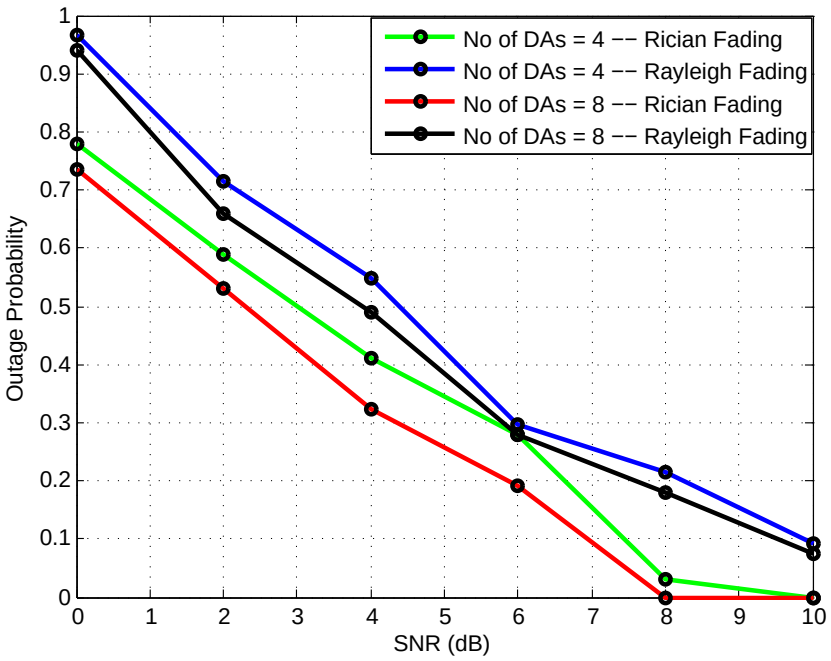

Figure 5.15. A Plot of transmission outage probability vs SNR over Rician and Rayleigh propagation for 4 and 8 DA per service cloud.

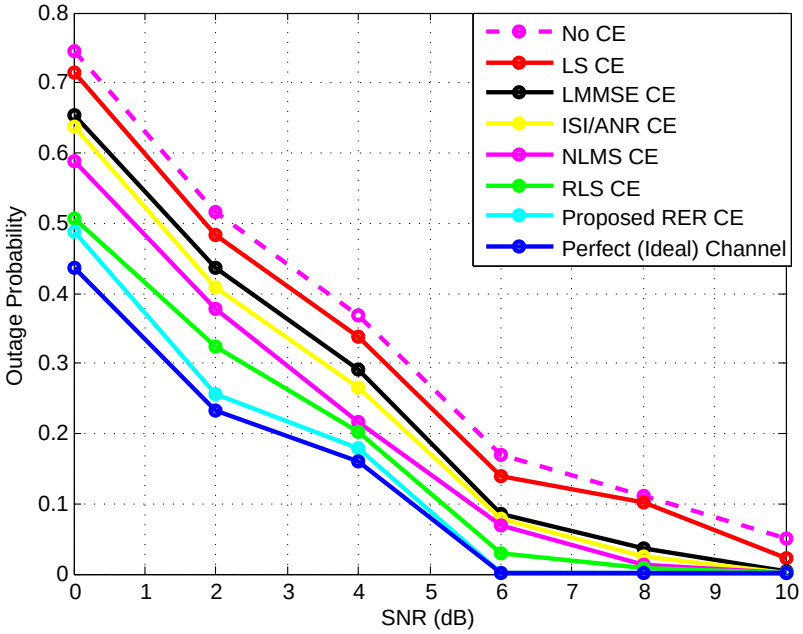

Figure 5.18. A plot of average probability of outage performance vs SNR over Rician fading marine channel environment for different channel estimators.

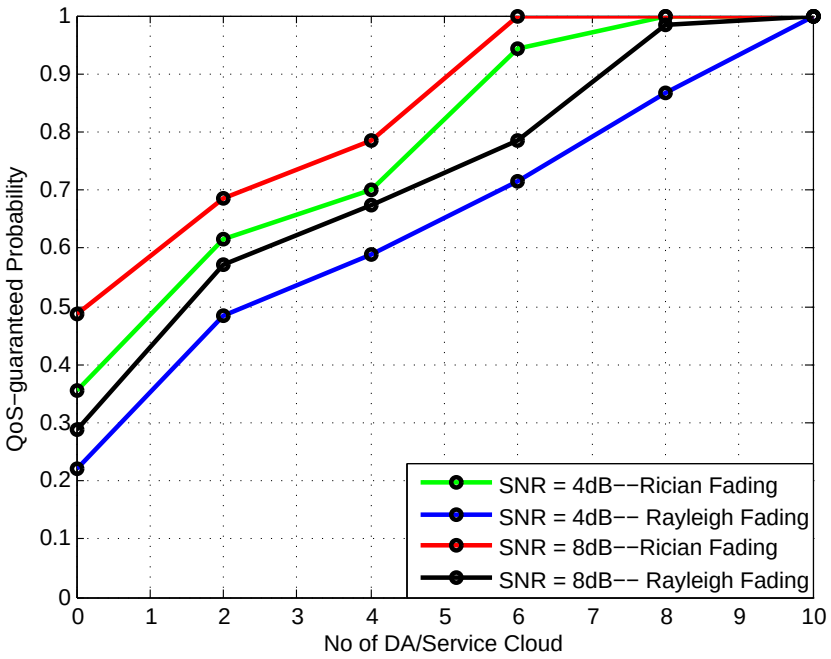

Figure 5.16. A Plot of transmission QoS guaranteed probability vs number of DA per service cloud over Rician and Rayleigh propagation for SNR values of 4 and 8 dB.

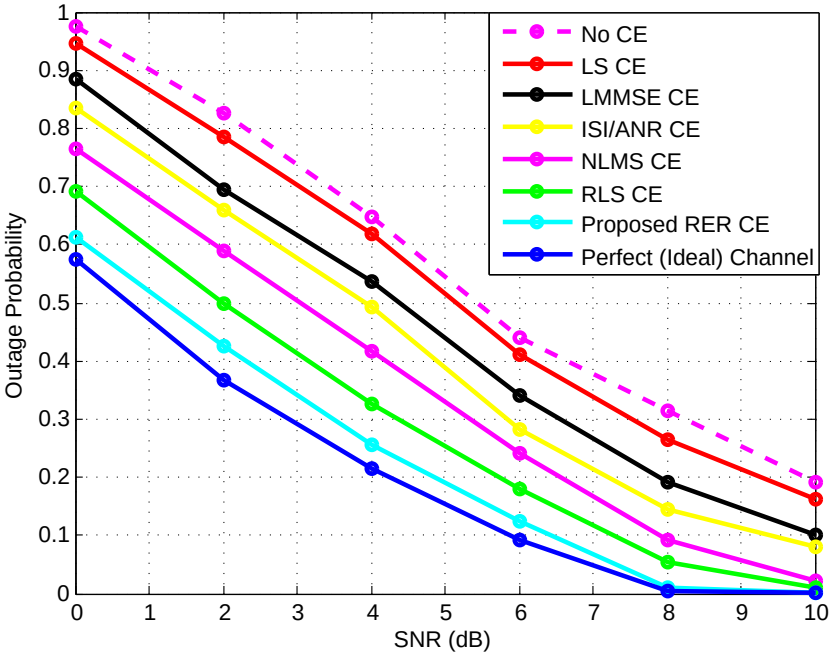

Figure 5.19. A plot of average probability of outage performance vs SNR over Rayleigh fading marine channel environment for different channel estimators.

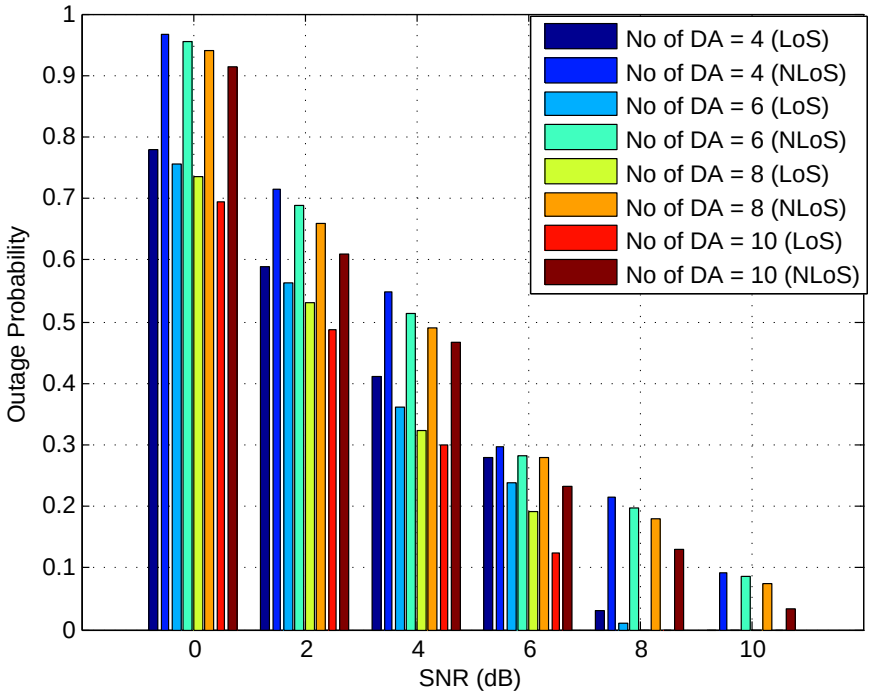

Figure 5.17. A plot of average probability of outage vs SNR over LoS and NLoS propagation at different numbers of DA per service cloud.

marine users are more likely to experience unwanted transaction delays, economic loses in addition to seaport congestion and probable collisions

It is further demonstrated in Figure 5.18 and 5.19 that the QoE of marine users can be improved with appropriate CE techniques which further justify our hypothesis in this research work. In both figures, it can be observed that the application of adequate CE methods can significantly reduce the transmission outage probability which subsequently strengthens the reception of aggregated CH signals at the BS of the maritime network thus, improving the QoS and QoE of the marine network as a result. From these figures, adopting the proposed RER CE method can considerably reduce the system outage probability in comparison to other techniques since the receiver will have much knowledge about the actual condition of the maritime environment before and during the transmission of the aggregated ship-implanted MUE signals. Similarly, marine communication systems will experience a higher probability of transmission outage in a small-scale Rayleigh fading environment over their Rician counterparts. At higher SNR values, the outage probabilities across both fading channels reduce proportionately.

The chart presented in Figure 5.17 also show a comparative graphical analysis of the system outage probabilities at different levels of SNR values. It is clearly visible from this graph that the system outage probability increases sharply as the SNR values rapidly decrease. For instance, when the noise power and the signal power are equal (i. e. SNR = 0 dB) the probability that network outage or breakage will occur is highest as presented in this figure. However, as the SNR values gradually increase from 1 to 10 dB, the outage probability decreases substantially in an inverse proportionate manner. These characteristics are similar for both LoS and NLoS communication networks. However, the system outage probabilities are exceedingly higher for NLoS communication systems in comparison to LoS propagations are clearly shown in this figure in particular.

The QoS-guaranteed probability is also evaluated over different SNR values and DAs per service cloud over similar channel models as shown in Figure 5.16 respectively. It can also be deduced from Figure 5.16 that the use of monumental antennas can sharply increase the QoS-guaranteed probability of marine users especially at higher SNR values. Hence, transmissions over 8 dB Rician fading channel will converge faster than transmissions over its Rayleigh fading counterpart. Thus, fewer DAs will be required for optimal signal transmissions over LoS propagations as the network QoS-guaranteed probability will converge when the number of DAs employed per service cloud is 6 as compared to 9 for its NLoS counterpart when the SNR is in this region of 8 dB.

5.4 SUMMARY OF RESEARCH FINDINGS

In this chapter, the performances of our proposed CE algorithms are evaluated in comparison with some conventional linear and adaptive algorithms. Additionally, the QoS requirement analysis for nautical communication networks are evaluated and documented. Both performances were analysed assuming heavy frequent maritime Rayleigh fading channel and light infrequent Rician fading maritime fading channels that correspond to NLoS and LoS propagations respectively. Several general research findings were observed and are recorded as follows.

To begin with, it can be noted that the relative CE performances of the estimation schemes when signals propagate under slow fading channel environmental conditions are noticeably superior in comparison to system performances of corresponding channels that are characterised by fast fading CIR scenarios. This is because the propagating CH information sent from the vessel to the on-shore mounted base

station can be easily trailed when the CSI oscillates slowly over a given period of time as compared to the expeditious changes that mark the CSI characteristics of fast fading channel propagation. Another preeminent trend that is worth noting is that the MSE performances of the proposed CE schemes decrease steadily with increases in the SNR values since the varying characteristics of the fading channel will be better tracked when the signal quality is way higher than the unwanted effects of the channel noises. More so, the results obtained proved that the adaptive schemes show better estimation performances for marine signal tracking in comparison with their linear counterparts because they recursively obtain the CIR that minimizes a cost function, which relates to the previous estimates and the CH information.

Furthermore, simulation results illustrate that as the number of DA increases per service cloud over offshore navigating vessels, the data rate increases proportionately over the communication network since the effects of environmental interference are drastically reduced which is further improved by CE. Likewise, it is inferred that the data rate improves as the number of DAs per service cloud and SNR values increases over LoS and NLoS communication scenarios in both situations where the CH-DA transmission is enabled over Rician and Rayleigh fading channels respectively. Conversely, the outage probabilities of marine networks decreases as the number of service cloud DAs increase at rising SNR values while the QoS-guaranteed probability rises with increase in costline mounted DAs even at extreme transmission conditions.

Additional simulation results obtained show that accurate CE techniques over the maritime communication network can improve the QoS and QoE of pelagic communication networks. These evaluations justify our second research hypothesis which states that "adopting accurate CE methods in nautical radio networks can result in a considerable increase in the QoS and QoE of marine users during the explorations of the maritime environment". Based on the hypothesis and simulation results discussed, it can be concluded that in a nautical radio network, CE can be used to enhance the QoS and QoE requirements of ocean-going communications. Also, the proposed adaptive RER CE method has offered the maritime network better performance stability when the receiver attempts to evaluate and estimate the behaviour of the communication channel. Similarly, our ISI/ANR shows a more improved estimation performance over other considered linear methods in a given nautical radio network. Thus, when CE becomes imperative for strengthening the quality of the received CH information on ocean-ward positioned BS, it is recommended that the proposed RER technique be adopted for the saltwater communication system since this method will offer significant comparable performance in contrast

with perfect channel scenarios. Finally, the superior performance of this proposed technique over other considered traditional methods (and scenarios where CE is not considered for the maritime network) has shown that effective CE can improve the data rate and reduce network outage probabilities for a maritime radio network according to Figure 5.13 and 5.14 respectively.

CHAPTER 6 CONCLUSION AND FUTURE RESEARCH DIRECTIONS

6.1 CHAPTER OVERVIEW

The penultimate chapter presents an elaborate discussion of results obtained for improving maritime communication networks through CE and QoS in terms of outage probability and data rate. This chapter discuses the conclusions drawn from this research work as presented in Section 6.2 where possible future research directions for the IoMT are suggested in Section 6.3.

6.2 CONCLUSION

The IoT paradigm finds valuable applications in the industries including agriculture, energy, automobile, healthcare and maritime industry etc. The benefits of this technology can be exploited in these industries by the use of tiny sensor and actuator devices which are capable of reading several environmental parameters and conditions. In the maritime industry, the IoT technology can be employed to boost operational activities including oil & gas explorations, fishing, scuba diving, sailing etc in what is termed IoMT. Here, sensor-inserted MUE are located at cardinal positions across the entire marine environment. To further support the QoS and QoE of marine networks, communication techniques such as EC, CE, SDN, NFV, energy balanced routing communication protocols and machine learning etc, are required.

In this thesis, a comprehensive review of the concept of IoT is presented. A general overview of the concept of IoT is reviewed as applicable to the industrial environment. The architectural concept of SDN-assisted EC is propounded for managing emergency situations as applicable to the maritime

IIoT, in order to mitigate the detrimental effects of oil and gas spillages onto marine environments for higher throughput and gain maximization in offshore oil and gas explorations. In SDN technology, the communication network control is decoupled from the conventional hardware devices with the underlying aim of providing network adaptability and efficiency for dedicated transmission functions. Nonetheless, the EC technology is described as a set of things with their functionalities and services that connect and cooperate temporarily to achieve a goal. To preserve the deep sea environment, this technology (EC) can be deployed to preserve lives in maritime environments during explorations of hydrocarbons from quick responses to emergency situations. The benefits of EC technology can also be exploited for onshore oil and gas production and across other industrial applications.

Channel estimation can be employed to predict the transmission and reception nature of saltwater communications. As the aggregated MUE information is clustered and transmitted to the remote seashore-located maritime BS, environmental factors such as the effects of multipath propagation, shadowing and signal fading may hinder the QoS and QoE of nautical radio networks. This research work has shown that accurate CE methods could improve the QoS and QoE of pelagic communication networks. From the results obtained, it is concluded from this study that, the adaptive estimators in comparison to their linear counterparts offer better estimation of channel properties which consequently give rise to ameliorate signal receptions for useful maritime decision making procedures. Specifically, the proposed RER CE scheme in addition to the RLS and NLMS methods offer better MSE performances in contrast to their linear counterparts including the ISI/ANR method, conventional ML estimator and the traditional LMMSE and LS techniques. This is achieved for both slow and fast fading marine channel environments under both Rayleigh and Rician fading models. Furthermore, in a nautical radio environment, the proposed ISI/ANR estimator will provide improved CE performances in comparison to other linear methods such as LS, LMMSE and ML estimators for the enhancement of maritime radio networks. Likewise, the developed RER CE approach in this work tremendously improves the estimation performances of maritime radio channels in comparison to other adaptive schemes such as conventional RLS and NLMS methods. More so, this proposed adaptive RER technique outperforms all other linear methods including LS, LMMSE traditional ML-scheme and even the proposed linear ISI/ANR technique. The superior performances of our proposed RER CE scheme are consistent over both LoS and NLoS signal propagations in conditions of both slow and fast fading maritime radio channels. In the proposed RER technique, the Manhattan distance of the CIR is taken, which is subsequently normalised by a stability constant $(\ddot{\varepsilon})$ whose responsibility is for correcting any potential numerical system instability that may arise during the updating stages of the CIR. In

order to decrease the received signal error, the log-sum penalty function is eventually multiplied by an adjustable leakage factor $(\hat{\epsilon})$ that provides additional stability to the oscillating channel behaviour in addition to minimizing the stalling of the channel coefficients under different marine fading conditions. This leakage factor is made adaptive using the variable leakage factor technique where we introduce a reweighting attractor for shrinking (or further reducing) the system CE error. Hence, the step size parameter for adaptive RER estimator should be chosen in the range $0.40 \leq \mu \leq 0.50$ which guarantees optimal estimation performance selected at 0.5. Optimal stability is also achieved by the aid of the RER variable leakage factor when this constant is assigned a value of 0.10. However, the stability range for choosing this constant for the proposed RER technique falls within $0.06 \leq (\ddot{\epsilon}) \leq 0.1$. Thus, it is generally concluded from this research that the proposed RER scheme will provide considerable estimation performance in comparison to other considered techniques for improving the QoS and QoE of coastal networks. Therefore, this particular scheme is recommended for use in maritime radio networks for combating the dynamics of nautical channels especially under frequent heavy shadowing (Non-LOS) maritime communication scenarios.

6.3 SUMMARY OF RESEARCH CONTRIBUTIONS AND POSSIBLE DIRECTIONS

The contributions of this research work are summarised as follows.

- Development of a comprehensive literature review on the applications of IoT technology across industrial activities particularly in the maritime sector.
- Design of an IoT-based framework for improving the QoS requirements in nautical radio management and operations, where off-shore navigating vessels are equipped with environmental sensing equipment in communication with a cluster head MUE that transmits aggregated seawater sensor information via the marine channel to a shoreward located central BS.
- Development of two novel CE techniques for improving the performances of maritime communication systems named RER and ISI/ANR CE. The estimators attempt to improve the performance of conventional schemes such as ML-based estimation and RLS techniques in order to reduce the CE error of the maritime communication network using combinational techniques that involve summing the instantaneous square error with a log-sum penalty which is subsequently realised by the normalisation of the Manhattan distance of the system CIR.

Additionally, a simple step by step procedures for deriving our considered marine estimators is elaborately documented for the benefits of intending readers.

- Evaluation of the QoS performances in terms of system data-rate, outage probability and QoS-guaranteed probabilities for improving nautical user QoE over signal transmissions in both heavy frequent and light infrequent shadowing conditions of oceanic signal propagation.

The propounded novel ubiquitous computing SDN-based architecture developed in Chapter 2 of this thesis can be further developed to address other aspects of communications such as security and efficient network interoperability in order to drastically mitigate the detrimental effects and conditions experienced during marine explorations. As such, developing unorthodox communication technologies/ algorithms based on software-defined networking (SDN), network functions virtualization (NFV), gateway solutions and content-centric networking (CCN) etc, can still be considered for enhancing the designs of marine hardware architectures for the IoMT with the aim of improving the overall network transmission data rates, spectral efficiencies, channel estimation, navigation security/ access control and the holistic QoS-guaranteed probabilities of oceanographic communications. More so, the development of software architectures that will enhance computation, mining, unsupervised and reinforcement learning, and aggregation of marine data with huge volumes, varieties and speed is still an open research issue for nautical communication systems. As such, the extensive deploration and improvement of fog and cloud computing technologies can go a mile to significantly support nautical explorations ranging from oil and gas drilling/maintenance to maritime cargo transportations and to underwater navigation/explorations etc. At this point, it is important to bear in mind that the development of marine IoT-enabled communication technologies is currently an interesting research area that is worthy of drawing the attention of numerous researchers and scholars in the field, where the safety, security, energy efficiency and environmental sustainabilities of nautical communication networks can be tremendously considered and improved. Hence, a summary of possible research directions in application to IoMT is listed as follows:

- In this thesis, we analysed the MSE performance of some estimators in comparison to various levels of SNR. Nevertheless, the MSE performance comparison of CE schemes in terms of Signal-to-Interference-plus-Noise Ratio (SINR) is an open research area to be developed. More so, analysing and evaluating the performances of the estimators in disconnected (or faulty) sensor networks with tremendous time delays will also be an interesting area of future research works.
- Designing unprecedented system architectures based on network technologies such as SDN,

cloud repatriation, edge computing, quantum computing, serverless computing and intent-based networking etc, for enabling EC in industries such as agriculture, smart energy, healthcare and transportation among others, is an open research problem.

- Developing novel network layer and energy-efficient routing protocols for enabling ubiquitous computing aided SDN-enabled EC procedures in solving the energy-hole problem of marine sensor networks for oil & gas exploration is still an open research issue.
- Exploiting the benefits of artificial intelligence and machine learning techniques for facilitating autonomous IoMT-aided networks is an enormously interesting research area. The integration of these technologies for maritime operations can be adopted for monitoring and safeguarding the aquatic lives across global deep oceans. Here, sensors will be placed on universal ocean bodies which can monitor the environmental conditions of marine surroundings so as to preserve aquatic lives from possible harm and extinctions that may arise from anthropogenic activities during oceanic explorations.
- Establishing ultra-modern cryptographic algorithms for addressing security concerns such as marine user confidentiality, end device security, virtualization security and core/edge network security for IoMT applications is an unreserved research domain awaiting explorations.

Keeping in view the coverage of this thesis, it is presumed that this study will spring up possible research directions in improving the autonomous extraction procedures of oil & gas across deep waters using contemporary IoT-based communication technologies. For future works, we consider to present a detailed comparative data analysis that compares the output performances of an SDN-aided EC-enabled oil and gas extraction technology in comparison to exploration scenarios where the EC process is not aided. A comparative analysis of existing maritime routing protocols such as the MAC-based routing protocol for TRITON (MRPT), OLSR, AoDV and AoMDV protocols etc in comparison with our MSPT routing protocol for oil and gas explorations will be elaborately provided.

REFERENCES

[1] Y. Yang, L. Wu, G. Yin, L. Li, and H. Zhao, "A survey on security and privacy issues in internet-of-things," *IEEE Internet of Things Journal*, vol. 4, no. 5, pp. 1250–1258, 2017.

[2] O. Elijah, T. A. Rahman, I. Orikumhi, C. Y. Leow, and M. N. Hindia, "An overview of internet of things (IoT) and data analytics in agriculture: Benefits and challenges," *IEEE Internet of Things Journal*, vol. 5, no. 5, pp. 3758–3773, 2018.

[3] Y. Kim, Y. Song, and S. H. Lim, "Hierarchical maritime radio networks for internet of maritime things," *IEEE Access*, vol. 7, no. 4, pp. 54 218–54 227, 2019.

[4] Y. Xu, "Quality of service provisions for maritime communications based on cellular networks," *IEEE Access*, vol. 5, no. 10, pp. 23 881–23 890, 2017.

[5] P. Sethi and S. R. Sarangi, "Internet of things: Architectures, protocols, and applications," *Journal of Electrical and Computer Engineering*, vol. 2017, no. 9324035, pp. 1–25, Jan. 2017.

[6] S. Forsstrom and U. Jennehag, "A performance and cost evaluation of combining OPC-UA and microsoft azure IoT hub into an industrial internet-of-things system," in *2017 Global Internet of Things Summit (GIoTS)*, Geneva, Switzerland, Jun 2017, pp. 1–6.

[7] O. Hahm, E. Baccelli, H. Petersen, and N. Tsiftes, "Operating systems for low-end devices in the internet of things: A survey," *IEEE Internet of Things Journal*, vol. 3, no. 5, pp. 720–734, Oct 2016.

[8] N. Ye, Y. Zhang, R. Wang, and R. Malekian, "Vehicle trajectory prediction based on hidden markov model." *KSII Transactions on Internet & Information Systems*, vol. 10, no. 7, 2016.

[9] A. J. Onumanyi, A. M. Abu-Mahfouz, and G. P. Hancke, "Cognitive radio in low power wide area network for IoT applications: Recent approaches, benefits and challenges," *IEEE Transactions on Industrial Informatics*, vol. 8, no. 11, pp. 1–10, 2019.

[10] S. Bera, S. Misra, and A. V. Vasilakos, "Software-defined networking for internet of things: A survey," *IEEE Internet of Things Journal*, vol. 4, no. 6, pp. 1994–2008, 2017.

[11] M. Mongiello, T. Di Noia, F. Nocera, E. Di Sciascio, and A. Parchitelli, "Context-aware design of reflective middleware in the internet of everything," in *Federation of International Conferences on Software Technologies: Applications and Foundations*. Marburg, Germany: Springer, Dec 2016, pp. 423–435.

[12] R. Parashar, A. Khan, and Neha, "A survey: The internet of things," *International Journal of Technical Research and Applications*, vol. 4, no. 3, pp. 251–257, 2016.

[13] D. Evans, "The internet of things: How the next evolution of the internet is changing everything," *Cisco white paper*, pp. 1 – 11, 2011.

[14] A. Kamilaris and A. Pitsillides, "Mobile phone computing and the internet of things: A survey," *IEEE Internet of Things Journal*, vol. 3, no. 6, pp. 885–898, 2016.

[15] Y. Li, Y. Tu, J. Lu, and Y. Wang, "A security transmission and storage solution about sensing image for blockchain in the internet of things," *Sensors*, vol. 20, no. 3, pp. 1 – 13, 2020.

[16] A. Zgank, "Bee swarm activity acoustic classification for an iot-based farm service," *Sensors*, vol. 20, no. 1, pp. 1 – 14, 2020.

[17] V. C. Gungor and G. P. Hancke, "Industrial wireless sensor networks: Challenges, design principles, and technical approaches," *IEEE Transactions on Industrial Electronics*, vol. 56, no. 10, pp. 4258–4265, 2009.

[18] S. S. Oyewobi, G. P. Hancke, A. M. Abu-Mahfouz, and A. J. Onumanyi, "An effective spectrum handoff based on reinforcement learning for target channel selection in the industrial internet of things," *Sensors*, vol. 19, no. 6, pp. 1 – 21, 2019.

[19] F. Alkhabbas, M. Ayyad, R. C. Mihailescu, and P. Davidsson, "A commitment-based approach to realize emergent configurations in the internet of things," in *2017 IEEE International Conference on Software Architecture Workshops (ICSAW)*, Gothenburg, Sweden, Apr 2017, pp. 88–91.

[20] X. Shi, X. An, Q. Zhao, H. Liu, L. Xia, X. Sun, and Y. Guo, "State-of-the-art internet of things in protected agriculture," *Sensors*, vol. 19, no. 8, pp. 1 – 24, 2019.

[21] E. Botha, R. Malekian, and O. E. Ijiga, "IoT in agriculture: Enhanced throughput in South African farming applications," in *2019 IEEE 2nd Wireless Africa Conference (WAC)*, Pretoria, South Africa, Aug 2019, pp. 1–5.

[22] A. Sheth, P. Anantharam, and C. Henson, "Physical-cyber-social computing: An early 21st century approach," *IEEE Intelligent Systems*, vol. 28, no. 1, pp. 78–82, 2013.

[23] J. Zeng, L. T. Yang, M. Lin, H. Ning, and J. Ma, "A survey: cyber-physical-social systems and their system-level design methodology," *Elservier Journal on Future Generation Computer Systems*, vol. 105, no. 4, pp. 1–15, 2016.

[24] M. Chiang and T. Zhang, "Fog and IoT: An overview of research opportunities," *IEEE Internet of Things Journal*, vol. 3, no. 6, pp. 854–864, 2016.

[25] B. Chen, J. Wan, L. Shu, P. Li, M. Mukherjee, and B. Yin, "Smart factory of industry 4.0: Key technologies, application case, and challenges," *IEEE Access*, vol. 6, no. 12, pp. 6505–6519, 2018.

[26] C. Qiu, F. R. Yu, H. Yao, C. Jiang, F. Xu, and C. Zhao, "Blockchain-based software-defined industrial internet of things: A dueling deep Q -learning approach," *IEEE Internet of Things Journal*, vol. 6, no. 3, pp. 4627–4639, 2019.

[27] A. Čolaković and M. Hadžialić, "Internet of things (IoT): A review of enabling technologies, challenges, and open research issues," *Computer Networks*, vol. 144, no. 7, pp. 17–39, 2018.

[28] B. B. Letswamotse, R. Malekian, C.-Y. Chen, and K. M. Modieginyane, "Software defined wireless sensor networks (sdwsn): a review on efficient resources, applications and technologies," *Journal of Internet Technology*, vol. 19, no. 5, pp. 1303–1313, 2018.

[29] B. B. Letswamotse, R. Malekian, C.-Y. Chen, and K. M. Modieginyane, "Software defined wireless sensor networks and efficient congestion control," *IET Networks*, vol. 7, no. 6, pp. 460–464, 2018.

[30] Y. Ma, Y. Chen, and J. Chen, "SDN-enabled network virtualization for industry 4.0 based on iots and cloud computing," in *2017 19th International Conference on Advanced Communication Technology (ICACT)*, Bongpyeong, South Korea, Feb 2017, pp. 199–202.

[31] R. Chaudhary, G. S. Aujla, S. Garg, N. Kumar, and J. J. P. C. Rodrigues, "SDN-enabled multi-attribute-based secure communication for smart grid in IIoT environment," *IEEE Transactions on Industrial Informatics*, vol. 14, no. 6, pp. 2629–2640, 2018.

[32] P. Fraga-Lamas, T. M. Fernandez-Carames, M. Suarez-Albela, L. Castedo, and M. Gonzalez-Lopez, "A review on internet of things for defense and public safety," *Sensors*, vol. 16, no. 1644, pp. 1–45, 2016.

[33] C. Gomez, S. Chessa, A. Fleury, G. Roussos, and D. Preuveneers, "Internet of things for enabling smart environments: A technology-centric perspective," *Journal of Ambient Intelligence and Smart Environments*, vol. 11, no. 1, pp. 23–43, 2019.

[34] A. Al-Fuqaha, M. Guizani, M. Mohammadi, M. Aledhari, and M. Ayyash, "Internet of things: A survey on enabling technologies, protocols, and applications," *IEEE Communications Surveys & Tutorials*, vol. 17, no. 4, pp. 2347–2376, 2015.

[35] P. A. Laplante and N. Laplante, "The internet of things in healthcare: Potential applications and challenges," *IT Professional*, vol. 18, no. 3, pp. 2–4, 2016.

[36] E. Solaiman, R. Ranjan, P. P. Jayaraman, and K. Mitra, "Monitoring internet of things application ecosystems for failure," *IT Professional*, vol. 18, no. 5, pp. 8–11, 2016.

[37] M. Ramadan, "Industry 4.0: Development of smart sunroof ambient light manufacturing system for automotive industry," in *2019 Advances in Science and Engineering Technology International Conferences (ASET)*, Dubai, United Arab Emirates, Mar 2019, pp. 1–5.

[38] A. Zanella, N. Bui, A. Castellani, L. Vangelista, and M. Zorzi, "Internet of things for smart cities," *IEEE Internet of Things Journal*, vol. 1, no. 1, pp. 22–32, 2014.

[39] O. O. Ogundile, M. B. Balogun, O. E. Ijiga, and E. O. Falayi, "Energy-balanced and energy-efficient clustering routing protocol for wireless sensor networks," *IET Communications*, vol. 13, no. 10, pp. 1449–1457, 2019.

[40] O. Ogundile and A. Alfa, "A survey on an energy-efficient and energy-balanced routing protocol for wireless sensor networks," *Sensors*, vol. 17, no. 5, pp. 1 – 51, 2017.

[41] I. B. Aris, R. K. Z. Sahbusdin, and A. F. M. Amin, "Impacts of IoT and big data to automotive industry," in *2015 10th Asian Control Conference (ASCC)*, Sabah, Malaysia, May 2015, pp. 1–5.

[42] O. Jo, Y. Jo, and J. Kim, "Internet of things for smart railway: Feasibility and applications," *IEEE Internet of Things Journal*, vol. 5, no. 2, pp. 482–490, 2018.

[43] X. Jin, J. Shao, X. Zhang, W. An, and R. Malekian, "Modeling of nonlinear system based on deep learning framework," *Nonlinear Dynamics*, vol. 84, no. 3, pp. 1327–1340, 2016.

[44] I. F. Akyildiz, S. Nie, S.-C. Lin, and M. Chandrasekaran, "5G roadmap: 10 key enabling technologies," *Computer Networks*, vol. 106, no. 9, pp. 17–48, 2016.

[45] O. E. Ijiga, O. O. Ogundile, A. D. Familua, and D. J. Versfeld, "Review of channel estimation for candidate waveforms of next generation networks," *Electronics*, vol. 8, no. 9, pp. 1 – 50, 2019.

[46] N. Abbas, Y. Zhang, A. Taherkordi, and T. Skeie, "Mobile edge computing: A survey," *IEEE Internet of Things Journal*, vol. 5, no. 1, pp. 450–465, 2018.

[47] J. Lin, W. Yu, N. Zhang, X. Yang, H. Zhang, and W. Zhao, "A survey on internet of things: Architecture, enabling technologies, security and privacy, and applications," *IEEE Internet of Things Journal*, vol. 4, no. 5, pp. 1125–1142, 2017.

[48] M. R. Palattella, M. Dohler, A. Grieco, G. Rizzo, J. Torsner, T. Engel, and L. Ladid, "Internet of things in the 5G era: Enablers, architecture, and business models," *IEEE Journal on Selected Areas in Communications*, vol. 34, no. 3, pp. 510–527, 2016.

[49] A. Ijaz, L. Zhang, M. Grau, A. Mohamed, S. Vural, A. U. Quddus, M. A. Imran, C. H. Foh, and R. Tafazolli, "Enabling massive IoT in 5G and beyond systems: Phy radio frame design considerations," *IEEE Access*, vol. 4, no. 6, pp. 3322–3339, 2016.

[50] G. A. Akpakwu, B. J. Silva, G. P. Hancke, and A. M. Abu-Mahfouz, "A survey on 5G networks for the internet of things: Communication technologies and challenges," *IEEE Access*, vol. 6, no. 12, pp. 3619–3647, 2018.

[51] C. Qiu, F. R. Yu, H. Yao, C. Jiang, F. Xu, and C. Zhao, "Blockchain-based software-defined industrial internet of things: A dueling deep q-learning approach," *IEEE Internet of Things Journal*, vol. 6, no. 3, pp. 1–14, 2018.

[52] P. Lade, R. Ghosh, and S. Srinivasan, "Manufacturing analytics and industrial internet of things," *IEEE Intelligent Systems*, vol. 32, no. 3, pp. 74–79, 2017.

[53] V. Scilimati, A. Petitti, P. Boccadoro, R. Colella, D. Di Paola, A. Milella, and L. A. Grieco, "Industrial internet of things at work: a case study analysis in robotic-aided environmental monitoring," *IET wireless sensor systems*, vol. 7, no. 5, pp. 155–162, 2017.

[54] T. Ulz, T. Pieber, C. Steger, S. Haas, H. Bock, and R. Matischek, "Bring your own key for the industrial internet of things," in *2017 IEEE International Conference on Industrial Technology (ICIT)*, Toronto, ON, Canada, Mar 2017, pp. 1430–1435.

[55] C. Sha, Y. Sun, and R. Malekian, "Research on cost-balanced mobile energy replenishment strategy for wireless rechargeable sensor networks," *IEEE Transactions on Vehicular Technology*, vol. 69, no. 3, pp. 3135–3150, 2019.

[56] S. R. Vijayalakshmi and S. Muruganand, "A survey of internet of things in fire detection and fire industries," in *2017 International Conference on I-SMAC (IoT in Social, Mobile, Analytics and Cloud) (I-SMAC)*, Palladam, India, Feb 2017, pp. 703–707.

[57] S. H. Javadi and A. Mohammadi, "Fire detection by fusing correlated measurements," *Journal of Ambient Intelligence and Humanized Computing*, vol. 10, no. 4, pp. 1443–1451, 2019.

[58] I. Koutsopoulos and M. Halkidi, "Distributed energy-efficient estimation in spatially correlated wireless sensor networks," *Computer Communications*, vol. 45, no. 6, pp. 47–58, 2014.

[59] S. G. Iyengar, P. K. Varshney, and T. Damarla, "A parametric copula based framework for multimodal signal processing," in *2009 IEEE International Conference on Acoustics, Speech and Signal Processing*, Taipei, Taiwan, May 2009, pp. 1893–1896.

[60] S. G. Iyengar, P. K. Varshney, and T. Damarla, "A parametric copula-based framework for hypothesis testing using heterogeneous data," *IEEE Transactions on Signal Processing*, vol. 59, no. 5, pp. 2308–2319, 2011.

[61] V. Scilimati, A. Petitti, P. Boccadoro, R. Colella, D. D. Paola, A. Milella, and L. A. Grieco, "Industrial internet of things at work: a case study analysis in robotic-aided environmental monitoring," *IET Wireless Sensor Systems*, vol. 7, no. 5, pp. 155–162, 2017.

[62] D. Miller, "Blockchain and the internet of things in the industrial sector," *IT Professional*, vol. 20, no. 3, pp. 15–18, 2018.

[63] T. Qiu, Y. Zhang, D. Qiao, X. Zhang, M. L. Wymore, and A. K. Sangaiah, "A robust time synchronization scheme for industrial internet of things," *IEEE Transactions on Industrial Informatics*, vol. 14, no. 8, pp. 1–11, 2017.

[64] U. Baroudi, M. Bin-Yahya, M. Alshammari, and U. Yaqoub, "Ticket-based QoS routing optimization using genetic algorithm for WSN applications in smart grid," *Journal of Ambient Intelligence and Humanized Computing*, vol. 10, no. 4, pp. 1325–1338, 2019.

[65] S. Al-Rubaye, E. Kadhum, Q. Ni, and A. Anpalagan, "Industrial internet of things driven by SDN platform for smart grid resiliency," *IEEE Internet of Things Journal*, vol. 6, no. 1, pp. 1–11, 2017.

[66] R. Basir, S. Qaisar, M. Ali, M. Aldwairi, M. I. Ashraf, A. Mahmood, and M. Gidlund, "Fog computing enabling industrial internet of things: State-of-the-art and research challenges," *Sensors*, vol. 19, no. 21, pp. 1 – 38, 2019.

[67] K. R. Choo, S. Gritzalis, and J. H. Park, "Cryptographic solutions for industrial internet-of-things: Research challenges and opportunities," *IEEE Transactions on Industrial Informatics*, vol. 14, no. 8, pp. 3567–3569, 2018.

[68] S. Jo and W. Shim, "LTE-maritime: High-speed maritime wireless communication based on LTE technology," *IEEE Access*, vol. 7, no. 4, pp. 53 172–53 181, 2019.

[69] F. Bekkadal and K. Yang, "Novel maritime communications technologies," in *2010 10th Mediterranean Microwave Symposium*, Guzelyurt, Cyprus, Aug 2010, pp. 338–341.

[70] T. Yang, Z. Zheng, H. Liang, R. Deng, N. Cheng, and X. Shen, "Green energy and content-aware data transmissions in maritime wireless communication networks," *IEEE Transactions on Intelligent Transportation Systems*, vol. 16, no. 2, pp. 751–762, 2015.

[71] P. Kong, J. S. Pathmasuntharam, H. Wang, Y. Ge, C. Ang, W. Su, M. Zhou, and H. Harada, "A routing protocol for WiMAX based maritime wireless mesh networks," in *VTC Spring 2009 - IEEE 69th Vehicular Technology Conference*, Barcelona, Spain, Apr 2009, pp. 1–5.

[72] M. Manoufali, H. Alshaer, P.-Y. Kong, and S. Jimaa, "An overview of maritime wireless mesh communication technologies and protocols," *International Journal of Business Data Communications and Networking (IJBDCN)*, vol. 10, no. 1, pp. 1–29, 2014.

[73] M. Manoufali, H. Alshaer, P. Kong, and S. Jimaa, "Technologies and networks supporting maritime wireless mesh communications," in *6th Joint IFIP Wireless and Mobile Networking Conference (WMNC)*, Dubai, United Arab Emirates, Apr 2013, pp. 1–8.

[74] D. Kidston and T. Kunz, "Challenges and opportunities in managing maritime networks," *IEEE Communications Magazine*, vol. 46, no. 10, pp. 162–168, 2008.

[75] Y. Xu, S. Jiang, and F. Liu, "A LTE-based communication architecture for coastal networks," in *Proceedings of the 11th ACM International Conference on Underwater Networks & Systems*, Shanghai, China, Oct 2016, pp. 1–2.

[76] J. Dhivvya, S. N. Rao, and S. Simi, "Towards maximizing throughput and coverage of a novel heterogeneous maritime communication network," in *Proceedings of the 18th ACM International Symposium on Mobile Ad Hoc Networking and Computing*, Chennai, India, Jul 2017, pp. 1–2.

[77] F. Bekkadal, "Novel maritime communications technologies," *International Journal on Marine Navigation and Safety of Sea Transportation*, vol. 4, no. 2, pp. 129–135, 2010.

[78] A. Xiao, N. Ge, L. Yin *et al.*, "A voyage-based cooperative resource allocation scheme in maritime broadband access network," in *2017 IEEE 86th Vehicular Technology Conference (VTC-Fall)*, Toronto, ON, Canada, Sep 2017, pp. 1–5.

[79] D. Yoo, H. Kim, J. Choi, B. Jang, and S. Ro, "A novel antenna tracking technique for maritime broadband communication (maricomm) system," in *2015 17th International Conference on Advanced Communication Technology (ICACT)*, Seoul, South Korea, Aug 2015, pp. 225–229.

[80] C. Liu, W. Feng, T. Wei, and N. Ge, "Fairness-oriented hybrid precoding for massive mimo maritime downlink systems with large-scale csit," *China Communications*, vol. 15, no. 1, pp. 52–61, 2018.

[81] Y. Shi and X. Ma, "Performance analysis of land-to-ship marine communication based on block markov superposition transmission and spatial modulation," in *2018 10th International*

Conference on Wireless Communications and Signal Processing (WCSP), Hangzhou, China, Oct 2018, pp. 1–6.

[82] R. Duan, J. Wang, H. Zhang, Y. Ren, and L. Hanzo, "Joint multicast beamforming and relay design for maritime communication systems," *IEEE Transactions on Green Communications and Networking*, vol. 4, no. 1, pp. 139–151, 2020.

[83] M. Manoufali, H. Alshaer, P.-Y. Kong, and S. Jimaa, "An overview of maritime wireless mesh communication technologies and protocols," *International Journal of Business Data Communications and Networking (IJBDCN)*, vol. 10, no. 1, pp. 1–29, 2014.

[84] F. Alkhabbas, R. Spalazzese, and P. Davidsson, "Architecting emergent configurations in the internet of things," in *2017 IEEE International Conference on Software Architecture (ICSA)*, Gothenburg, Sweden, Apr 2017, pp. 221–224.

[85] F. Alkhabbas and R. Spalazzese and P. Davidsson, "Emergent configurations in the internet of things as system of systems," in *2017 IEEE/ACM Joint 5th International Workshop on Software Engineering for Systems-of-Systems and 11th Workshop on Distributed Software Development, Software Ecosystems and Systems-of-Systems (JSOS)*, Buenos Aires, Argentina, May 2017, pp. 70–71.

[86] F. Alkhabbas, R. Spalazzese, and P. Davidsson., "ECo-IoT: an architectural approach for realizing emergent configurations in the internet of things," in *European Conference on Software Architecture, ECSA 2018*, Madrid, Spain, Sep 2018, pp. 86 – 102.

[87] T. Di Noia, M. Mongiello, F. Nocera, and U. Straccia, "A fuzzy ontology-based approach for tool-supported decision making in architectural design," *Knowledge and Information Systems*, vol. 58, no. 1, pp. 83–112, 2019.

[88] F. Nocera, M. Mongiello, E. Di Sciascio, and T. Di Noia, "MoSAIC: a middleware-induced software architecture design decision support system," in *Proceedings of the 12th European Conference on Software Architecture: Companion Proceedings. ACM*, Madrid, Spain, Sep 2018, pp. 1 – 4.

[89] N. Mäkitalo, F. Nocera, M. Mongiello, and S. Bistarelli, "Architecting the web of things for the fog computing era," *IET Software*, vol. 12, no. 5, pp. 381–389, 2018.

[90] G. Shao, Y. Ma, R. Malekian, X. Yan, and Z. Li, "A novel cooperative platform design for coupled USV-UAV systems," *IEEE Transactions on Industrial Informatics*, vol. 15, no. 9, pp. 4913 – 4922, 2019.

[91] B. Dicks, "The environmental impact of marine oil spills-effects, recovery and compensation," in *1998 International seminar on tanker safety, polution prevention, spill response and compensation)*, Tokyo, Japan, Nov 1998, pp. 1–8.

[92] O. L. Osen, H. Wang, K. B. Hjelmervik, and H. Schoyen, "Organizing data from industrial internet of things for maritime operations," in *OCEANS 2017 - Aberdeen*, Aberdeen, UK, Jun 2017, pp. 1–5.

[93] M. Lennon, N. Thomas, V. Mariette, S. Babichenko, and G. Mercier, "Oil slick detection and characterization by satellite and airborne sensors: experimental results with sar, hyperspectral and lidar data," in *Proceedings. 2005 IEEE International Geoscience and Remote Sensing Symposium, 2005. IGARSS '05*, Seoul, South Korea, Jul 2005, pp. 292 – 295.

[94] Open Network Foundation (ONF), "Software-defined networking: The new norm for networks," *ONF White Paper*, pp. 1–12, 2012.

[95] O. Choi and S. Han, "Ubiquitous computing services discovery and execution using a novel intelligent web services algorithm," *Sensors*, vol. 7, no. 7, pp. 1287–1305, 2007.

[96] B. N. Grosof, M. D. Gandhe, T. W. Finin *et al.*, "Sweetjess: Translating DAMLRuleML to JESS." in *Proceedings of the International Workshop on Rule Markup Languages for Business Rules on the Semantic Web*, Sardinia, Italy, Jun 2002, pp. 1–21.

[97] H. Sharma and S. Sharma, "A review of sensor networks: Technologies and applications," in *2014 Recent Advances in Engineering and Computational Sciences (RAECS)*, Chandigarh, India, Mar 2014, pp. 1–4.

[98] S. S. I. Samuel, "A review of connectivity challenges in IoT-smart home," in *2016 3rd MEC International Conference on Big Data and Smart City (ICBDSC)*, Muscat, Oman, Mar 2016, pp. 1–4.

[99] T. Elarabi, V. Deep, and C. K. Rai, "Design and simulation of state-of-art zigbee transmitter for IoT wireless devices," in *2015 IEEE International Symposium on Signal Processing and Information Technology (ISSPIT)*, Abu Dhabi, UAE, Dec 2015, pp. 297–300.

[100] M. B. Yassein, M. Q. Shatnawi, and D. Al-zoubi, "Application layer protocols for the internet of things: A survey," in *2016 International Conference on Engineering & MIS (ICEMIS)*, Agadir, Morocco, Sep 2016, pp. 1–4.

[101] L. Nastase, "Security in the internet of things: A survey on application layer protocols," in *2017 21st International Conference on Control Systems and Computer Science (CSCS)*, Bucharest, Romania, May 2017, pp. 659–666.

[102] P. P. Ray, "A survey on internet of things architectures," *Journal of King Saud University-Computer and Infromation Sciences*, vol. 30, no. 3, pp. 1–29, 2016.

[103] M. Saadeh, A. Sleit, M. Qatawneh, and W. Almobaideen, "Authentication techniques for the internet of things: A survey," in *2016 Cybersecurity and Cyberforensics Conference (CCC)*, Amman, Jordan, Aug 2016, pp. 28–34.

[104] S. Mijovic, E. Shehu, and C. Buratti, "Comparing application layer protocols for the internet of things via experimentation," in *2016 IEEE 2nd International Forum on Research and Technologies for Society and Industry Leveraging a better tomorrow (RTSI)*, Bologna, Italy, Sep 2016, pp. 1–5.

[105] M. Manoufali, H. Alshaer, P.-Y. Kong, and S. Jimaa, "An overview of maritime wireless mesh communication technologies and protocols," *International Journal of Business Data Communications and Networking (IJBDCN)*, vol. 10, no. 1, pp. 1–29, 2014.

[106] T. K. Sarkar, Zhong Ji, Kyungjung Kim, A. Medouri, and M. Salazar-Palma, "A survey of

various propagation models for mobile communication," *IEEE Antennas and Propagation Magazine*, vol. 45, no. 3, pp. 51–82, 2003.

[107] T. S. Rappaport, *Wireless Communications: Principles and Practice*. New Jersey: Prentice-Hall Inc, 2002.

[108] O. O. Oyerinde and S. H. Mneney, "Review of channel estimation for wireless communication systems," *IETE Technical review*, vol. 29, no. 4, pp. 282–298, 2012.

[109] V. K. Jones and G. C. Raleigh, "Channel estimation for wireless OFDM systems," in *IEEE GLOBECOM*, 1998, pp. 980–985.

[110] O. E. Ijiga, "Channel estimation techniques for filter bank multicarrier based transceivers for next generation of wireless networks systems," *M. S. dissertation*, University of the Witwatersrand, Johannesburg, South Africa, 2017.

[111] O. Edfors, M. Sandell, J.-J. Van de Beek, S. K. Wilson, and P. O. Borjesson, "OFDM channel estimation by singular value decomposition," *IEEE Transactions on communications*, vol. 46, no. 7, pp. 931–939, 1998.

[112] J.-J. Van De Beek, O. Edfors, M. Sandell, S. K. Wilson, and P. O. Borjesson, "On channel estimation in OFDM systems," in *1995 IEEE 45th Vehicular Technology Conference. Countdown to the Wireless Twenty-First Century*, Chicago, IL, USA, Aug 1995, pp. 815–819.

[113] S. S. Haykin, *Adaptive filter theory*, 4th ed. India: Pearson Ed., 2005.

[114] I. F. Akyildiz, S. Nie, S.-C. Lin, and M. Chandrasekaran, "5G roadmap: 10 key enabling technologies," *Elsevier Journal of Computer Networks*, vol. 106, no. 9, pp. 17 – 48, 2016.

[115] O. Hahm, E. Baccelli, H. Petersen, and N. Tsiftes, "Operating systems for low-end devices in the internet of things: A survey," *IEEE Internet of Things Journal*, vol. 3, no. 5, pp. 720–734, 2016.

[116] S. Ramesh and M. Govindarasu, "An efficient framework for privacy-preserving computations on encrypted IoT data," *IEEE Internet of Things Journal*, vol. 7, no. 5, pp. 1–8, 2020.

[117] L. Chettri and R. Bera, "A comprehensive survey on internet of things (IoT) toward 5G wireless systems," *IEEE Internet of Things Journal*, vol. 7, no. 1, pp. 16–32, 2020.

[118] S. Chen, H. Xu, D. Liu, B. Hu, and H. Wang, "A vision of IoT: Applications, challenges, and opportunities with China perspective," *IEEE Internet of Things Journal*, vol. 1, no. 4, pp. 349–359, 2014.

[119] M. Christiansen, K. Fagerholt, B. Nygreen, and D. Ronen, "Maritime transportation," *"Elsevier Handbooks in Operations Research and Management Science*, vol. 14, no. 12, pp. 189–284, 2007.

[120] G. Kahyarara, "Maritime transport in Africa: Challenges, opportunities, and an agenda for future research," in *2018 UNCTAD framework of the IAME Conference*, Mombasa, Kenya, Sept 2018, pp. 1– 49.

[121] M. Manoufali, H. Alshaer, P.-Y. Kong, and S. Jimaa, "An overview of maritime wireless mesh communication technologies and protocols," *International Journal of Business Data Communications and Networking (IJBDCN)*, vol. 10, no. 1, pp. 1–29, 2014.

[122] T. Mrkvička, M. Muška, and J. Kubečka, "Two step estimation for Neyman-Scott point process with inhomogeneous cluster centers," *Statistics and Computing*, vol. 24, no. 1, pp. 91–100, 2014.

[123] C. Saha, M. Afshang, and H. S. Dhillon, "Poisson cluster process: Bridging the gap between PPP and 3GPP HetNet models," in *2017 Information Theory and Applications Workshop (ITA)*, San Diego, CA, USA, Aug 2017, pp. 1–9.

[124] B. Błaszczyszyn and D. Yogeshwaran, *Clustering comparison of point processes, with applications to random geometric models*. New York, NY, USA: Springer, 2015.

[125] N. Hajri, N. Youssef, and M. Patzold, "On the statistical properties of phase crossings and random FM noise in double rayleigh fading channels," *IEEE Transactions on Vehicular Technology*, vol. 65, no. 4, pp. 1859–1867, 2016.

[126] V. Erceg, S. J. Fortune, J. Ling, A. J. Rustako, and R. A. Valenzuela, "Comparisons of a computer-based propagation prediction tool with experimental data collected in urban microcellular environments," *IEEE Journal on Selected Areas in Communications*, vol. 15, no. 4, pp. 677–684, 1997.

[127] P. S. Bithas, K. Maliatsos, and A. G. Kanatas, "The bivariate double rayleigh distribution for multichannel time-varying systems," *IEEE Wireless Communications Letters*, vol. 5, no. 5, pp. 524–527, 2016.

[128] I. S. Gradshteyn and I. M. Ryzhik, *Table of integrals, series, and products*, 6th ed. New York, NY, USA: Academic press, 2000.

[129] G. K. Karagiannidis, N. C. Sagias, and P. T. Mathiopoulos, "$N*$Nakagami: A novel stochastic model for cascaded fading channels," *IEEE Transactions on Communications*, vol. 55, no. 8, pp. 1453–1458, 2007.

[130] G. K. Karagiannidis, T. A. Tsiftsis, and R. K. Mallik, "Bounds for multihop relayed communications in nakagami-m fading," *IEEE Transactions on Communications*, vol. 54, no. 1, pp. 18–22, 2006.

[131] V. S. Adamchik and O. I. Marichev, "The algorithm for calculating integrals of hypergeometric type functions and its realization in reduce system," in *ACM Proceedings of the International Symposium on Symbolic and Algebraic Computation*, New York, NY, USA, 1990, pp. 212–224.

[132] N. Bouhlel and A. Dziri, "Maximum likelihood parameter estimation of nakagami-gamma shadowed fading channels," *IEEE Communications Letters*, vol. 19, no. 4, pp. 685–688, 2015.

[133] Lingzhi Cao and N. C. Beaulieu, "A simple efficient method for generating independent nakagami-m fading samples," in *2005 IEEE 61st Vehicular Technology Conference*, Stockholm,

Sweden, May 2005, pp. 44–47.

[134] J. C. Silveira Santos Filho and M. D. Yacoub, "On the simulation and correlation properties of phase-envelope nakagami fading processes," *IEEE Transactions on Communications*, vol. 57, no. 4, pp. 906–909, 2009.

[135] T. J. Rouphael, *RF and Digital SIGNAL processing for Software-defined radio*, 1st ed. Newnes: Elsevier, 2008.

[136] Yuping Zhao and Aiping Huang, "A novel channel estimation method for OFDM mobile communication systems based on pilot signals and transform-domain processing," in *1997 IEEE 47th Vehicular Technology Conference. Technology in Motion*, Phoenix, AZ, USA, May 1997, pp. 2089–2093.

[137] Yilun Chen, Y. Gu, and A. O. Hero, "Sparse LMS for system identification," in *2009 IEEE International Conference on Acoustics, Speech and Signal Processing*, Taipei, Taiwan, Apr 2009, pp. 3125–3128.

[138] Z. Xu, F. Bai, and G. Zheng Bang, "Improved variable ZA-LMS algorithm based on discrete cosine transform for high noise reduction," in *2016 35th Chinese Control Conference (CCC)*, Chengdu, China, Jul 2016, pp. 5116–5121.

[139] O. J. Tobias and R. Seara, "On the LMS algorithm with constant and variable leakage factor in a nonlinear environment," *IEEE Transactions on Signal Processing*, vol. 54, no. 9, pp. 3448–3458, 2006.

[140] X. Wu and Z. Ma, "Modeling and performance analysis of cellular and device-to-device heterogeneous networks," in *2017 IEEE Globecom Workshops (GC Wkshps)*, Singapore, Singapore, Dec 2017, pp. 1–6.

[141] M. R. Bhatnagar and M. Arti, "On the closed-form performance analysis of maximal ratio combining in shadowed-rician fading LMS channels," *IEEE Communications Letters*, vol. 18, no. 1, pp. 54–57, 2014.

[142] D. Schafhuber and G. Matz, "MMSE and adaptive prediction of time-varying channels for OFDM systems," *IEEE Transactions on Wireless Communications*, vol. 4, no. 2, pp. 593–602, 2005.

[143] O. O. Oyerinde and S. H. Mneney, "Regularized adaptive algorithms-based CIR predictors for time-varying channels in ofdm systems," *IEEE Signal Processing Letters*, vol. 18, no. 9, pp. 505–508, 2011.

[144] O. O. Oyerinde and S. H. Mneney, "Subspace tracking-based decision directed CIR estimator and adaptive cir prediction," *IEEE Transactions on Vehicular Technology*, vol. 61, no. 5, pp. 2097–2107, 2012.

[145] L. L. Scharf, *Statistical signal processing: Detection, estimation and time series analysis*. Boston, MA, USA: Addison-Wesley, 1991.

[146] A. K. Jagannatham, "Estimation for wireless communications: MIMO/ OFDM cellular and sensor networks," in *National Programme on Technology Enhanced Learning (NPTEL)*, Bombay, India, Jan 2016.

ADDENDUM A DERIVATION OF CHANNEL ESTIMATION FOR IoMT

A.1 DERIVATION OF CE TECHNIQUES FOR IOMT

In this section of the addendum, the expressions for the considered CE algorithms are elaborately derived as presented in section A.2, A.3, A.4 and A.5 respectively.

A.2 PROOF OF LMMSE CHANNEL ESTIMATE FOR IOMT

The aggregated CH sensor information $\mathbf{g}[D_i,i]$ can be used to form a diagonal matrix represented as:

$$\mathbf{G}[D_i,i] = diag\Big[\mathbf{g}[D_i,i]\Big] = diag\Big[g[D_i,1],g[D_i,2],...,g[D_i,d]\Big] \tag{A.1}$$

The DA received signals according to (4.15) can similarly be expressed as:

$$\mathbf{y}[D_i,i] = \Big[y[D_i,1],y[D_i,2],...,y[D_i,d]\Big] \tag{A.2}$$

To derive the LMMSE channel estimate for the proposed maritime framework, we consider the possible auto- and cross-covariance matrices between $\mathbf{C}[D_i,i]$ and the received signals $\mathbf{y}[D_i,i]$. Let the possible auto-covariance matrices between the channel and the received aggregated CH information

be respectively denoted as $\mathbf{A}_{cc}[D_i,i]$ and $\mathbf{A}_{yy}[D_i,i]$ while the possible cross-covariance matrices be represented as $\mathbf{A}_{cy}[D_i,i]$ and $\mathbf{A}_{yc}[D_i,i]$. Then, the structure of the overall covariance matrix $\left(\mathbf{A}[D_i,i]\right)$ can be given as:

$$\mathbf{A}[D_i,i] = \begin{bmatrix} \mathbf{A}_{cc}[D_i,i] & \mathbf{A}_{cy}[D_i,i] \\ W & W \\ \mathbf{A}_{yc}[D_i,i] & \mathbf{A}_{yy}[D_i,i] \end{bmatrix} \tag{A.3}$$

Using the rules of *inverse of a partitioned matrix* and *Matrix inversion lemma*, the inverse of the structured covariance matrix according to (A.3) can be obtained [145]. From this rule, the inverse partition matrix $\mathbf{A^{-1}}[D_i,i]$ as obtained from (A.3) is given as:

$$\mathbf{A}^{-1} = \begin{bmatrix} \mathbf{B}^{-1} & \mathbf{L}\mathbf{Q}^{-1} \\ W & W \\ \mathbf{P}\mathbf{Q}^{-1} & \mathbf{Q}^{-1} \end{bmatrix} \tag{A.4}$$

where

$$\begin{aligned} \mathbf{B} &= \mathbf{A}_{cc}[D_i,i] - \mathbf{A}_{cy}[D_i,i]\mathbf{A}_{yy}^{-1}[D_i,i]\mathbf{A}_{yc}[D_i,i] \\ \mathbf{B}^{-1} &= \mathbf{A}_{cc}^{-1}[D_i,i] + \mathbf{L}\mathbf{Q}^{-1}\mathbf{P} \\ \mathbf{L}.\mathbf{A}_{cc}[D_i,i] &= -\mathbf{A}_{cy}[D_i,i] \\ \mathbf{P}\mathbf{A}_{cc}[D_i,i] &= -\mathbf{A}_{yc}[D_i,i] \\ \mathbf{Q} &= \mathbf{A}_{cc}[D_i,i] - \mathbf{A}_{yc}[D_i,i]\mathbf{A}_{cc}^{-1}[D_i,i]\mathbf{A}_{cy}[D_i,i] \end{aligned} \tag{A.5}$$

Thus, from the theorem of partitioned matrix inverse,

$$\mathbf{A}^{-1}[D_i,i] = \begin{bmatrix} \mathbf{A}_{cc}^{-1}[D_i,i] & 0 \\ W & W \\ 0 & 0 \end{bmatrix} + \begin{bmatrix} \mathbf{L} \\ W \\ \boldsymbol{I}[m] \end{bmatrix} + \begin{bmatrix} \mathbf{P} & I[m] \end{bmatrix} \begin{bmatrix} \mathbf{Q}^{-1} \end{bmatrix} \tag{A.6}$$

where $\boldsymbol{I}[m]$ is an $M \times M$ identity matrix. Hence, directly substituting the expressions in (A.5) to (A.6) yields:

$$\mathbf{A}^{-1}[D_i,i] = \begin{bmatrix} \mathbf{A}_{cc}^{-1}[D_i,i] & 0 \\ W & W \\ 0 & 0 \end{bmatrix} + \begin{bmatrix} -\mathbf{A}_{cc}[D_i,i]\mathbf{A}_{cy}[D_i,i] \\ W \\ \boldsymbol{I}[m] \end{bmatrix} + \begin{bmatrix} -\mathbf{A}_{yc}[D_i,i]\mathbf{A}_{cc}^{-1}[D_i,i] & \boldsymbol{I}[m] \end{bmatrix} \begin{bmatrix} \mathbf{Q}^{-1} \end{bmatrix} \tag{A.7}$$

In this expression as in (A.7), $\mathbf{Q}$ is known as the Schur component of $\mathbf{A}_{yy}[D_i,i]$ which is given as expressed in (A.5). The component also constitute the variance of the noise σ_w^2. Thus, the linear expression presented in (4.15) can be equivalently written in matrix form as:

$$\begin{bmatrix} \mathbf{C}[D_i,i] \\ W \\ \mathbf{y}[D_i,i] \end{bmatrix} = \begin{bmatrix} \boldsymbol{I}[m] & 0 \\ W & W \\ \mathbf{G}[D_i,i] & \boldsymbol{I}[m] \end{bmatrix} + \begin{bmatrix} \mathbf{C}[D_i,i] \\ W \\ \mathbf{w}[D_i,i] \end{bmatrix} \tag{A.8}$$

The structured covariance matrix can then be given as:

$$\mathbf{A}[D_i,i] = \mathbb{E}\begin{bmatrix} \mathbf{C}[D_i,i] \\ W \\ \mathbf{y}[D_i,i] \end{bmatrix} \begin{bmatrix} \mathbf{C}^H[D_i,i] & \mathbf{y}^H[D_i,i] \end{bmatrix} = \begin{bmatrix} \boldsymbol{I}[m] & 0 \\ W & W \\ \mathbf{G}[D_i,i] & \boldsymbol{I}[m] \end{bmatrix} \begin{bmatrix} \mathbf{A}_{cc}[D_i,i] & 0 \\ W & W \\ 0 & \sigma_w^2\boldsymbol{I}[m] \end{bmatrix} \begin{bmatrix} \boldsymbol{I}[m] & \mathbf{G}^H[D_i,i] \\ W & W \\ 0 & \boldsymbol{I}[m] \end{bmatrix}$$

$$= \begin{bmatrix} \mathbf{A}_{cc}[D_i,i] & \mathbf{A}_{cc}[D_i,i]\mathbf{G}^H[D_i,i] \\ W & W \\ \mathbf{G}[D_i,i]\mathbf{A}_{cc}[D_i,i] & \mathbf{G}[D_i,i]\mathbf{A}_{cc}[D_i,i]\mathbf{G}^H[D_i,i] + \sigma_w^2\boldsymbol{I}[m] \end{bmatrix} = \begin{bmatrix} \mathbf{A}_{cc}[D_i,i] & \mathbf{A}_{cy}[D_i,i] \\ W & W \\ \mathbf{A}_{yc}[D_i,i] & \mathbf{A}_{yy}[D_i,i] \end{bmatrix} \tag{A.9}$$

where $(.)^H$ represents the hermitian transpose operator and $\mathbb{E}$ is the expectation operator.

By comparing the expressions in (A.9), the following conclusions can be made:

$$\mathbf{A}_{cy}[D_i,i] = \mathbb{E}\left[\mathbf{C}[D_i,i]\ \ \mathbf{y}^H[D_i,i]\right] = \mathbf{A}_{cc}[D_i,i]\mathbf{G}^H[D_i,i] \tag{A.10}$$

$$\mathbf{A}_{yc}[D_i,i] = \mathbb{E}\left[\mathbf{y}[D_i,i]\ \ \mathbf{C}^H[D_i,i]\right] = \mathbf{A}_{cc}[D_i,i]\mathbf{G}[D_i,i] \tag{A.11}$$

$$\mathbf{A}_{yy}[D_i,i] = \mathbb{E}\left[\mathbf{y}[D_i,i]\ \ \mathbf{y}^H[D_i,i]\right] = \mathbf{G}[D_i,i]\mathbf{A}_{cc}[D_i,i]\mathbf{G}^H[D_i,i] + \sigma_w^2\boldsymbol{I}[m] \tag{A.12}$$

According to the Weiner-Hopf equation, the orthogonality condition of the LMMSE estimator must satisfy the expression [145]:

$$\mathbf{A}_{yc}[D_i,i] = \mathbb{E}\left[(\mathbf{C}[D_i,i] - \Xi[D_i,i]\mathbf{y}[D_i,i])\mathbf{y}^H[D_i,i]\right] = 0 \tag{A.13}$$

where $\Xi[D_i,i]$ is a matrix that satisfies the Weiner-Hopf equation. To determine $\Xi[D_i,i]$, the orthogonality condition according to (A.13) is expressed as [145]:

$$\begin{aligned}\mathbf{A}_{cy}[D_i,i] - \Xi^H[D_i,i]\mathbf{y}[D_i,i]\mathbf{y}^H[D_i,i] &= 0\\ \Xi^H[D_i,i] &= \mathbf{A}_{cy}[D_i,i]\mathbf{A}_{yy}^{-1}[D_i,i]\end{aligned} \tag{A.14}$$

For a Gaussian and uncorrelated maritime channel $\mathbf{C}[D_i,i]$ with noise $\mathbf{w}[D_i,i]$, it can be concluded that the linear estimator which minimizes the MSE is represented as [111, 112]:

$$\hat{\mathbf{C}}_{LMMSE}[D_i,i] = \Xi[D_i,i]\mathbf{y}[D_i,i] = \mathbf{A}_{cy}[D_i,i]\mathbf{A}_{yy}^{-1}[D_i,i]\mathbf{y}[D_i,i] \tag{A.15}$$

Substituting (A.10) and (A.12) into (A.15) yields the LMMSE CE expression in (A.16).

$$\begin{aligned}\hat{\mathbf{C}}_{LMMSE}[D_i,i] &= \mathbf{A}_{cc}[D_i,i]\mathbf{G}^H[D_i,i]\left[\mathbf{G}[D_i,i]\mathbf{A}_{cc}[D_i,i]\mathbf{G}^H[D_i,i] + \sigma_w^2\boldsymbol{I}[m]\right]^{-1}\mathbf{y}[D_i,i] \\ &= \frac{\mathbf{A}_{cc}[D_i,i]\mathbf{G}^H[D_i,i]\mathbf{y}[D_i,i]}{\mathbf{G}[D_i,i]\mathbf{A}_{cc}[D_i,i]\mathbf{G}^H[D_i,i] + \sigma_w^2\boldsymbol{I}[m]} \\ &= \frac{\mathbf{A}_{cc}[D_i,i]\mathbf{G}^H[D_i,i]\mathbf{y}[D_i,i]}{\mathbf{G}[D_i,i]\mathbf{G}^H[D_i,i]\left[\mathbf{A}_{cc}[D_i,i] + (\mathbf{G}^H[D_i,i]\mathbf{G}[D_i,i])^{-1}\sigma_w^2\boldsymbol{I}[m]\right]}\end{aligned}$$

Thus,

$$\hat{\mathbf{C}}_{LMMSE}[D_i,i] = \frac{\mathbf{A}_{cc}[D_i,i]\mathbf{y}[D_i,i]}{\mathbf{G}[D_i,i]\left[\mathbf{A}_{cc}[D_i,i] + (\mathbf{G}^H[D_i,i]\mathbf{G}[D_i,i])^{-1}\sigma_w^2\boldsymbol{I}[m]\right]} \tag{A.16}$$

A.3 PROOF OF NLMS CHANNEL ESTIMATE

Expanding (3.8), the cost function for minimizing the mean square error (MSE) of marine fading channel is given as:

$$\begin{aligned}\mathbf{J}_{cf}[D_i,i] &= \mathbb{E}\Big[(\mathbf{y}[D_i,i]\mathbf{y}^*[D_i,i]) - (\mathbf{y}[D_i,i]\mathbf{C}[D_i,i]\mathbf{g}^H[D_i,i]) - (\mathbf{y}^*[D_i,i]\mathbf{C}^H[D_i,i]\mathbf{g}[D_i,i]) \\ &\quad + (\mathbf{C}^H[D_i,i]\mathbf{g}[D_i,i]\mathbf{C}[D_i,i]\mathbf{g}^H[D_i,i])\Big] \\ &= \mathbb{E}\left[(\mathbf{y}[D_i,i]\mathbf{y}^*[D_i,i])\right] - \mathbb{E}\left[(\mathbf{y}[D_i,i]\mathbf{C}[D_i,i]\mathbf{g}^H[D_i,i])\right] - \mathbb{E}\left[(\mathbf{y}^*[D_i,i]\mathbf{C}^H[D_i,i]\mathbf{g}[D_i,i])\right] \\ &\quad + \mathbb{E}\left[(\mathbf{C}^H[D_i,i]\mathbf{g}[D_i,i]\mathbf{C}[D_i,i]\mathbf{g}^H[D_i,i])\right] \\ &= \mathbb{E}\left[(\mathbf{y}[D_i,i]\mathbf{y}^*[D_i,i])\right] - \mathbf{C}[D_i,i]\,\mathbb{E}[(\mathbf{y}[D_i,i]\mathbf{g}^H[D_i,i])] - \mathbf{C}^H[D_i,i]\,\mathbb{E}[(\mathbf{y}^*[D_i,i]\mathbf{g}[D_i,i])] \\ &\quad + \mathbf{C}^H[D_i,i]\mathbf{C}[D_i,i]\,\mathbb{E}\left[(\mathbf{g}[D_i,i]\mathbf{g}^H[D_i,i])\right]\end{aligned} \tag{A.17}$$

If the aggregated MUE sensor information and the received signal at the coastal-based control station are jointly stationary, the individual expectations in $\mathbf{J}_{cf}[D_i,i]$ according to (A.17) can simply be define as follows [113]:

◇ If $\mathbf{y}[D_i,i]$ has zero mean, then

$$\sigma_y^2 = \mathbb{E}\left[(\mathbf{y}[D_i,i]\mathbf{y}^*[D_i,i])\right] \tag{A.18}$$

◇ Let $\varkappa$ be the $d\times 1$ cross-correlation vector between the received signal $\mathbf{y}[D_i,i]$ and the aggregated CH information $\mathbf{g}[D_i,i]$. As such,

$$\varkappa = \mathbb{E}\left[(\mathbf{y}^*[D_i,i]\mathbf{g}[D_i,i])\right] \tag{A.19}$$

◇ From (A.19), the expression in (A.20) can be obtained.

$$\varkappa^H = \mathbb{E}\left[(\mathbf{y}[D_i,i]\mathbf{g}^H[D_i,i])\right] \tag{A.20}$$

◇ The $d\times d$ correlation matrix between $\mathbf{g}[D_i,i]$ is given as:

$$\bar{\Upsilon}[D_i,i] = \mathbb{E}\left[(\mathbf{g}[D_i,i]\mathbf{g}^H[D_i,i])\right] \tag{A.21}$$

Inserting (A.18), (A.19), (A.20) and (A.21) into the cost function $(\mathbf{J}_{cf}[D_i,i])$ as represented in (A.17), then

$$\mathbf{J}_{cf}[D_i,i] = \sigma_y^2 - \varkappa^H\mathbf{C}[D_i,i] - \varkappa\mathbf{C}^H[D_i,i] + \mathbf{C}^H[D_i,i]\mathbf{C}[D_i,i]\bar{\Upsilon}[D_i,i] \tag{A.22}$$

To obtain the gradient $\nabla[D_i,i]$, the MSE expression in (A.22) is differentiated with respect to (wrt) $\mathbf{C}[D_i,i]$ given as:

$$\nabla[D_i,i] = \frac{\mathrm{d}\mathbf{J}_{cf}[D_i,i]}{\mathrm{d}\mathbf{C}[D_i,i]} = -2\varkappa + 2\bar{\Upsilon}[D_i,i]\mathbf{C}[D_i,i] \tag{A.23}$$

When differentiating wrt a vector as done in (A.23), the following equations must be considered.

$$\frac{\mathrm{d}\left(\varkappa^H\mathbf{C}[D_i,i]\right)}{\mathrm{d}\mathbf{C}[D_i,i]} = 0 \tag{A.24}$$

$$\frac{\mathrm{d}\left(\varkappa \mathbf{C}[D_i,i]\right)}{\mathrm{d}\mathbf{C}[D_i,i]} = 2\varkappa \tag{A.25}$$

$$\frac{\mathrm{d}\left(\mathbf{C}^H[D_i,i]\mathbf{C}[D_i,i]\bar{\Upsilon}[D_i,i]\right)}{\mathrm{d}\mathbf{C}[D_i,i]} = 2\bar{\Upsilon}[D_i,i]\mathbf{C}[D_i,i] \tag{A.26}$$

If the instantaneous estimates for $\bar{\Upsilon}[D_i,i]$ and $\varkappa$ is considered, then

$$\hat{\varkappa} = \left[(\mathbf{y}^*[D_i,i]\mathbf{g}[D_i,i])\right] \tag{A.27}$$

$$\hat{\bar{\Upsilon}}[D_i,i] = \left[(\mathbf{g}[D_i,i]\mathbf{g}^H[D_i,i])\right] \tag{A.28}$$

Consequently, the instantaneous estimate of $\nabla[D_i,i]$ as derived from (A.23) is formulated as:

$$\begin{aligned}\hat{\nabla}[D_i,i] &= -2\hat{\varkappa} + 2\hat{\bar{\Upsilon}}[D_i,i]\mathbf{C}[D_i,i] \\ &= -2\Big[(\mathbf{y}^*[D_i,i]\mathbf{g}[D_i,i])\Big] + 2\Big[(\mathbf{g}[D_i,i]\mathbf{g}^H[D_i,i])\Big]\mathbf{C}[D_i,i]\end{aligned} \tag{A.29}$$

From the method of steepest decent, the CIR vector updated value at time (D_i+1) is represented as:

$$\hat{\mathbf{C}}_{LMS}[D_i+1,i] = \mathbf{C}[D_i,i] + \frac{1}{2}\mu\left[-\hat{\nabla}[D_i,i]\right] \tag{A.30}$$

where μ has been described as the step size parameter which assumes a positive constant that is real-valued. Hence, substituting (A.29) into (A.30) yields:

$$\begin{aligned}\hat{\mathbf{C}}_{LMS}[D_i+1,i] &= \mathbf{C}[D_i,i]+\frac{1}{2}\mu\left[2(\mathbf{y}^*[D_i,i]\mathbf{g}[D_i,i])\right]-\frac{1}{2}\mu\left[2(\mathbf{g}[D_i,i]\mathbf{g}^H[D_i,i])\right]\mathbf{C}[D_i,i]\\ &= \mathbf{C}[D_i,i]+\mu\mathbf{y}^*[D_i,i]\mathbf{g}[D_i,i]-\mu\mathbf{C}[D_i,i]\mathbf{g}^H[D_i,i]\mathbf{g}[D_i,i]\\ &= \mathbf{C}[D_i,i]+\mu\mathbf{g}[D_i,i]\left[\mathbf{y}^*[D_i,i]-\mathbf{C}[D_i,i]\mathbf{g}^H[D_i,i]\right] \qquad \text{(A.31)}\end{aligned}$$

Substituting the error expression in (3.9) into (A.31) gives the LMS channel estimate as expressed in (3.10). Thereafter, LMS channel estimate is normalized using the power of the aggregated CH information to obtain the NLMS channel estimate according to (3.11).

A.4 PROOF OF PROPOSED ISI/ANR CHANNEL ESTIMATE

The PDF of the received signal according to (4.15) is given as:

$$f_Y(\mathbf{y}[D_i,i]) = \frac{1}{\sqrt{2\pi\sigma_w^2}}\times\exp\left(-\frac{1}{2\sigma_w^2}\left(\mathbf{y}[D_i,i]-\mathbf{C}[D_i,i]\mathbf{g}[D_i,i]\right)^2\right) \qquad \text{(A.32)}$$

If the channel noise $\mathbf{w}[D_i,i]$ are independent and identically distributed (iid), then the received observation $\mathbf{y}[D_i,i]$ will also be iid such that the joint PDF of the received signal is expressed as a product of the individual PDFs of the received signal observation [146]. It is important to note that the likelihood function of a channel estimate $\Lambda_L[\mathbf{y}[D_i,i],\mathbf{C}]$ is denoted as the joint PDF of the received signal vector which is specified by the CIR. This is simply derived as the product of the PDF of individual received observation shown as:

$$\Lambda_L[\mathbf{y}[D_i,i],\mathbf{C}] = f_{Y(1)Y(2)\ldots Y(d)}[y(1),y(2),\ldots,y(d)]) = f_{Y(1)}y(1)\times f_{Y(2)}y(2)\times\ldots\times f_{Y(d)}y(d) \qquad \text{(A.33)}$$

where the PDF of individual sample of received observation is given in (4.15). Hence, the joint PDF of received observation $\Lambda_L[\mathbf{y}[D_i,i],\mathbf{C}]$ according to the Gaussian PDF can be expressed as:

$$f_{Y(1)Y(2)\ldots Y(d)}[y(1),y(2),\ldots,y(d)]) = \frac{1}{\sqrt{2\pi\sigma_w^2}}\exp\left(-\frac{1}{2\sigma_w^2}\left(\mathbf{y}[1]-\mathbf{C}[1]\mathbf{g}[1]\right)^2\right)$$
$$\times\frac{1}{\sqrt{2\pi\sigma_w^2}}\exp\left(-\frac{1}{2\sigma_w^2}\left(\mathbf{y}[2]-\mathbf{C}[2]\mathbf{g}[2]\right)^2\right)\times\ldots\times\frac{1}{\sqrt{2\pi\sigma_w^2}}\exp\left(-\frac{1}{2\sigma_w^2}\left(\mathbf{y}[d]-\mathbf{C}[d]\mathbf{g}[d]\right)^2\right)$$

Hence,

$$\Lambda_L[\mathbf{y}[D_i,i],\mathbf{C}] = \left(\frac{1}{\sqrt{2\pi\sigma_w^2}}\right)^d\exp\left(-\frac{1}{2\sigma_w^2}\sum_{k=1}^{d}\left(\mathbf{y}[k]-\mathbf{C}[k]\mathbf{g}[k]\right)^2\right) \tag{A.34}$$

If the logarithm of the likelihood function according to (A.34) is evaluated, then the log-likelihood function of the unknown channel $\Lambda_{\log L}[\mathbf{y}[D_i,i],\mathbf{C}]$ can be represented as:

$$\begin{aligned}\Lambda_{\log L}[\mathbf{y}[D_i,i],\mathbf{C}] &= \log_e\left(\Lambda_L[\mathbf{y}[D_i,i],\mathbf{C}]\right) = \ln\left(\Lambda_L[\mathbf{y}[D_i,i],\mathbf{C}]\right)\\ &= \ln\left(\left(\frac{1}{\sqrt{2\pi\sigma_w^2}}\right)^d\exp\left(-\frac{1}{2\sigma_w^2}\times\sum_{k=1}^{d}\left(\mathbf{y}[k]-\mathbf{C}[k]\mathbf{g}[k]\right)^2\right)\right)\\ &= \ln\left(\left(\frac{1}{\sqrt{2\pi\sigma_w^2}}\right)^d\right)+\ln\left(\exp\left(-\frac{1}{2\sigma_w^2}\sum_{k=1}^{d}\left(\mathbf{y}[k]-\mathbf{C}[k]\mathbf{g}[k]\right)^2\right)\right)\\ &= d\ln\left(\frac{1}{\sqrt{2\pi\sigma_w^2}}\right)-\left(\frac{1}{2\sigma_w^2}\sum_{k=1}^{d}\left(\mathbf{y}[k]-\mathbf{C}[k]\mathbf{g}[k]\right)^2\right)\end{aligned} \tag{A.35}$$

The maximum likelihood estimate of the channel fading coefficients $\hat{\mathbf{C}}_{ML}[D_i,i]$ is obtained by evaluating the parameter that maximizes the log-likelihood function expressed in (A.35). Hence,

$$\hat{\mathbf{C}}_{ML}[D_i,i] = \max\Lambda_{\log L}[\mathbf{y}[D_i,i],\mathbf{C}] = \frac{\partial\left(\Lambda_{\log L}[\mathbf{y}[D_i,i],C]\right)}{\partial C} = 0$$

Therefore,

$$\hat{\mathbf{C}}_{ML}[D_i,i] = \frac{\partial\left(d\ln\left(\frac{1}{\sqrt{2\pi\sigma_w^2}}\right)\right)}{\partial C} - \frac{\partial\left(\left(\frac{1}{2\sigma_w^2}\sum_{k=1}^{d}\left(\mathbf{y}[k]-\mathbf{C}[k]\mathbf{g}[k]\right)^2\right)\right)}{\partial C}$$
$$= \left(-\frac{1}{2\sigma_w^2}\right)\times 2\left(\sum_{k=1}^{d}\left(\mathbf{y}[k]-\mathbf{C}[k]\mathbf{g}[k]\right)\times\left(-\mathbf{g}[k]\right)\right) = 0 \tag{A.36}$$

This implies that

$$\sum_{k=1}^{d}\left(\mathbf{y}[k]-\mathbf{C}[k]\mathbf{g}[k]\right)\times\left(\mathbf{g}[k]\right) = 0$$
$$\therefore \sum_{k=1}^{d}\left(\mathbf{y}[k]\mathbf{g}[k]-\mathbf{C}[k]\mathbf{g}^2[k]\right) = 0$$

Hence,

$$\sum_{k=1}^{d}\mathbf{y}[k]\mathbf{g}[k] - \sum_{k=1}^{d}\mathbf{C}[k]\mathbf{g}^2[k] = 0$$

or

$$\sum_{k=1}^{d}\mathbf{C}[k]\mathbf{g}^2[k] = \sum_{k=1}^{d}\mathbf{y}[k]\mathbf{g}[k]$$

Finally,

$$\hat{\mathbf{C}}_{ML}[D_i,i] = \frac{\sum_{k=1}^{d}\mathbf{y}[k]\mathbf{g}[k]}{\mathbf{g}^2[k]} = \frac{\mathbf{y}[k]\mathbf{g}[k]}{\mathbf{g}^2[k]} \tag{A.37}$$

A.5 PROOF OF PROPOSED RER CHANNEL ESTIMATE

It is previously mentioned that the $d\times d$ correlation matrix between the aggregated CH sensor information $\left(\mathbf{g}[D_i,i]\right)$ is given based on NLMS CE according to (A.21). The product $\left[(\mathbf{g}[D_i,i]\mathbf{g}^H[D_i,i])\right]$ as obtained from this correlation matrix is re-weighted by an exponential factor given as $\breve{\lambda}^{D_i-i}$. As such, the $d\times d$ correlation matrix for the derivation of RLS CE is presented as:

$$\bar{\Upsilon}_{RLS}[D_i,i] = \sum_{i=1}^{D_i} \breve{\lambda}^{D_i-i}\left(\mathbf{g}[D_i,i]\mathbf{g}^H[D_i,i]\right) \tag{A.38}$$

From the expression in (A.38), if $(D_i = 1)$ is isolated from the summation, then the RLS-based correlation matrix can be written as:

$$\bar{\Upsilon}_{RLS}[D_i,i] = \breve{\lambda}\left[\sum_{i=1}^{D_i-1} \breve{\lambda}^{D_i-i-1}\Big(\mathbf{g}[D_i,i]\mathbf{g}^H[D_i,i]\Big)\right] + \Big(\mathbf{g}[D_i,i]\mathbf{g}^H[D_i,i]\Big) \tag{A.39}$$

Comparing the expressions (A.38) and (A.39), the RLS-based correlation matrix based on previous estimate $\left(\bar{\Upsilon}_{RLS}[D_i-1,i]\right)$ can then be formulated as:

$$\bar{\Upsilon}_{RLS}[D_i-1,i] = \sum_{i=1}^{D_i-1} \breve{\lambda}^{D_i-i-1}\Big(\mathbf{g}[D_i,i]\mathbf{g}^H[D_i,i]\Big) \tag{A.40}$$

Substituting (A.40) into (A.39) gives the expression in (A.41) which is used for updating the deterministic correlation matrix:

$$\bar{\Upsilon}^{-1}_{RLS}[D_i,i] = \breve{\lambda}\bar{\Upsilon}_{RLS}[D_i-1,i] + \mathbf{g}[D_i,i]\mathbf{g}^H[D_i,i] \tag{A.41}$$

The use of matrix inversion lemma can be adopted for deriving the RLS-based channel estimate where the inverse autocorrelation matrix $\bar{\Upsilon}^{-1}_{RLS}[D_i,i]$ is obtained. The properties of this lemma is summarized as follows. Let two positive-definite $D_i \times D_i$ matrix be represent as $\acute{\mathbf{Y}}$ and $\acute{\mathbf{B}}$ such that they are related by:

$$\acute{\mathbf{Y}} = \acute{\mathbf{B}}^{-1} + \acute{\mathbf{U}}\acute{\mathbf{V}}^{-1}\acute{\mathbf{U}}^H \tag{A.42}$$

In (A.42), $\acute{\mathbf{U}}$ is a $D_i \times E_i$ matrix while $\acute{\mathbf{V}}$ is an $E_i \times E_i$ small positive-definite matrix. From this expression, the matrix inversion lemma can then be used to obtain the inverse of $\acute{\mathbf{Y}}$ which is given as:

$$\acute{\mathbf{Y}}^{-1} = \acute{\mathbf{B}} - \acute{\mathbf{B}}\acute{\mathbf{U}}\left(\acute{\mathbf{V}} + \acute{\mathbf{U}}^{H}\acute{\mathbf{B}}\acute{\mathbf{U}}\right)^{-1}\acute{\mathbf{U}}^{H}\acute{\mathbf{B}} \tag{A.43}$$

The product of (A.42) and (A.43) gives unity. As such, from the matrix inversion lemma, the RLS inverse correlation matrix $\left(\bar{\boldsymbol{\Upsilon}}^{-1}_{RLS}[D_i,i]\right)$ can be obtained if the following substitutions below are inserted into (A.43) [113]:

$\acute{\mathbf{Y}} = \bar{\boldsymbol{\Upsilon}}^{-1}_{RLS}[D_i,i], \acute{\mathbf{U}} = \mathbf{g}[D_i,i], \acute{\mathbf{B}}^{-1} = \check{\lambda}\bar{\Upsilon}_{RLS}[D_i-1,i], \acute{\mathbf{V}} = 1$ Thus, $\left(\bar{\boldsymbol{\Upsilon}}^{-1}_{RLS}[D_i,i]\right)$ can be obtained as the expression in (A.44).

$$\begin{aligned}
\bar{\boldsymbol{\Upsilon}}^{-1}_{RLS}[D_i,i] &= \left[\check{\lambda}\bar{\boldsymbol{\Upsilon}}_{RLS}[D_i-1,i]\right]^{-1} - \Big(\left[\check{\lambda}\bar{\boldsymbol{\Upsilon}}_{RLS}[D_i-1,i]\right]^{-1}\mathbf{g}[D_i,i]\left(1+\mathbf{g}^{H}[D_i,i]\left[\check{\lambda}\bar{\boldsymbol{\Upsilon}}_{RLS}[D_i-1,i]\right]^{-1}\right.\\
&\left.\mathbf{g}[D_i,i]\right)^{-1}\Big)\mathbf{g}^{H}[D_i,i]\left[\check{\lambda}\bar{\boldsymbol{\Upsilon}}_{RLS}[D_i-1,i]\right]^{-1}\\
&= \check{\lambda}^{-1}\bar{\boldsymbol{\Upsilon}}^{-1}_{RLS}[D_i-1,i] - \Big(\check{\lambda}^{-1}\bar{\boldsymbol{\Upsilon}}^{-1}_{RLS}[D_i-1,i]\mathbf{g}[D_i,i]\left(1+\mathbf{g}^{H}[D_i,i]\check{\lambda}^{-1}\bar{\boldsymbol{\Upsilon}}^{-1}_{RLS}[D_i-1,i]\mathbf{g}[D_i,i]\right)^{-1}\cdot\\
&\mathbf{g}^{H}[D_i,i]\check{\lambda}^{-1}\bar{\boldsymbol{\Upsilon}}^{-1}_{RLS}[D_i-1,i]\Big)\\
&= \check{\lambda}^{-1}\bar{\boldsymbol{\Upsilon}}^{-1}_{RLS}[D_i-1,i] - \left[\frac{\check{\lambda}^{-1}\bar{\boldsymbol{\Upsilon}}^{-1}_{RLS}[D_i-1,i]\mathbf{g}[D_i,i]\mathbf{g}^{H}[D_i,i]\check{\lambda}^{-1}\bar{\boldsymbol{\Upsilon}}^{-1}_{RLS}[D_i-1,i]}{1+\mathbf{g}^{H}[D_i,i]\check{\lambda}^{-1}\bar{\boldsymbol{\Upsilon}}^{-1}_{RLS}[D_i-1,i]\mathbf{g}[D_i,i]}\right] \Longrightarrow\\
\bar{\boldsymbol{\Upsilon}}^{-1}_{RLS}[D_i,i] &= \check{\lambda}^{-1}\bar{\boldsymbol{\Upsilon}}^{-1}_{RLS}[D_i-1,i] - \left[\frac{\check{\lambda}^{-2}\bar{\boldsymbol{\Upsilon}}^{-1}_{RLS}[D_i-1,i]\mathbf{g}[D_i,i]\mathbf{g}^{H}[D_i,i]\bar{\boldsymbol{\Upsilon}}^{-1}_{RLS}[D_i-1,i]}{1+\mathbf{g}^{H}[D_i,i]\check{\lambda}^{-1}\bar{\boldsymbol{\Upsilon}}^{-1}_{RLS}[D_i-1,i]\mathbf{g}[D_i,i]}\right]
\end{aligned} \tag{A.44}$$

Let the inverse autocorrelation matrix $\bar{\boldsymbol{\Upsilon}}^{-1}_{RLS}[D_i,i]$ for computational convenience be denoted as $\hat{\boldsymbol{\rho}}_{RLS}[D_i,i]$ such that:

$$\hat{\boldsymbol{\rho}}_{RLS}[D_i,i] = \bar{\boldsymbol{\Upsilon}}^{-1}_{RLS}[D_i,i] \tag{A.45}$$

As such;

$$\hat{\boldsymbol{\rho}}_{RLS}[D_i-1,i]=\bar{\boldsymbol{\Upsilon}}^{-1}_{RLS}[D_i-1,i] \tag{A.46}$$

From the expression in (A.44), if the gain vector is represented according to (3.14), then this (gain) vector can be represented using the notation given in (A.46) as:

$$\vec{\eth}[D_i,i]=\frac{\check{\lambda}^{-1}\hat{\boldsymbol{\rho}}_{RLS}[D_i-1,i]\mathbf{g}[D_i,i]}{1+\mathbf{g}^H[D_i,i]\check{\lambda}^{-1}\hat{\boldsymbol{\rho}}_{RLS}[D_i-1,i]\mathbf{g}[D_i,i]} \tag{A.47}$$

Hence, the inverse autocorrelation matrix $\hat{\boldsymbol{\rho}}_{RLS}[D_i,i]$ can be derived by simply substituting (A.45), (A.46) and (A.47) into the expression in (A.44). Thus,

$$\hat{\boldsymbol{\rho}}_{RLS}[D_i,i]=\check{\lambda}^{-1}\hat{\boldsymbol{\rho}}_{RLS}[D_i-1,i]-\check{\lambda}^{-1}\vec{\eth}[D_i,i]\mathbf{g}^H[D_i,i]\hat{\boldsymbol{\rho}}_{RLS}[D_i-1,i] \tag{A.48}$$

It is worth noting that (A.48) can also be given as:

$$\bar{\boldsymbol{\Upsilon}}^{-1}_{RLS}[D_i-1,i]=\check{\lambda}^{-1}\bar{\boldsymbol{\Upsilon}}^{-1}_{RLS}[D_i-1,i]-\check{\lambda}^{-1}\vec{\eth}[D_i,i]\mathbf{g}^H[D_i,i]\bar{\boldsymbol{\Upsilon}}^{-1}_{RLS}[D_i-1,i] \tag{A.49}$$

The expression in (A.47) can further be simplified as follows:

$$\begin{aligned}
&\vec{\eth}[D_i,i]\left(1+\mathbf{g}^H[D_i,i]\lambda^{-1}\hat{\boldsymbol{\rho}}_{RLS}[D_i-1,i]\mathbf{g}[D_i,i]\right)=\check{\lambda}^{-1}\hat{\boldsymbol{\rho}}_{RLS}[D_i-1,i]\mathbf{g}[D_i,i]\Big(\vec{\eth}[D_i,i]+\vec{\eth}[D_i,i].\\
&\mathbf{g}^H[D_i,i]\check{\lambda}^{-1}\hat{\boldsymbol{\rho}}_{RLS}[D_i-1,i]\mathbf{g}[D_i,i]\Big)\\
&=\check{\lambda}^{-1}\hat{\boldsymbol{\rho}}_{RLS}[D_i-1,i]\mathbf{g}[D_i,i]-\vec{\eth}[D_i,i]\\
&\implies\vec{\eth}[D_i,i]=\check{\lambda}^{-1}\hat{\boldsymbol{\rho}}_{RLS}[D_i-1,i]\mathbf{g}[D_i,i]-\vec{\eth}[D_i,i]\mathbf{g}^H[D_i,i]\check{\lambda}^{-1}\hat{\boldsymbol{\rho}}_{RLS}[D_i-1,i]\mathbf{g}[D_i,i]\\
&=\mathbf{g}[D_i,i]\left[\check{\lambda}^{-1}\hat{\boldsymbol{\rho}}_{RLS}[D_i-1,i]-\vec{\eth}[D_i,i]\mathbf{g}^H[D_i,i]\check{\lambda}^{-1}\hat{\boldsymbol{\rho}}_{RLS}[D_i-1,i]\right]
\end{aligned} \tag{A.50}$$

Inserting the expression in (A.48) into (A.50),

$$\vec{\eth}[D_i,i] = \hat{\boldsymbol{\rho}}_{RLS}[D_i,i]\mathbf{g}[D_i,i] \tag{A.51}$$

When the performance index according to (3.12) attains its minimum value, then the optimum RLS channel estimate can be obtained using the expression in (A.52) [113].

$$\hat{\mathbf{C}}_{RLS}[D_i,i] = \bar{\boldsymbol{\Upsilon}}^{-1}_{RLS}[D_i,i]\omega[D_i,i] \tag{A.52}$$

where ω is a $D_i \times 1$ cross-correlation vector between $\mathbf{g}[D_i,i]$ and $\mathbf{y}[D_i,i]$ which can be compared to (A.38) such that $(*)$ represents complex conjugation by the expression:

$$\omega[D_i,i] = \sum_{i=1}^{D_i} \breve{\lambda}^{D_i-i}\Big(\mathbf{g}[D_i,i]\mathbf{y}^*[D_i,i]\Big) \tag{A.53}$$

The notation $\omega[D_i,i]$ can also be similarly expressed in comparison with the auto correlation matrix according to (A.41). Thus,

$$\omega[D_i,i] = \breve{\lambda}\,\omega[D_i-1,i] + \mathbf{g}[D_i,i]\mathbf{y}^*[D_i,i] \tag{A.54}$$

Substituting A.54 into A.52, the following expressions are obtained.

$$\begin{aligned}\hat{\mathbf{C}}_{RLS}[D_i,i] &= \bar{\boldsymbol{\Upsilon}}^{-1}_{RLS}[D_i,i]\Big[\breve{\lambda}\,\omega[D_i-1,i] + \mathbf{g}[D_i,i]\mathbf{y}^*[D_i,i]\Big] \\ &= \hat{\boldsymbol{\rho}}_{RLS}[D_i,i]\Big[\breve{\lambda}\,\omega[D_i-1,i] + \mathbf{g}[D_i,i]\mathbf{y}^*[D_i,i]\Big] \\ &= \hat{\boldsymbol{\rho}}_{RLS}[D_i,i]\breve{\lambda}\,\omega[D_i-1,i] + \hat{\boldsymbol{\rho}}_{RLS}[D_i,i]\mathbf{g}[D_i,i]\mathbf{y}^*[D_i,i]\end{aligned} \tag{A.55}$$

Substituting (A.48) into (A.55) yields

$$\begin{aligned}
\hat{\mathbf{C}}_{RLS}[D_i,i] &= \breve{\lambda}\left[\breve{\lambda}^{-1}\hat{\boldsymbol{\rho}}_{RLS}[D_i-1,i] - \breve{\lambda}^{-1}\vec{\partial}[D_i,i]\mathbf{g}^H[D_i,i]\hat{\boldsymbol{\rho}}_{RLS}[D_i-1,i]\right]\omega[D_i-1,i] \\
&+ \hat{\boldsymbol{\rho}}_{RLS}[D_i,i]\mathbf{g}[D_i,i]\mathbf{y}^*[D_i,i] \\
&= \left[\hat{\boldsymbol{\rho}}_{RLS}[D_i-1,i] - \vec{\partial}[D_i,i]\mathbf{g}^H[D_i,i]\hat{\boldsymbol{\rho}}_{RLS}[D_i-1,i]\right]\omega[D_i-1,i] \\
&+ \hat{\boldsymbol{\rho}}_{RLS}[D_i,i]\mathbf{g}[D_i,i]\mathbf{y}^*[D_i,i] \\
&= \hat{\boldsymbol{\rho}}_{RLS}[D_i-1,i]\omega[D_i-1,i] - \vec{\partial}[D_i,i]\mathbf{g}^H[D_i,i]\hat{\boldsymbol{\rho}}_{RLS}[D_i-1,i]\omega[D_i-1,i] \\
&+ \hat{\boldsymbol{\rho}}_{RLS}[D_i,i]\mathbf{g}[D_i,i]\mathbf{y}^*[D_i,i] \\
&= \bar{\boldsymbol{\Upsilon}}^{-1}_{RLS}[D_i-1,i]\omega[D_i-1,i] - \vec{\partial}[D_i,i]\mathbf{g}^H[D_i,i]\bar{\boldsymbol{\Upsilon}}^{-1}_{RLS}[D_i-1,i]\omega[D_i-1,i] \\
&+ \hat{\boldsymbol{\rho}}_{RLS}[D_i,i]\mathbf{g}[D_i,i]\mathbf{y}^*[D_i,i] \qquad \text{(A.56)}
\end{aligned}$$

Similarly to the expression in (A.52), the previous estimate can be formulated as:

$$\hat{\mathbf{C}}[D_i-1,i] = \bar{\boldsymbol{\Upsilon}}^{-1}_{RLS}[D_i-1,i]\omega[D_i-1,i] \qquad \text{(A.57)}$$

Substituting this expression of A.57 into (A.56) yields:

$$\hat{\mathbf{C}}_{RLS}[D_i,i] = \hat{\mathbf{C}}[D_i-1,i] - \vec{\partial}[D_i,i]\mathbf{g}^H[D_i,i]\hat{\mathbf{C}}[D_i-1,i] + \hat{\boldsymbol{\rho}}_{RLS}[D_i,i]\mathbf{g}[D_i,i]\mathbf{y}^*[D_i,i] \qquad \text{(A.58)}$$

Inserting the expression in (A.51) into (A.58) yields:

$$\begin{aligned}
\hat{\mathbf{C}}_{RLS}[D_i,i] &= \hat{\mathbf{C}}[D_i-1,i] - \vec{\partial}[D_i,i]\mathbf{g}^H[D_i,i]\hat{\mathbf{C}}[D_i-1,i] + \vec{\partial}[D_i,i]\mathbf{y}^*[D_i,i] \\
&= \hat{\mathbf{C}}[D_i-1,i] + \vec{\partial}[D_i,i]\left[\mathbf{y}^*[D_i,i] - \mathbf{g}^H[D_i,i]\hat{\mathbf{C}}[D_i-1,i]\right] \qquad \text{(A.59)}
\end{aligned}$$

Finally, substituting the error expression of (3.9) into (A.59) yields the RLS channel estimate according to (3.16).

ADDENDUM B DERIVATION OF QoS REQUIREMENTS for IoMT

B.1 DERIVATION OF AVERAGE DATA RATE EXPRESSIONS FOR IOMT

In this section of the addendum, the average data rate expressions assuming frequent heavy shadowing and infrequent light shadowing marine propagation are elaborately derived as presented in section B.2 and B.3 respectively.

B.2 AVERAGE DATA RATE DERIVATION ASSUMING RAYLEIGH FADING

The data rate expression according to (4.29) can be further simplified as:

$$\vec{\hat{R}}_i = \mathbb{E}_{\mathbf{C}[D_i,i]}\left[\log_2\left(1+\frac{\overline{E}_p\hat{\tau}_h}{\sigma_w^2}\right)\right] \tag{B.1}$$

where $\hat{\tau}_h$ is given as in (4.30). Considering the PDF expression represented in (4.31), the integral form of the data rate of vessel i can be mathematically written as:

$$\begin{aligned}\vec{\hat{R}}_i &= \int_0^g \log_2\left(1+\frac{\overline{E}_p g}{\sigma_w^2}\right) f_{\hat{\tau}_h}(\mathbf{g})\mathrm{d}g = \int_0^g \log_2\left(1+\frac{\overline{E}_p g}{\sigma_w^2}\right)\sum_{k=1}^{d}\varpi_k(0)\zeta_k e^{-\zeta_k g}\mathrm{d}g \\ &= \sum_{k=1}^{d}\zeta_k\varpi_k(0)\int_0^g \log_2\left(1+\frac{\overline{E}_p g}{\sigma_w^2}\right)e^{-\zeta_k g}\mathrm{d}g\end{aligned} \tag{B.2}$$

From the expression in (B.2), the relation in (B.3) can be defined after applying linearity property. Hence,

$$\int_0^g \log_2\left(1+\frac{\overline{E}_p g}{\sigma_w^2}\right)e^{-\zeta_k g}\mathrm{d}g = \frac{1}{\log_e(2)}\int_0^g\left[\log_e\left(1+\frac{\overline{E}_p g}{\sigma_w^2}\right)e^{-\zeta_k g}\right]\mathrm{d}g \tag{B.3}$$

The solution of the integral in (B.3) can be achieved using integration by parts. Solving this expression by parts yield:

$$\int_0^g\left[\log_e\left(1+\frac{\overline{E}_p g}{\sigma_w^2}\right)e^{-\zeta_k g}\right]\mathrm{d}g = \left[-\frac{e^{-\zeta_k g}\log_e\left(1+\frac{\overline{E}_p g}{\sigma_w^2}\right)}{\zeta_k} - \int_0^g -\frac{\overline{E}_p e^{-\zeta_k g}}{\zeta_k\sigma_w^2\left(1+\frac{\overline{E}_p g}{\sigma_w^2}\right)}\mathrm{d}g\right] \tag{B.4}$$

From (B.4), the expression $\left[\int_0^g -\frac{\overline{E}_p e^{-\zeta_k g}}{\zeta_k\sigma_w^2\left(1+\frac{\overline{E}_p g}{\sigma_w^2}\right)}\mathrm{d}g\right]$ can easily be solved using the concept of *exponential integrals* such that $\left[\ddot{t} = \left(\zeta_k g + \frac{\zeta_k\sigma_w^2}{\overline{E}_p}\right)\right]$. The exponential integral is a special function that consist of the ratio between an exponential function (e) and its argument generally given as $E_1(\dot{t}) = \int_{-g}^{\infty}\left(\frac{e^{-\ddot{t}}}{\ddot{t}}\right)\mathrm{d}\ddot{t}$. Thus, the solution to this expression is given as:

$$\int_0^g -\frac{\overline{E}_p.e^{-\zeta_k g}}{\zeta_k\sigma_w^2\left(1+\frac{\overline{E}_p g}{\sigma_w^2}\right)}\mathrm{d}g = \frac{1}{\zeta_k}\left(e^{\frac{\zeta_k\sigma_w^2}{\overline{E}_p}}E_1\left(\zeta_k g+\frac{\zeta_k\sigma_w^2}{\overline{E}_p}\right)\right) \tag{B.5}$$

Plugging (B.5) into the integral expression in (B.4), the equation in (B.4) can be simplified as in (B.6):

$$\int_0^g\left[\log_e\left(1+\frac{\overline{E}_p g}{\sigma_w^2}\right)e^{-\zeta_k g}\right]\mathrm{d}g = \left[-\frac{e^{-\zeta_k g}\log_e\left(1+\frac{\overline{E}_p g}{\sigma_w^2}\right)}{\zeta_k} - \frac{1}{\zeta_k}\left(e^{\frac{\zeta_k\sigma_w^2}{\overline{E}_p}}E_1\left(\zeta_k g+\frac{\zeta_k\sigma_w^2}{\overline{E}_p}\right)\right)\right] \tag{B.6}$$

Thus, (B.3) can be further simplified as presented in (B.7).

$$\int_0^g \log_2\left(1+\frac{\overline{E}_p g}{\sigma_w^2}\right)e^{-\zeta_k g}\mathrm{d}g = \frac{1}{\log_e(2)}\left[-\frac{e^{-\zeta_k g}\log_e\left(1+\frac{\overline{E}_p g}{\sigma_w^2}\right)}{\zeta_k} - \frac{1}{\zeta_k}\left(e^{\frac{\zeta_k\sigma_w^2}{\overline{E}_p}}E_1\left(\zeta_k g+\frac{\zeta_k\sigma_w^2}{\overline{E}_p}\right)\right)\right] \tag{B.7}$$

Lastly, if the expression in (B.7), is substituted into (B.2), then the average data rate expression assuming Rayleigh fading (NLOS) propagation can be obtained as (4.33).

B.3 AVERAGE DATA RATE ASSUMING SHADOWED RICIAN FADING

The PDF $f_{\|\mathbf{C}[D_i,i]\|^2}(g)$ can be expressed in terms of confluent hypergeometric (Kummer's) function of the first kind as [3, 141]:

$$f_{\|\mathbf{C}[D_i,i]\|^2}(g) = (2P_E)^{\left((m-1)|D_i|\right)}.\eta^{(m|D_i|-\varphi)}\sum_{\hat{l}=0}^{\xi}\left(\frac{g^{\varphi-\hat{l}-1}}{\Gamma(\varphi-\hat{l})}.{}_1F_1(\varphi;\varphi-\hat{l};-\eta g)\right.$$
$$\left.+\frac{\phi.\eta^{\hat{l}-1}}{\Gamma(\varphi-\hat{l}+1)}.{}_1F_1(\varphi+1;\varphi-\hat{l}+1;-\eta g)\right)dg \tag{B.8}$$

From the expression in (4.34), $\ln\left(1+\bar{\gamma}g\right) = G_{2,2}^{1,2}\left(-\bar{\gamma}g\middle|\begin{matrix}1,1\\1,0\end{matrix}\right)$ while in general, ${}_1F_1(k;m;n) = \frac{\Gamma(m)}{\Gamma(k)}G_{1,2}^{1,1}\left(-n\middle|\begin{matrix}1-k\\0,1-m\end{matrix}\right)$.

The data rate expression of the Rican fading channel according to (4.34) can then be simplified as:

$$\vec{\mathring{R}}_i = \frac{1}{\ln 2}\int_0^{\infty} \ln\left(1+\bar{\gamma}g\right).(2P_E)^{\left((m-1)|D_i|\right)}.\eta^{(m|D_i|-\varphi)}\sum_{\hat{l}=0}^{\xi}\left(\frac{g^{\varphi-\hat{l}-1}}{\Gamma(\varphi-\hat{l})}.{}_1F_1(\varphi;\varphi-\hat{l};-\eta g)\right.$$
$$\left.+\frac{\phi.g^{\varphi-\hat{l}}}{\Gamma(\varphi-\hat{l}+1)}.{}_1F_1(\varphi+1;\varphi-\hat{l}+1;-\eta g)\right)\mathrm{d}g$$
$$=\frac{1}{\ln 2}(2P_E)^{\left((m-1)|D_i|\right)}.\eta^{(m|D_i|-\varphi)}\sum_{\hat{l}=0}^{\xi}\int_0^{\infty}G_{2,2}^{1,2}\left(-\bar{\gamma}g\middle|\begin{matrix}1,1\\1,0\end{matrix}\right)\left[\left(\frac{g^{\varphi-\hat{l}-1}}{\Gamma(\varphi-\hat{l})}\right)\left(\frac{\Gamma(\varphi-\hat{l})}{\Gamma(\varphi)}\right).\right.$$
$$\left.G_{1,2}^{1,1}\left(\eta g\middle|\begin{matrix}1-\varphi\\0,1-(\varphi-\hat{l})\end{matrix}\right)+\left(\frac{\phi.g^{\varphi-\hat{l}}}{\Gamma(\varphi-\hat{l}+1)}\right)\left(\frac{\Gamma(\varphi-\hat{l}+1)}{\Gamma(\varphi+1)}\right)G_{1,2}^{1,1}\left(\eta g\middle|\begin{matrix}1-(\varphi+1)\\0,1-(\varphi-\hat{l}+1)\end{matrix}\right)\right]\mathrm{d}g$$
$$=\frac{1}{\ln 2}(2P_E)^{\left((m-1)|D_i|\right)}.\eta^{(m|D_i|-\varphi)}\sum_{\hat{l}=0}^{\xi}\int_0^{\infty}G_{2,2}^{1,2}\left(-\bar{\gamma}g\middle|\begin{matrix}1,1\\1,0\end{matrix}\right).\left[\left(\frac{g^{\varphi-\hat{l}-1}}{\Gamma(\varphi)}\right)G_{1,2}^{1,1}\left(\eta g\middle|\begin{matrix}1-\varphi\\0,(1-\varphi+\hat{l})\end{matrix}\right)\right.$$
$$\left.+\left(\frac{\phi.g^{\varphi-\hat{l}}}{\Gamma(\varphi+1)}\right)G_{1,2}^{1,1}\left(\eta g\middle|\begin{matrix}-\varphi\\0,(-\varphi+\hat{l})\end{matrix}\right)\right]\mathrm{d}g \tag{B.9}$$

Bearing in mind that $g^{\varphi-\hat{l}-1}G_{1,2}^{1,1}\left(\eta g\middle|\begin{matrix}1-\varphi\\0,(1-\varphi+\hat{l})\end{matrix}\right)=\eta^{-(\varphi-\hat{l}-1)}G_{1,2}^{1,1}\left(\eta g\middle|\begin{matrix}-\hat{l}\\(\varphi-\hat{l}-1),0\end{matrix}\right)$ and that the integration of the product of two Meijer-G functions $\int_0^{\infty}G_{1,2}^{1,1}\left(\eta g\middle|\begin{matrix}-\hat{l}\\(\varphi-\hat{l}-1,0\end{matrix}\right).$ $G_{2,2}^{1,2}\left(-\bar{\gamma}g\middle|\begin{matrix}1,1\\1,0\end{matrix}\right)\mathrm{d}g$ is given as $\frac{1}{\eta}G_{4,3}^{2,3}\left(\frac{-\bar{\gamma}}{\eta}\middle|\begin{matrix}-\varphi+\hat{l}+1,1,1,0\\\hat{l},1,0\end{matrix}\right)$ then the data rate expression of (B.9) reduces to:

$$\vec{\mathring{R}}_i=\frac{1}{\ln 2}(2P_E)^{\left((m-1)|D_i|\right)}.\eta^{(m|D_i|-\varphi)}\sum_{\hat{l}=0}^{\xi}\left[\left(\frac{\eta^{-(\varphi-\hat{l}-1)}}{\Gamma(\varphi)}\right)\int_0^{\infty}G_{1,2}^{1,1}\left(\eta g\middle|\begin{matrix}-\hat{l}\\(\varphi-\hat{l}-1),0\end{matrix}\right)\right.$$
$$\left.\times G_{2,2}^{1,2}\left(-\bar{\gamma}g\middle|\begin{matrix}1,1\\1,0\end{matrix}\right)\mathrm{d}g+\left(\frac{\phi.\eta^{-(\varphi-\hat{l})}}{\Gamma(\varphi+1)}\right)\int_0^{\infty}G_{1,2}^{1,1}\left(\eta g\middle|\begin{matrix}1-\hat{l}\\(\varphi-\hat{l}),0\end{matrix}\right)G_{2,2}^{1,2}\left(-\bar{\gamma}g\middle|\begin{matrix}1,1\\1,0\end{matrix}\right)\mathrm{d}g\right].$$
$$=\frac{1}{\ln 2}(2P_E)^{\left((m-1)|D_i|\right)}.\eta^{(m|D_i|-\varphi)}\sum_{\hat{l}=0}^{\xi}.\left[\left(\frac{\eta^{-(\varphi-\hat{l}-1)}}{\Gamma(\varphi)}\right)\frac{1}{\eta}G_{4,3}^{2,3}\left(\frac{-\bar{\gamma}}{\eta}\middle|\begin{matrix}-\varphi+\hat{l}+1,1,1,0\\\hat{l},1,0\end{matrix}\right)\right.$$
$$\left.+\left(\frac{\phi.\eta^{\varphi-\hat{l}}}{\Gamma(\varphi+1)}\right).\frac{1}{\eta}G_{4,3}^{2,3}\left(\frac{-\bar{\gamma}}{\eta}\middle|\begin{matrix}-\varphi+\hat{l},1,1,0\\\hat{l},1,0\end{matrix}\right)\right] \tag{B.10}$$